

UNIVERSITÉ DE SHERBROOKE

Faculté de Génie

Département de génie mécanique

Caractérisation des propriétés thermiques et
rhéologiques des nanofluides eau-alumine :
compréhension des mécanismes
thermophysiques, régimes de dispersion et
étude du phénomène d'hystérésis.

Thèse de doctorat

Spécialité : Génie mécanique

Nizar BOUGUERRA

Sherbrooke (Québec) Canada

Novembre 2018

Membres du Jury

Dr. Jérôme Pollak (examineur)

Prof. Armand Soldera (examineur)

Prof. Nicolas Galanis (examineur)

Prof. Julien Sylvestre (rapporteur)

Prof. Sébastien Poncet (codirecteur)

Prof. Saïd Elkoun (directeur)

Résumé:

Les échangeurs de chaleur sont utilisés dans la quasi-totalité des applications qui font intervenir des procédés de récupération de chaleur. Afin de réduire les coûts énergétiques, les industriels ont souvent tendance à recourir à des méthodes qui permettent de réaliser le maximum d'économie dans leurs installations. Dans ce sens, l'utilisation des nanofluides fait partie des méthodes passives permettant d'améliorer l'efficacité des systèmes. En effet, la faible conductivité thermique des fluides couramment utilisés constitue la limitation majeure dans le développement des fluides caloporteurs. L'intérêt croissant pour les nanofluides est justifié par la prise de conscience qu'avec l'avènement récent des nanotechnologies il est possible de développer des fluides à haut rendement avec des propriétés thermiques qui sont radicalement différentes de celles des fluides classiques. Cette nouvelle classe de fluides caloporteurs bénéficie de la conductivité thermique très élevée des nanoparticules dispersées dans un fluide de base, le mélange résultant constitue la suspension nommée nanofluide.

Le concept est une idée centenaire qui s'est limitée, jusqu'au début des années 90, à l'ajout de particules de taille micrométrique. A cette échelle, ce type de suspensions est caractérisé par une sédimentation rapide des particules et cause la dégradation des installations hydrauliques par érosion. Les nanofluides permettent potentiellement de minimiser considérablement ces problèmes tout en bénéficiant d'un rapport surface d'échange sur volume amélioré d'un facteur 10^3 . Cependant, bien qu'ils permettent d'améliorer la conductivité thermique, l'ajout des nanoparticules entraîne une augmentation de la viscosité des mélanges. Cette propriété est une caractéristique du fluide importante en raison de son impact sur la puissance de pompage requise et les performances énergétiques globales des nanofluides. Par conséquent, l'évaluation du comportement thermo-fluidique des nanofluides doit systématiquement considérer le double examen de leur conductivité thermique et de leur viscosité dynamique.

Bien que le domaine des nanofluides soit devenu en vogue ces 20 dernières années, l'élaboration de suspensions homogènes et stables dans le temps, même pour des échantillons de petite taille, reste un défi à l'heure actuelle. Dans ce contexte, l'objectif principal de ce projet de doctorat est de caractériser de manière approfondie le comportement thermique et rhéologique des nanofluides à base d'eau et d'alumine utilisés tout au long de ce travail afin de quantifier les principaux paramètres influençant leurs propriétés thermo-physiques, de contrôler leurs conditions de préparation et de stabilisation et de comprendre les mécanismes conduisant à l'amélioration des propriétés thermiques des nanofluides. Pour ce faire, diverses études paramétriques ont été réalisées expérimentalement dans le cadre de cette thèse. Les propriétés thermofluides des nanofluides ont été étudiées et caractérisées en fonction d'une multitude de paramètres dont les principaux sont : la concentration en nanoparticules, le diamètre moyen des nanoparticules, le pH de la solution, la concentration en tensioactif utilisé pour stabiliser la suspension et la température. Une analyse expérimentale détaillée a permis d'identifier les différents régimes de dispersion que peuvent présenter les nanofluides à base d'eau et d'alumine et de déterminer les conditions de préparation pour les obtenir. Un protocole expérimental permettant d'identifier les conditions expérimentales offrant la plus grande augmentation de conductivité thermique a été développé. L'évaluation des performances énergétiques globales des suspensions a été réalisée en considérant un critère de mérite permettant de les comparer et d'identifier le meilleur nanofluide. L'effet de la température sur les propriétés des nanofluides a été examiné et dans ce sens le phénomène d'hystérésis a été étudié dans les conditions relatives aux différents régimes de dispersion préalablement identifiés.

Mots clés : Nanofluides, régimes de dispersion, stabilité des suspensions, conductivité thermique, viscosité, mesures expérimentales, pH, phénomène d'hystérésis, critère de performance.

Abstract:

Heat exchangers have been essentially used in almost all applications that involve heat recovery processes. In order to reduce energy costs, industrialists often tend to use methods that make it possible to achieve maximum savings in their installations. In that sense, the addition of nanoparticles in base fluids is regarded as one of the passive methods to improve the efficiency of thermal systems. In fact, the low thermal conductivity of commonly used fluids is the main limitation for the development of heat transfer fluids. The growing interest in nanofluids is justified by the fact that, with the recent advent of nanotechnology, the development of high-performance fluids, with substantially better thermal properties as compared to those of conventional fluids, has become possible. This new class of heat transfer fluids benefits from the higher thermal conductivity of the nanoparticles dispersed in a base fluid. The resulting mixtures lead to suspensions named nanofluids.

This concept is a century old idea that was limited to the addition of micrometric particles until the beginning of the 90s. At this scale, this type of suspension was characterized by a rapid sedimentation of the particles that may causes the degradation of the hydraulic installations by erosion. Nanofluids have the potential of significantly minimizing these problems as they benefit from an improved surface/volume ratio of about 10^3 . Despite their potential of improving the thermal conductivity, the addition of nanoparticles lead to an increase in the overall viscosity of the mixtures. This property is of a great importance due to its impact on the required pumping power and the overall energy performance of thermal systems. Therefore, the evaluation of the thermo-fluidic behavior of nanofluids must systematically consider the examination of both thermal conductivity and dynamic viscosity.

Although, nanofluids exhibit a very attractive thermophysical behavior, the development of homogeneous and stable suspensions over time, even for small samples, remains a challenge. In this context, the main objective of this thesis was to characterize in depth the thermal and rheological behavior of alumina/water-based nanofluids, in order to quantify the main parameters affecting their thermo-physical properties, to control their preparation conditions, and to understand the mechanisms leading to the improvement of their thermal properties. Thus, the effect of the concentration of nanoparticles, the average diameter of the nanoparticles, the pH of the solution, the concentration of surfactant used to stabilize the suspension and temperature on the thermo-fluidic properties of alumina/water-based nanofluids were investigated. Detailed and comprehensive experimental analysis allowed to identify five different dispersion regimes of alumina/water-based nanofluids and to determine their stability state as a function of the preparation conditions. An experimental protocol to identify the experimental conditions offering the greatest increase in thermal conductivity was developed. The evaluation of the overall energy performance of the suspensions was carried out by considering a merit criterion making it possible to compare and identify the best nanofluid. Eventually, the effect of temperature on nanofluids properties was examined and the hysteresis phenomenon was studied for two selected dispersion regimes.

Keywords: Nanofluids, Dispersion Regimes, Thermal Conductivity, Dynamic Viscosity, Experimental Measurements, pH, Hysteresis Phenomenon, Alumina/water-based Nanofluids, Suspensions Stability, Performance Criteria.

Remerciements :

Je tiens à remercier les membres de mon jury pour le temps accordé à la lecture de ce manuscrit ainsi que pour leur participation à ma soutenance.

Table des matières :

Table des matières

Chapitre I	Introduction	1
I-1	Contexte de l'étude et motivations	1
I-2	Objectifs et originalité	3
I-3	Organisation du mémoire.....	3
Chapitre II	: Conductivité thermique des nanofluides à base d'eau et d'Alumine: revisiter les effets du pH et du tensioactif.	5
II-1	Résumé Français	6
II-2	Abstract	7
II-3	Introduction.....	7
II-4	Experimental methods	10
II-4.1	Measurement Technique for the Thermal Conductivity	10
II-4.2	Preparation of Alumina-Water Nanofluids	11
II-4.3	Experimental Procedure	12
II-5	Results and Discussions.....	13
II-5.1	Effect of SDBS on the Thermal conductivity at an arbitrary pH value	13
II-5.2	Effect of pH on the Thermal Conductivity.....	16
II-5.3	Effect of the SDBS Surfactant on the Thermal Conductivity at Adjusted Optimum pH	19
II-5.4	Effect of the Nanoparticle Size on the Thermal Conductivity	24
II-5.5	Effect of Nanoparticle Concentration on Thermal Conductivity	25
II-6	Conclusion	26
II-7	References.....	29
Chapitre III	Régimes de dispersion des nanofluides à base d'eau et d'alumine : mesures simultanées de la conductivité thermique et de la viscosité dynamique.	32
III-1	Résumé français	33

III-2	Abstract	34
III-3	Introduction	35
III-4	Experimental methods.....	36
III-5	Results and discussion.....	38
III-6	Conclusions	45
III-7	References	46
Chapitre IV Effet de la température sur les nanofluides à base d'eau et d'Alumine : Relation entre le phénomène d'hystérésis et les régimes de dispersion.		
IV-1	Résumé français	51
IV-2	Abstract	52
IV-3	Introduction	53
IV-4	Experimental methods.....	59
IV-4.1	Thermal conductivity measurements	59
IV-4.2	Dynamic viscosity measurements.....	61
IV-4.3	Preparation of alumina/water-based nanofluids and experimental procedure	63
IV-5	Hysteresis phenomenon on the dynamic viscosity and thermal conductivity.....	65
IV-5.1	Effect of temperature on suspensions with initial state located within the W.D. regime	66
IV-5.2	Effect of temperature on suspensions with initial state located within the C- L.Agg. regime.....	76
IV-6	Conclusion.....	84
IV-7	Références	86
Chapitre V Conclusion générale		90

Liste des Figures :

Figure II-1 THW-L1 Liquid Thermal Conductivity System from Thermtest Thermophysical Instruments	11
Figure II-2 Variation of the thermal conductivity and pH with weight fraction of SDBS	14
Figure II-3 Variation of the thermal conductivity with weight fraction of SDBS without fixing the pH value	15
Figure II-4 Thermal conductivity as a function of pH with the enhancement percentage without adding SDBS	17
Figure II-5 Thermal conductivity as a function of pH (optimal range)	17
Figure II-6 Thermal conductivity as a function of pH for different nanoparticle sizes	18
Figure II-7 Variation of the thermal conductivity with the weight fraction of SDBS at fixed optimum pH	20
Figure II-8 Samples at different pH values from 4 to 7.5, at 0.1 wt.% SDBS	21
Figure II-9 Samples at 0.1 wt.% SDBS and different pH values, from left to right: pH=8 - 9.3 - 10 - 10.7 - 11.4 - 2 - 2.6 - 3	21
Figure II-10 Samples at 0.01 wt.% SDBS and different pH values, from left to right: pH=7.2 - 6.9 - 6.5 - 6.3 - 5.9 - 5.6 - 5.3 - 5 - 4.8 - 4.5 - 4.2 - 4	22
Figure II-11 Samples at 0.015 wt.% SDBS and different pH values, from left to right: pH=6.4 - 6.6 - 7.1 - 6 - 5.8 - 5.6 - 5.4 - 5.2 - 4.9 - 4.5 - 3.9	22
Figure II-12 Variation of the thermal conductivity with the weight fraction of SDBS at optimum pH	23
Figure II-13 Variation of the thermal conductivity ratio with the size of nanoparticles	25
Figure II-14 Evolution of the thermal conductivity ratio with the volume fraction of Al ₂ O ₃	26
=====	
=====	
Figure III-1 (a) Ratios of the effective thermal conductivity and dynamic viscosity as a function of pH for $\phi=1\%$; (b) corresponding efficiency ratio.	40
Figure III-2 Same legend as Figure III-1 for $\phi=0.5\%$.	42
Figure III-3 Same legend as Figure III-1 for $\phi=0.2\%$.	43

Figure III-4 Same legend as Figure III-1 for $\phi=2\%$. 44

Figure IV-1 Variation of the thermal conductivity of distilled water as a function of temperature 61

Figure IV-2 Variation of the dynamic viscosity of distilled water as a function of temperature. 63

Figure IV-3 Dispersion regimes – Relative thermal conductivity and dynamic viscosity as a function of pH for $\phi=0.7$ vol. % at $T=25^\circ\text{C}$. 66

Figure IV-4 : Influence of the temperature on the (a) thermal conductivity, (b) dynamic viscosity and (c) pH for the suspension (b) (center of the W.D. zone: initial pH = 5.35 at $T=25^\circ\text{C}$ in Figure IV-3). 70

Figure IV-5 Relative thermal conductivity and dynamic viscosity as a function of temperature for the suspension (b) (center of the well-dispersed area: initial pH = 5.35 at $T=25^\circ\text{C}$ in Figure IV-3). 71

Figure IV-6 . Influence of the temperature on the (a) thermal conductivity, (b) dynamic viscosity and (c) pH for the suspension (a) (low end of the W.D. area: initial pH = 5.05 at $T=25^\circ\text{C}$ in Figure IV-3). 73

Figure IV-7 Relative thermal conductivity and dynamic viscosity as a function of temperature for the suspension (a) (low end of the W.D. area: initial pH = 5.05 at $T=25^\circ\text{C}$ in Figure IV-3). 74

Figure IV-8 Influence of the temperature on the (a) thermal conductivity, (b) dynamic viscosity and (c) pH for the suspension (c) (upper end of the W.D. area: initial pH = 5.6 at $T=25^\circ\text{C}$ in Figure IV-3). 75

Figure IV-9 Relative thermal conductivity and dynamic viscosity as a function of temperature for the suspension (c) (upper end of the W.D. area: initial pH = 5.6 at $T=25^\circ\text{C}$ in Figure IV-3). 76

Figure IV-10 Influence of the temperature on the (a) thermal conductivity, (b) dynamic viscosity and (c) pH for the suspension (e) (center of C-L agg. zone: initial pH = 6 at $T=25^\circ\text{C}$ in Figure IV-3). 78

Figure IV-11 Relative thermal conductivity and dynamic viscosity as a function of temperature for the suspension (e) (center of C-L agg. Zone: initial pH = 6 at $T=25^\circ\text{C}$ in Figure IV-3). 79

Figure IV-12 Influence of the temperature on the (a) thermal conductivity, (b) dynamic viscosity and (c) pH for the suspension (f) (upper end of C-L. agg zone: initial pH = 6.2 at T=25°C in Figure IV-3). 81

Figure IV-13 Relative thermal conductivity and dynamic viscosity as a function of temperature for the suspension (f) (upper end of C-L. agg zone: initial pH = 6.2 at T=25°C in Figure IV-3). 82

Figure IV-14 Influence of the temperature on the (a) thermal conductivity, (b) dynamic viscosity and (c) pH for the suspension (d) (lower end of C-L. agg. zone: initial pH = 5.8 at T=25°C in Figure IV-3). 83

Figure IV-15 Relative thermal conductivity and dynamic viscosity as a function of temperature for the suspension (d) (lower end of C-L. agg. zone: initial pH = 5.8 at T=25°C in Figure IV-3). 84

Liste des tableaux :

Table II-1 : Conditions of the first experience (variation of thermal conductivity and pH with weight fraction of SDBS)	14
Tableau II-2 Conditions of the Second Experience (Variation of Thermal Conductivity with Weight Fraction of SDBS without Fixing the pH Value)	15
Tableau II-3 Experimental Conditions (pH Effect)	16
Tableau II-4 Experimental Conditions (pH effect for Different Sizes)	18
Tableau II-5 Experimental Conditions (SDBS Effect at Adjusted Optimum pH)	19
Tableau II-6 Experimental Conditions (SDBS Effect – Optimum Range)	24
Tableau II-7 Experimental Conditions (Size Effect)	24
Tableau II-8 Experimental Conditions (Concentration Effect)	26

Chapitre I Introduction

I-1 Contexte de l'étude et motivations

Les nanofluides sont des suspensions contenant des particules de taille nanométrique (le diamètre est typiquement inférieur à 100 nm), appelées nanoparticules, dispersées dans un fluide de base afin d'en améliorer certaines propriétés, notamment thermiques. En effet, pour ce type d'applications, le terme « nanofluide » a été introduit pour la première fois par Choi et Eastman (1995) [1]. Dans le cas des fluides caloporteurs utilisés dans les échangeurs de chaleur par exemple, la principale propriété à prendre en compte afin d'évaluer le potentiel d'échange de chaleur est la conductivité thermique. Les fluides les plus utilisés sont l'eau, l'huile ou l'éthylène-glycol qui malheureusement se caractérisent par une conductivité thermique faible par rapport à celle des solides cristallins. A titre d'exemple, l'alumine a une conductivité thermique de 40 W/(m.K) alors que celle de l'eau pure à 20°C n'est que de 0.6 W/(m.K). Le graphène, quant à lui, peut atteindre une valeur de 5300 W/(m.K). Ainsi, l'ajout de particules au sein d'un fluide de base permettrait d'augmenter la conductivité thermique effective du mélange. Bien que cette idée remonte à Maxwell [2] en 1881, ce n'est que l'avènement récent des nanotechnologies qui a rendu possible la synthèse de particules de taille nanométrique permettant potentiellement de minimiser considérablement les problèmes de sédimentation rencontrés avec les particules micrométriques tout en augmentant le ratio surface d'échange sur volume d'un facteur 10^3 .

Les nanofluides ont donc suscité de nombreux travaux de recherche et de développement tant académiques qu'industriels visant essentiellement à améliorer les performances des systèmes énergétiques. Depuis 1995, l'activité de recherche sur les nanofluides croît de manière exponentielle. A titre d'exemple, 1108 articles contenant le terme « nanofluid » dans le titre ou les mots-clefs ont été publiés sur *Science Direct* uniquement en 2017.

Si cette thématique de recherche est devenue en vogue ces 20 dernières années, l'élaboration de nanofluides homogènes et stables dans le temps, même pour des échantillons de petite taille, reste un défi de taille à l'heure actuelle. Ceci explique notamment pourquoi il y a encore de nombreuses barrières à leur utilisation à plus grande échelle dans des installations thermiques réelles.

Les nombreux travaux de recherche actuellement en cours visent à renforcer la compréhension des mécanismes conduisant à l'amélioration des propriétés thermiques des nanofluides, maîtriser leur préparation et leur stabilité et ainsi les amener à un niveau de maturité suffisant pour être utilisé de manière efficace dans des échangeurs thermiques industriels. C'est dans cette optique que s'inscrit cette thèse.

Il s'agit d'un objectif ambitieux car les propriétés thermofluides des nanofluides ainsi que leur stabilité dépendent d'un grand nombre de paramètres dont les principaux sont : type de nanofluide (couple fluide/nanoparticule), concentration en nanoparticules, diamètre moyen et distribution de tailles des nanoparticules, pH de la solution, type et concentration en tensioactif utilisé pour stabiliser la suspension, durée de la sonification, etc. Pour être utilisable dans des échangeurs thermiques industriels, le nanofluide doit principalement avoir une bonne conductivité thermique et une viscosité peu modifiée par la présence des particules tout en étant peu coûteux, simple à préparer, stable sur plusieurs années et contenant des particules qui ne s'oxydent pas. Le nanofluide alumine (Al_2O_3) / eau étudié dans cette thèse est sans doute le nanofluide le plus largement étudié dans la littérature. Bien que sa conductivité soit relativement faible comparativement à d'autres types de nanoparticules, son faible coût (environ 500\$/kg, soit 2000 fois plus bas que le prix du graphène) et le fait qu'il ne s'oxyde pas par rapport au cuivre expliquent ce succès.

La multitude des paramètres à étudier et la pluridisciplinarité du domaine de recherche font que les résultats de certaines études sur le nanofluide alumine/eau sont parfois contradictoires. Ceci s'explique notamment par la méthode de préparation du nanofluide (achat de solutions déjà prêtes), et surtout par les méthodes de mesure employées. Pour avoir une idée de la taille, de la distribution et de la morphologie des nanoparticules, de nombreuses études font appel à la microscopie électronique à balayage qui ne peut être réalisée qu'en milieu sec et après élimination du fluide ayant servi à la dispersion des particules. Aussi, les techniques permettant d'évaluer les critères de stabilité des suspensions (le potentiel Zeta et la distribution de taille des nanoparticules) ne sont possibles qu'à des niveaux de concentrations volumiques très faibles ($< 0.1\%$); loin des concentrations utilisées dans les systèmes thermiques (jusqu'à 5%). Il n'existe donc pas, à ce jour, de méthode précise pour quantifier la dispersion des nanoparticules. De même, pour mesurer la conductivité thermique des nanofluides, un appareil nommé KD2pro, très sensible aux vibrations

et aux variations des conditions extérieures est largement utilisé, mais malheureusement non adapté aux fluides puisqu'il permet à la convection naturelle de se développer, conduisant ainsi à des mesures erronées.

I-2 Objectifs et originalité

L'objectif principal de cette thèse est donc **l'étude des propriétés thermofluides du nanofluide alumina/eau en se focalisant sur les différents régimes de dispersion possibles et les conditions expérimentales pour les obtenir.**

Les objectifs spécifiques sont les suivants :

- Identifier les conditions expérimentales (pH, type et concentration en tensioactif, paramètres de sonification) pour obtenir la plus grande augmentation de conductivité thermique;
- Développer un protocole expérimental permettant d'identifier les régimes de dispersion de ce nanofluide;
- Comparer les différents nanofluides obtenus à travers un paramètre objectif pertinent, en l'occurrence le nombre de Mouromtseff, afin d'identifier le meilleur nanofluide;
- Étudier le phénomène d'hystérésis pour un nanofluide donné en fonction de la température du mélange et ce pour tous les régimes de dispersion préalablement identifiés.

Trois diamètres moyens des nanoparticules seront considérés : $d=50$, 135 et 200 nm pour des concentrations volumiques allant de $\phi = 0.1$ à 2% . Des mesures simultanées de la viscosité dynamique et de la conductivité thermique de ces nanofluides permettront de caractériser précisément les différents régimes de dispersion, ce qui constitue en partie l'originalité de cette étude. Contrairement à la majorité écrasante des travaux reportés dans la littérature, la conductivité thermique sera évaluée via un dispositif de mesure basé sur la méthode « Transient Hot Wire » adapté aux nanofluides.

I-3 Organisation du mémoire

Ce mémoire de thèse s'articule autour de trois articles scientifiques. Chacun de ces articles rappelle les principales études publiées sur le sujet dans la littérature et décrit les méthodes expérimentales pour caractériser les propriétés des nanofluides.

Le manuscrit est organisé comme suit: le chapitre 2 propose une étude expérimentale sur la préparation et la stabilisation des nanofluides alumine/eau et notamment sur l'influence combinée du pH et du tensioactif et ce pour les trois tailles de nanoparticules énoncées précédemment. Le tensioactif n'ayant qu'un effet mineur pour ce nanofluide précis, le chapitre 3 présente les résultats sur les mesures combinées de conductivité thermique et de viscosité dynamique pour des nanoparticules de diamètre $d=50$ nm en fonction du pH de la solution. Les cinq régimes de dispersion déjà observés dans la littérature sont étudiés en détails pour des concentrations volumiques en nanoparticules allant de $\phi=0.2$ à 2%. Le phénomène d'hystérésis est étudié pour ces deux propriétés en fonction de la température du mélange au chapitre 4 pour $d=50$ nm et $\phi=0.7\%$. Une approche systématique est utilisée pour expliquer les phénomènes physico-chimiques liés à ce phénomène d'hystérésis pour les cinq régimes de dispersion. Le document se termine au chapitre 5 par les principales conclusions et les perspectives de ce travail.

Références:

- [1] Choi, S. U. S. and Eastman, J. A. (1995). Enhancing thermal conductivity of fluids with nanoparticles. In ASME International Mechanical Engineering Congress and Exposition, November 12-17, 1995, San Francisco, CA.
- [2] Maxwell, J. C. (1881). A Treatise on electricity and magnetism, Second Edition. Clarendon, Oxford.

Chapitre II : Conductivité thermique des nanofluides à base d'eau et d'Alumine: revisiter les effets du pH et du tensioactif.

Titre de l'article:

Thermal Conductivity of Al₂O₃/Water-Based Nanofluids: Revisiting the Influences of pH and Surfactant.

Auteurs et affiliations :

¹Nizar Bouguerra : Étudiant au doctorat, Université de Sherbrooke, Faculté de Génie, Département de Génie mécanique.

²Ahmed Khabou: Élève ingénieur, École Nationale d'Ingénieurs de Tunis (ENIT).

³Sébastien Poncet : Professeur agrégé, Université de Sherbrooke, Faculté de Génie, Département de Génie mécanique.

⁴Saïd Elkoun: Professeur, Université de Sherbrooke, Faculté de Génie, Département de Génie mécanique.

Date de soumission : Octobre 2016

Date d'acceptation : Décembre 2016

Statut actuel: Publié

Journal: International Journal of Mechanical,

Aerospace, Industrial, Mechatronic and Manufacturing Engineering.

Vol.10, n°12, p.1849-1858.

II-1 Résumé Français

Cette étude porte sur la préparation et la stabilisation des nanofluides à base d'eau et d' Al_2O_3 . Bien qu'ils aient été largement examinés par le passé, et au meilleur de nos connaissances, il n'y a pas de consensus clair sur la manière appropriée de les préparer et de les stabiliser avec le tensioactif adéquat. Dans cet article, une étude expérimentale minutieusement menée a été effectuée pour quantifier l'influence combinée du pH et du tensioactif sur la stabilité des nanofluides à base d'eau et d'alumine. Deux concentrations volumiques et trois tailles de nanoparticules ont été considérées. La bonne préparation et la stabilité de ces nanofluides sont examinées et évaluées à travers des mesures de la conductivité thermique. Les résultats montrent que la valeur optimale de la conductivité thermique est obtenue principalement en contrôlant le pH du mélange et que les agents tensioactifs ne sont pas nécessaires pour stabiliser la solution.

II-2 Abstract

The present work focuses on the preparation and the stabilization of Al_2O_3 -water based nanofluids. Though they have been widely considered in the past, to the best of our knowledge, there is no clear consensus about a proper way to prepare and stabilize them by the appropriate surfactant. In this paper, a careful experimental investigation is performed to quantify the combined influence of pH and the surfactant on the stability of Al_2O_3 -water based nanofluids. Two volume concentrations of nanoparticles and three nanoparticle sizes have been considered. The good preparation and stability of these nanofluids are evaluated through thermal conductivity measurements. The results show that the optimum value for the thermal conductivity is obtained mainly by controlling the pH of the mixture and surfactants are not necessary to stabilize the solution.

Keywords: Nanofluid, thermal conductivity, pH, transient hot wire, surfactant, Al_2O_3 , stability, dispersion, preparation.

II-3 Introduction

NANOFLUIDS are a new class of fluids with enhanced thermophysical properties, which can be applied in many thermal devices for better performances. A complete, unique and well established definition unfortunately does not exist to date. This can be explained by the fact that the field is very recent and some concepts are not yet entirely understood. However, several definitions can be found in the literature, almost all of them being inspired by the first definition announced by Choi and Eastman [1]. They defined “nanofluids” as innovative heat transfer fluids, which can be designed by suspending nanoparticles into conventional fluids. Thirteen years later, the authors have revisited this definition in a book entitled "Nanofluids, Science and Technology" [2]. This new definition emphasizes the preparation step of nanofluids and the importance of the nanoparticle size. It also clearly emerges dispersion and stabilization as key elements for the good preparation of nanofluids. This definition can be found in [2] and summarized as: “Nanofluids are engineered by suspending nanoparticles with average sizes below *100 nm* in traditional heat transfer fluids such as water, oil, and ethylene glycol. A very small amount of guest nanoparticles, when dispersed uniformly and suspended stably in host fluids, can provide dramatic improvements in the thermal properties of host fluids”.

The Maxwell's theory [3] revealed that an improvement of the thermal conductivity may be obtained by scattering millimeter or micrometer-sized solid particles into a base fluid. However, one major disadvantage related to the use of such large particles is their rapid settling, which may result into a complete separation of the two phases and so causes a decrease of the resulting thermal conductivity. As opposed to milli- or micro-sized suspensions, nanofluids achieved by introducing metallic, non-metallic or polymeric nanoparticles are more stable. Furthermore, nanoparticles benefit from a 10^3 times larger surface/volume ratio than that of microparticles and exhibit then much higher thermal conductivity.

There are numerous researches on the superior heat transfer properties of nanofluids, especially on the thermal conductivity. Choi and Eastman [1], Eastman et al. [4], Liu et al. [5], Hwang et al. [6], Yu et al. [7] and Mints et al. [8] observed an important improvement of the nanofluids' thermal conductivity compared to conventional coolants. Nevertheless, because of the difficulties in preparing comparable nanofluids and adjusting all the preparation parameters and the experimental conditions, the literature results are often contradictory. For example, Buongiorno et al. [9] performed a benchmark study on the thermal conductivity of nanofluids and did not observe anomalously high thermal conductivity enhancement. There is a wide range of techniques to measure the thermal conductivity of liquids, such as the cylindrical cell method, temperature oscillation method, steady-state parallel plate method, 3ω method, thermal constants analyzer method, thermal comparator method, and hot disk method or transient hot-wire (THW) [10, 11]. Some researchers argued that the nonobservation of the anomalous enhancement in some data is due to the inaccuracies of some thermal measurement methods [10, 11]. Indeed, some measurement techniques, initially designed for solids, are not suitable for the measurement of the liquid conductivity which is very affected by natural convection effects. KD2Pro Thermal Property Analyzer manufactured by Decagon Devices, Inc. may be cited as the best example. This instrument is mistakenly recurrently presented as a measurement technique based on the THW method while it is not as reliable. In the benchmark performed by Buongiorno et al. [9], the thermal conductivity tests were based, largely, on this non-accurate device, which may render highly questionable the conclusions drawn in this paper.

The present study is aimed to demonstrate experimentally that, by using appropriate measurement techniques and by optimizing the preparation conditions, it is possible to observe an

increase in the thermal conductivity of nanofluids, much higher than the one predicted by the classical Maxwell's theory [3].

Alumina/water based nanofluid is probably the most studied nanofluids. Such suspensions are mainly created using twostep methods by dispersing Al_2O_3 nanoparticles into base liquids. The stabilization steps involve using the appropriate surfactant, controlling the pH of the solution and dispersing the nanoparticles by mechanical or ultrasound techniques. Several experimental studies [10-13] focused on the Al_2O_3 /water nanofluids and revealed that their properties depend on a large number of parameters such as the size of nanoparticle, their volume fraction, the type and the concentration of the surfactant and the pH of the mixture. Effectively, because of the high surface energy of nanoparticles, it is easy for nanoparticles to coalesce and difficult to disperse them in water. Consequently, controlling the agglomeration of the nanoparticles has become a primary issue.

Huang et al. [14] investigated the dispersion behavior of Al_2O_3 /water based nanofluids. The authors measured the absorbency and zeta potential of the suspensions under different pH values. The results indicated that the stability of nanofluids was highly dependent on the pH values. Xie et al. [15] compared the thermal conductivity of various suspensions containing Al_2O_3 nanoparticles. The pH of the mixture was adjusted at three different values: 4, 7 and 11.5. The highest enhancement observed for 60.4 nm sized particle at a concentration level comprised between 1.8 and 5 vol.% was obtained for a pH equal to 4. Khairul et al. [16] studied the effects of surfactant on the stability and thermo-physical properties of metal oxide nanofluids. They found that the variation of weight concentrations of sodium dodecylbenzene sulfonate (SDBS) has an effect on pH, zeta potential, particle size distribution, viscosity and thermal conductivity of Al_2O_3 /DI-water. Dehkordi et al. [17] measured the dynamic viscosity and thermal conductivity of alumina/water nanofluids with the addition of SDBS. They observed that low concentrations of SDBS have a negligible effect on both the thermal conductivity and viscosity of the suspension, while at higher concentrations (>1 wt.%) SDBS leads to a reduction of the thermal conductivity and an augmentation of the viscosity which undesirably affects the application of SDBS for nanofluids.

Other studies dealing with the effects of surfactant and pH on the properties of alumina/water nanofluids exist, except that these studies focused much more on the stability indicators (zeta potential, absorbency, particle size...) [18-20]. Studies on the optimization of the

thermal conductivity based on two methods of pH control and surfactant addition exist but these works are usually done at low concentrations of nanoparticles or made based on inappropriate measurement techniques [16, 21-25].

The present study aims to investigate the effect of pH control and SDBS dispersant on the thermal conductivity of Al_2O_3 /water nanofluids. The goal is to identify the optimal preparation conditions for these two parameters through direct conductivity measurements at particle concentration levels that are found in applications covered by nanofluids (between 0.2 and 2% vol). Once these parameters are selected, the effects of the particle size and concentration at the optimal conditions of preparation are examined in details.

II-4 Experimental methods

II-4.1 Measurement Technique for the Thermal Conductivity

The thermal conductivity of nanofluids is measured using the THW-L1 Liquid Thermal Conductivity System from Thermtest Thermophysical Instruments (Fig. II-1). It measures the thermal conductivity, denoted k , based on the THW method. Coupled with a system controlling the temperature (heat exchanger + thermostat bath circulator), this device allows a complete characterization of the nanofluid thermal conductivity within the ranges $-40\text{ }^\circ\text{C}$ to $200\text{ }^\circ\text{C}$ and $0.01 \leq k \leq 2\text{ W/(m.K)}$. The THW-L1 allows a direct, accurate and fast measure of the thermal conductivity and diffusivity. The most important advantage of this method for its application to fluids is its capacity to experimentally eliminate the error due to natural convection. The principle of the hot-wire method is based on an ideal and constant heat generation source, an infinitely long and thin continuous line, dissipating the heat into an infinite test medium. A constant current is supplied to the wire (platinum) to generate the temperature rise. The wire serves as both the heat source and the temperature sensor [26]. Heating the wire by Joule effect causes the variation of its resistance, thus its temperature is measured as a function of time using a Wheatstone bridge and a data acquisition system. Finally, the thermal conductivity value is determined from the heating power and the slope of temperature change in a logarithmic time scale. Higher the thermal conductivity of the surrounding liquid is, lower will be the temperature rise of the wire [27]. The THW-L1 sensor has two key components: A thin platinum wire for heating the sample and recording raw data for the determination of the thermal conductivity and a PT100 Platinum resistance thermometer for independently measuring the temperature of the sample. The THW

sensor (including the sample cell) is made of stainless steel. The platinum wire is 0.1 mm in diameter and 35 mm in length. A platinum wire is chosen owing to its capable resistance–temperature relationship over a wide temperature range. Nanofluids containing metal particles are electrically conductive. Teflon spray is then used for the coating of the platinum wire to act as an electric insulation.

The main experimental cell (sample cell) is in fact a part of the Wheatstone bridge circuit for which the resistance of the wire has to be measured. In the bridge, two of the four resistors are the fixed resistors. The third resistance is variable which allows balancing the circuit. The required sample volume is 50 ml. The THW sensor is positioned at the center of the nanofluid sample cell and is placed inside the heat exchanger connected to the thermostat bath circulator to ensure constant temperature test. Water is used as the heating fluid in the bath.



Figure II-1 THW-L1 Liquid Thermal Conductivity System from Thermtest Thermophysical Instruments

II-4.2 Preparation of Alumina-Water Nanofluids

The preparation of nanofluids is the first step towards the characterization of their properties. There are two primary methods to obtain nanofluids: The single-step method (direct evaporation) and the two-step preparation method [12]. In this study, the mixtures are prepared based on the two-step method, which consists in the dispersion of nanoparticles in powder form into the base liquid. Stability is a big issue that is inherently related to this operation as the powders easily aggregate due to strong van der Waals forces between nanoparticles. In spite of such disadvantages, this process is still popular as the most economic process for nanofluid production

at a large scale [28]. In addition, particles in dispersion may adhere together and form aggregates of increasing size which may settle out due to gravity. Stability means that the particles do not aggregate at a significant rate. At this stage of the preparation, it is necessary to act in order to improve the dispersion and stability of suspension by chemical and mechanical ways. The most common methods of dispersion are: Addition of acid or base to modify the pH value of the suspension and consequently to control surface potential; addition of surfactants to prevent particles coming close to each other and the use of ultrasonic agitation.

The alumina nanoparticles used in our experimental protocol were directly purchased from US Research Nanomaterials, Inc, Houston, USA. The major part of our tests were performed with Al_2O_3 nanoparticles (80% alpha: 20%gamma, Purity: 99.9%, Size: 50 nm). In order to examine the effect of particle size on the thermal conductivity of suspensions, other alumina particles were used, their sizes varying from 50 nm to 1 μm . The anionic surfactant SDBS in technical grade, from Sigma-Aldrich Canada Co. (Oakville, Canada), was used for stabilizing the suspension. The pH was controlled using hydrochloric acid (HCl) and sodium hydroxide (NaOH) in analytical grade. The pH of the solution was measured with LabQuest 2 from Vernier (Beaverton, USA). Connected to the pH sensor and the temperature probe, this device offers the possibility to perform the simultaneous measurement of pH and temperature of the mixtures, which allows to obtain pH taking into account the correction due to the test temperature. Q700 Sonicator from Qsonica Sonicators is the ultra-sonicator used for the dispersal of particles in our experiences. This device is capable of delivering 700 watts, with a 20 kHz frequency. It delivers energy in forms of sound waves which can break the clusters. It can work in a continuous way for 72 hours or in an interrupted way. During the preparation of samples, it can be programmed to work in an interrupted way to avoid the overheating of samples. In addition, the preparation is plunged into a jacketed glass beaker, which is connected to a thermostat bath circulator.

II-4.3 Experimental Procedure

The first step in our experimental procedure is the weighing of the nanoparticles. Small and precise masses are measured with an analytical balance ("lab balance" 0.01 mg). This allows to obtain nanofluids with an ultra-precise concentration. In order to properly disperse the nanopowder into the water, nanoparticles must be homogenized in the medium. Since the purity of the nanofluid is important, particular attention has been made to avoid impurity. Particles are mixed directly with

water with no additive. A first homogenization is made using a magnetic stirrer. During this mechanical agitation, depending on the test to be performed, pH adjustments and the addition of surfactant may be carried out. The most effective method of breaking and evenly dispersing the nanopowder in a fluid is through application of ultrasonic vibration. Using this methodology, the water/alumina nanofluid was created and ultrasonic vibration was applied for generally 12 hours with 50% amplitude in an interrupted way (5s ON/2s OFF) for 500 ml of nanofluid. This initial solution of 500 ml was each time divided into samples of 50 ml which were sonicated between 10 min and 30 min for each test.

The next step is to calibrate the THW using a reference solution (Water Deionized Ultrafiltered Water DIUF). The reference exhibits a thermal conductivity equal to 0.6052 W/(m.K) at 20 °C. For that, we begin by turning on the temperature bath with a fixed temperature of 20 °C and by putting the reference in the THW cell. Then, we change the bath's temperature to 25 °C which is the fixed temperature of our experiences. The nanofluid was heated to the desired temperature after sonication. After taking the reading for each sample, the nanofluid was taken out and sonicated well before conducting the experiment for the next sample. During the experimentation, for well stabilized samples, we did not find any agglomeration for the nanofluid tested. For every sample, the glass beakers and the THW cell was well cleaned and dried with compressed air. The above procedure was repeated for different SDBS concentration, pH values, particle sizes and different volume concentrations of alumina nanoparticles.

II-5 Results and Discussions

II-5.1 Effect of SDBS on the Thermal conductivity at an arbitrary pH value

In the first experiment, the surfactant effect without adjusting the pH of the nanofluid is studied. In other words, the thermal conductivity k (W/ (m.K)) of the solution at different SDBS concentrations without fixing the pH is measured. This experiment is conducted using an initial solution of 500 ml of alumina/water nanofluid. Then, it is divided into several samples of 50 ml. The conditions of preparation are mentioned in Table II-1. The results of this experiment are shown in Fig II-2.

Table II-1 : Conditions of the first experience (variation of thermal conductivity and pH with weight fraction of SDBS)

Size of nanoparticles	50 nm
Volume fraction Al_2O_3	2 Vol.%
Weight fraction of SDBS	0 to 0.05 wt.%
Ultrasonication	12 h for 500 ml 10 min for each 50 ml
Temperature	25 °C

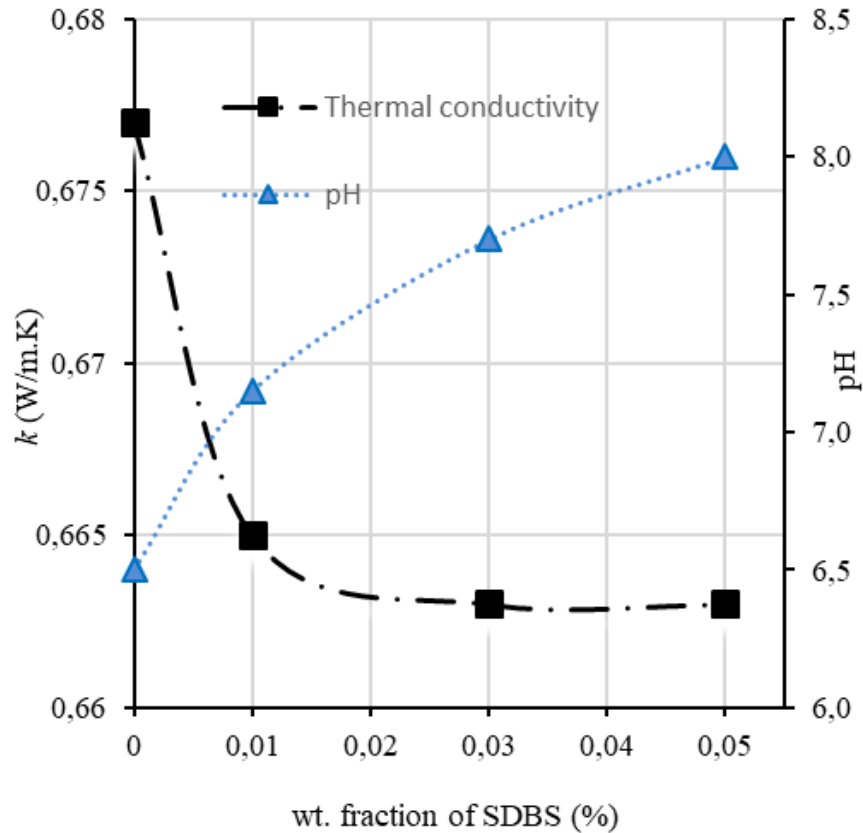


Figure II-2 Variation of the thermal conductivity and pH with weight fraction of SDBS

As seen in Fig. II-2, the addition of SDBS modifies the pH value. Moreover, the conductivity is not improved with the adjusted concentration of SDBS and this is because the pH values are not in the optimal range. The maximum enhancement (compared to distilled water, k (water, 25 °C) = 0.613 W/(m.K)) is attained here when the SDBS is not used (0 wt.%) and it is found to be 10.4% whereas, with the use of SDBS, one obtains an enhancement of around 8%.

The next step is then to identify the optimal range of SDBS concentration by improving the preparation conditions (sonication time). As in the first experience, the pH of the solutions is not adjusted and each sample has its own pH value depending on the quantity of added SDBS. The new preparation conditions as well as the results are presented in Table II-2 and Fig. II-3 respectively.

Tableau II-2 Conditions of the Second Experience (Variation of Thermal Conductivity with Weight Fraction of SDBS without Fixing the pH Value)

Size of nanoparticles	50 nm
Volume fraction Al_2O_3	2 Vol. %
Weight fraction of SDBS	0 to 0.3 wt. %
Ultrasonication	12 h for 500 ml 30 min for each 50ml
Temperature	25 °C

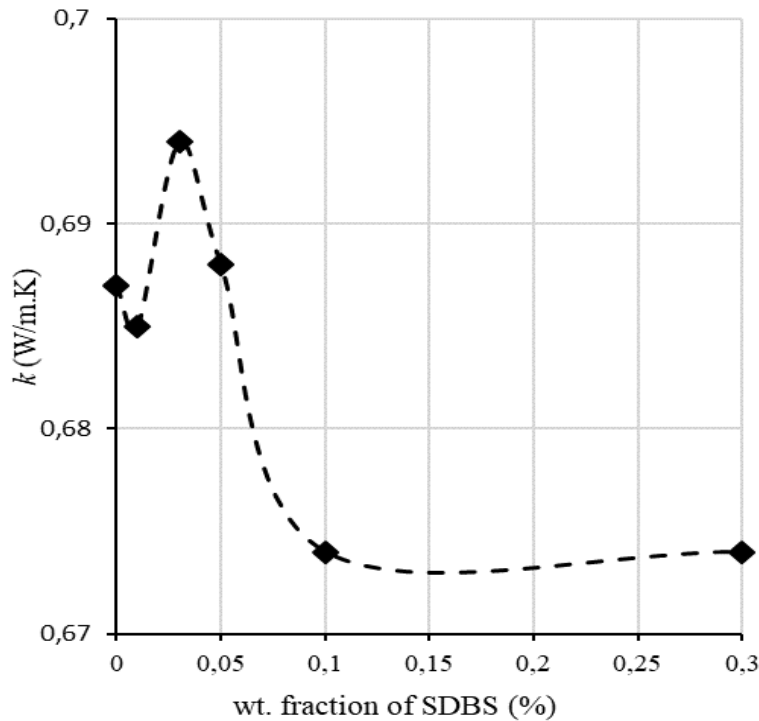


Figure II-3 Variation of the thermal conductivity with weight fraction of SDBS without fixing the pH value

As seen in Fig. II-3, the conductivity reaches its optimal value at 0.03 wt. % of SDBS with an enhancement of 13.2% compared to distilled water (base fluid). In fact, improving the nanofluid

conductivity can be obtained by optimizing the surfactant percentage but it is not necessary that one get an optimal value as the pH is not fixed yet. Thus, combining both effects to determine the optimal percentage of surfactant for a fixed pH value is imperative. Therefore, in order to fix an optimal range of pH values, a study of the pH effect on the thermal conductivity was conducted.

II-5.2 Effect of pH on the Thermal Conductivity

In this series of tests, one aims to isolate the effect of pH on the thermal conductivity k (W/(m.K)). Alumina-water mixtures at the same volume fraction (2 Vol.%) are prepared without addition of surfactant. The pH of solutions is varied from 3.5 to 7.5. For pH values outside this range, visual examination of the stability shows a strong sedimentation which explains the uselessness of presenting them in the conductivity measurements. The conditions of this experiment as well as the results are presented in Table II-3 and Fig. II-4 respectively. This study shows that an increase of the conductivity of more than 15% can be observed when the pH of the solution is between 5.3 and 6.1 and without addition of surfactant, values which are not reached with the use of the SDBS at uncontrolled pH values. Based on these results, a new study of the pH effect on the conductivity is made. The range of pH values from 5.3 to 6.1 is investigated to identify more precisely the optimal pH value (Fig. II-5).

Tableau II-3 *Experimental Conditions (pH Effect)*

Size of nanoparticles	50 nm
Volume fraction Al_2O_3	2 Vol.%
Weight fraction of SDBS	Without addition of surfactant
Ultrasonication	12 h for 500 ml 15 min for each 50ml
Temperature	25 °C

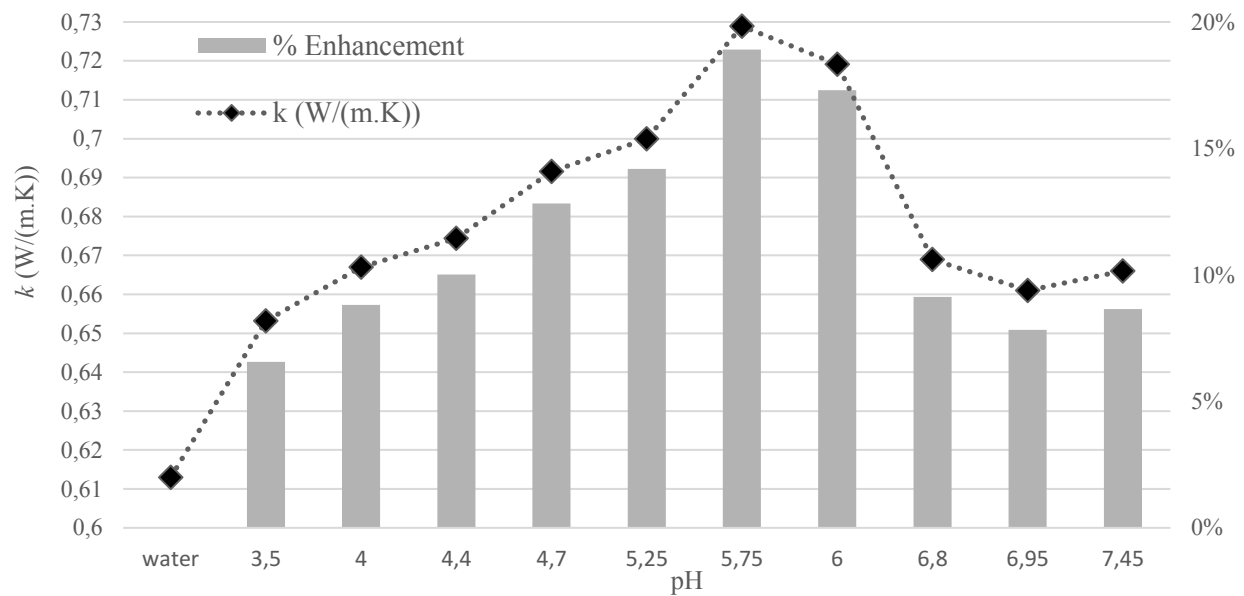


Figure II-4 Thermal conductivity as a function of pH with the enhancement percentage without adding SDBS

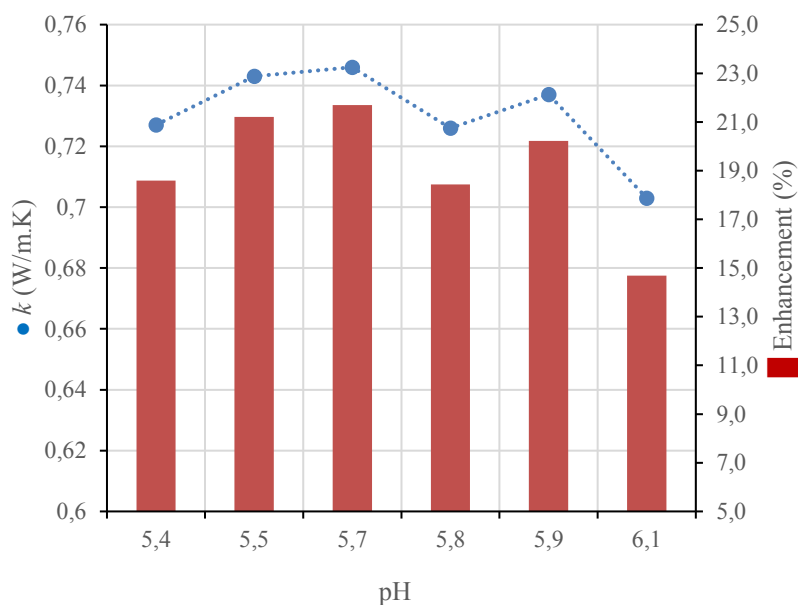


Figure II-5 Thermal conductivity as a function of pH (optimal range)

This study showed that the preparation of nanofluids is strongly dependent on the pH value. As it can be seen on Fig.II-5, the adjustment of the pH causes the improvement of the thermal conductivity. An enhancement of 21% is observed at pH=5.7 (optimal pH). To generalize this result to other particle sizes, the effect of the pH on the thermal conductivity is studied for three different

sizes, namely 50 nm, 135 nm and 200 nm. The experience is conducted without adding SDBS and the concentration of Al_2O_3 nanoparticles in water is fixed to 2 vol%. All conditions are presented in Table II-4, and the test results are illustrated in Fig. II-6 which shows the evolution of the relative improvement in the thermal conductivity of nanofluids compared to the base fluid ($R = k_{nf}/k_{bf}$).

Tableau II-4 Experimental Conditions (pH effect for Different Sizes)

Size of nanoparticles (nm)	50, 135 and 200
Volume fraction Al_2O_3	2 Vol.%
Weight fraction of SDBS	0
Ultrasonication	12 h for 500 ml 25 min for each 50 ml
Temperature	25 °C

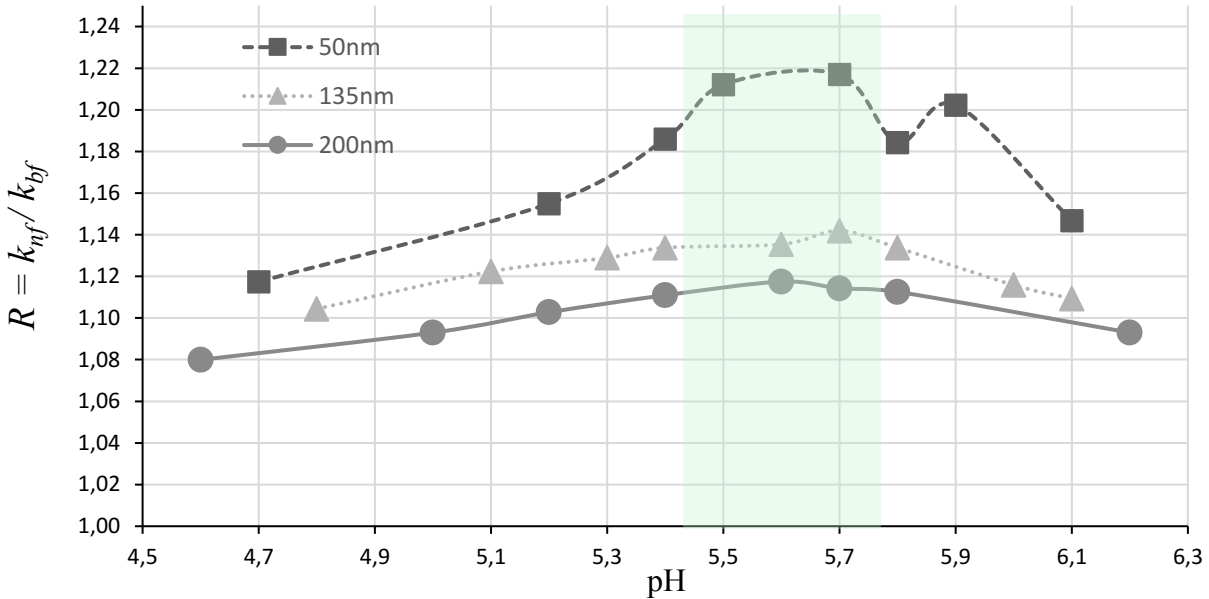


Figure II-6 Thermal conductivity as a function of pH for different nanoparticle sizes

As seen in Fig. II-6, the variation of the thermal conductivity with pH is not linear and an optimal zone between 5.4 and 5.8 may be identified for the three sizes. Thus, an approximation is made and the optimal pH value is fixed to 5.7 for the three sizes for the further experiences.

The maximum enhancements are 21.7%, 14.2% and 11.7% for 50 nm, 135 nm and 200 nm respectively. In the case of 200nm particle size, the conductivity values know a degradation while measuring. This can be explained by the fast sedimentation caused by the large particle size compared to the two other sizes. Fig. II-6 also shows the enhancement of the thermal conductivity

with the size of particles. In fact, when the size becomes larger, the thermal conductivity becomes lower. This result is also proved in Section II-5.4.

II-5.3 Effect of the SDBS Surfactant on the Thermal Conductivity at Adjusted Optimum pH

After fixing an optimal pH, a study of the SDBS effect at that optimal pH value is needed. In order to do that, various 50ml samples from a 500 ml sonicated solution are prepared. After adding the suitable SDBS concentration for each sample, the pH value is readjusted to 5.7. The preparation conditions for this experience as well as the results are presented in Table II-5 and Fig. II-7 respectively.

Tableau II-5 *Experimental Conditions (SDBS Effect at Adjusted Optimum pH)*

Size of nanoparticles	50 nm
Volume fraction Al_2O_3	2 Vol. %
Weight fraction of SDBS	0 to 0.1 wt. %
pH	5.7
Ultrasonication	11 h for 500 ml 15 min for each 50ml
Temperature	25 °C

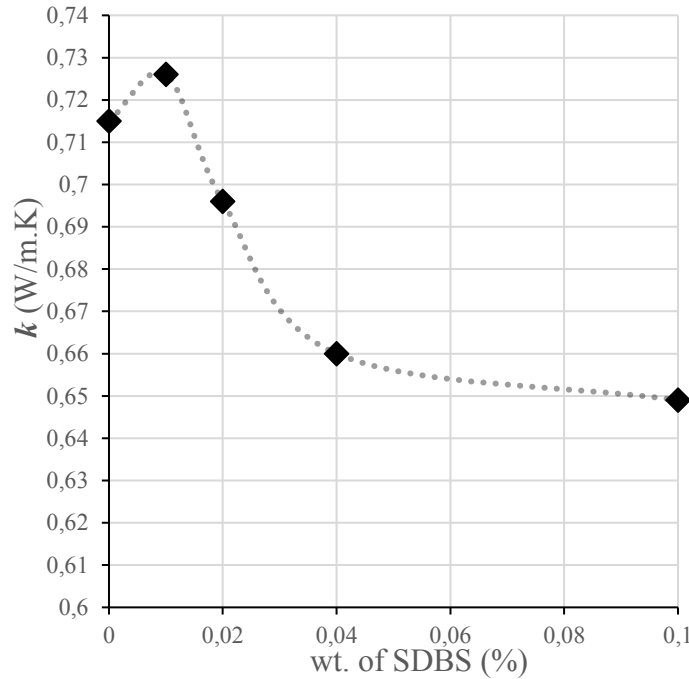


Figure II-7 Variation of the thermal conductivity with the weight fraction of SDBS at fixed optimum pH

Fig. II-7 shows that the thermal conductivity values decrease rapidly in a remarkable way as soon as the SDBS concentration exceeds 0.02 wt.% and a peak is observed at 0.01 wt.%. Thus, we decided to explore better the range of values between 0 and 0.04 wt.%. To make sure that the range of concentrations from 0.04 wt.% SDBS is not suitable, a verification through the sedimentation method is made. This test allows us to study the stability of suspensions with a fixed SDBS concentrations and a variable pH. An example of these visual inspections is illustrated by Figs. II-8 and II-9 in which the SDBS concentration is fixed at 0.1 wt.% and pH at a random value for each sample. For this SDBS concentration (0.1 wt.%), it can be noticed that for any pH value a strong sedimentation occurs. In addition, the conductivity measurement at pH=5.7 gives a value clearly lower than that without SDBS: k (0.1 wt.% SDBS, pH=5.7)=0.649 W/(m.K) while k (0 wt.% SDBS, pH 5.7)=0.741 W/(m.K). The percentage of SDBS is downgraded by browsing the concentration range between 0.04 wt.% and 0.1 wt.%, which leads to a slight improvement in conductivity compared to 0.1% but still has strong signs of sedimentation and a conductivity value well below to that without surfactant: k (SDBS 0.04 wt.%, pH=5.7)=0.661 W/(m.K). These surfactant concentration levels are detrimental to the dispersion and the stability of the mixtures. Visual examinations of the agglomeration and sedimentation of these mixtures at these surfactant

concentration levels substantially lead to the same conclusion than that relating to the SDBS concentration 0.1 wt.%. It is only by being at SDBS concentrations of 0.03 wt.% or less that the stability of the suspensions is improved. This finding is proved by the sedimentation method (see Figures. II-10 and II-11).



Figure II-8 Samples at different pH values from 4 to 7.5, at 0.1 wt.% SDBS



Figure II-9 Samples at 0.1 wt.% SDBS and different pH values, from left to right: pH=8 - 9.3 - 10 - 10.7 - 11.4 - 2 - 2.6 - 3



Figure II-10 Samples at 0.01 wt.% SDBS and different pH values, from left to right: pH=7.2 - 6.9 - 6.5 - 6.3 - 5.9 - 5.6 - 5.3 - 5 - 4.8 - 4.5 - 4.2 - 4



Figure II-11 Samples at 0.015 wt.% SDBS and different pH values, from left to right: pH=6.4 - 6.6 - 7.1 - 6 - 5.8 - 5.6 - 5.4 - 5.2 - 4.9 - 4.5 - 3.9

As it can be noticed, the stability of mixtures with SDBS concentrations less than 0.03 wt.% improves when the value of the pH is around 5.7. Quantification of the effect of the surfactant concentration at this level (< 0.03 wt.%) at an optimum pH (5.7) on the thermal conductivity is then necessary. In order to achieve that, another experience is conducted and the time of sonication for each sample is increased for better stability. Measurements of the thermal conductivity are realized by fixing the pH to 5.7 and by varying finely the percentage of SDBS from 0 to 0.03% wt. The preparation conditions for this experience as well as the results are presented in Table II-6 and Fig. II-12 respectively.

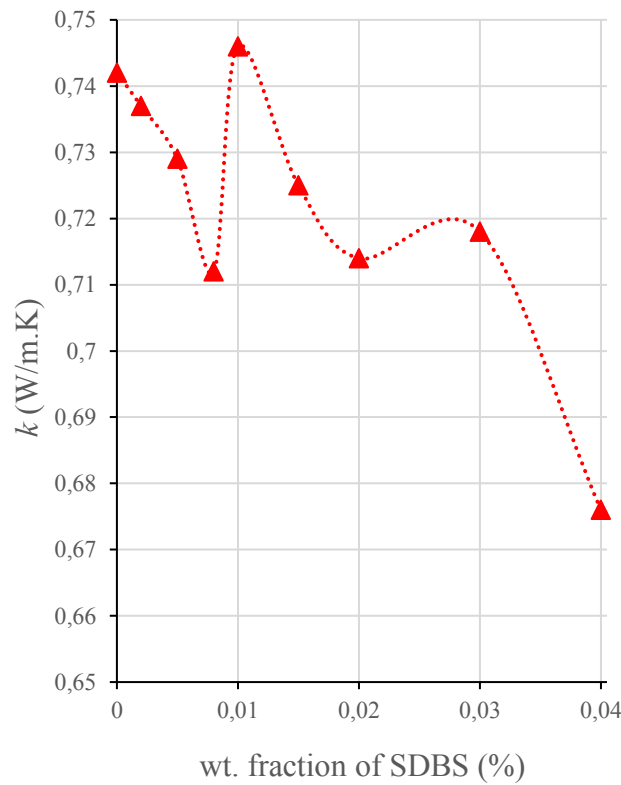


Figure II-12 Variation of the thermal conductivity with the weight fraction of SDBS at optimum pH

As seen in Fig. II-12, the optimal percentage of SDBS should not exceed 0.03 wt.%. Besides, the addition of SDBS when the pH is optimized does not imperatively enhance the thermal conductivity as for some SDBS concentrations, lower conductivity values are observed compared to that of optimized pH without SDBS. In fact, the evolution of the conductivity as a function of the SDBS concentration is not linear and exhibits a peak at 0.01 wt.%. This value is noticed as the optimal one with an enhancement of 21.7% compared to pure water (base fluid).

Tableau II-6 *Experimental Conditions (SDBS Effect – Optimum Range)*

Size of nanoparticles	50 nm
Volume fraction Al ₂ O ₃	2 Vol. %
Weight fraction of SDBS	0 to 0.03 wt. %
pH	5.7
Ultrasonication	12 h for 500 ml 30 min for each 50ml
Temperature	25 °C

II-5.4 Effect of the Nanoparticle Size on the Thermal Conductivity

To study the effect of the nanoparticle size on the thermal conductivity, two experiments are conducted at two different concentrations i.e. 1 vol.% and 2 vol.%. These experiences are then compared to the Maxwell's model [3] for each concentration. The preparation conditions for this experience as well as the results are presented in Table II-7 and Fig. II-13 respectively.

Tableau II-7 *Experimental Conditions (Size Effect)*

Size of nanoparticles (nm)	50 – 135 - 200 - 300 - 500 and 1000
Volume fraction Al ₂ O ₃	1 and 2 Vol. %
Weight fraction of SDBS	0
pH	5.7
Ultrasonication	12h for 500ml 30 min for each 50ml
Temperature	25 °C

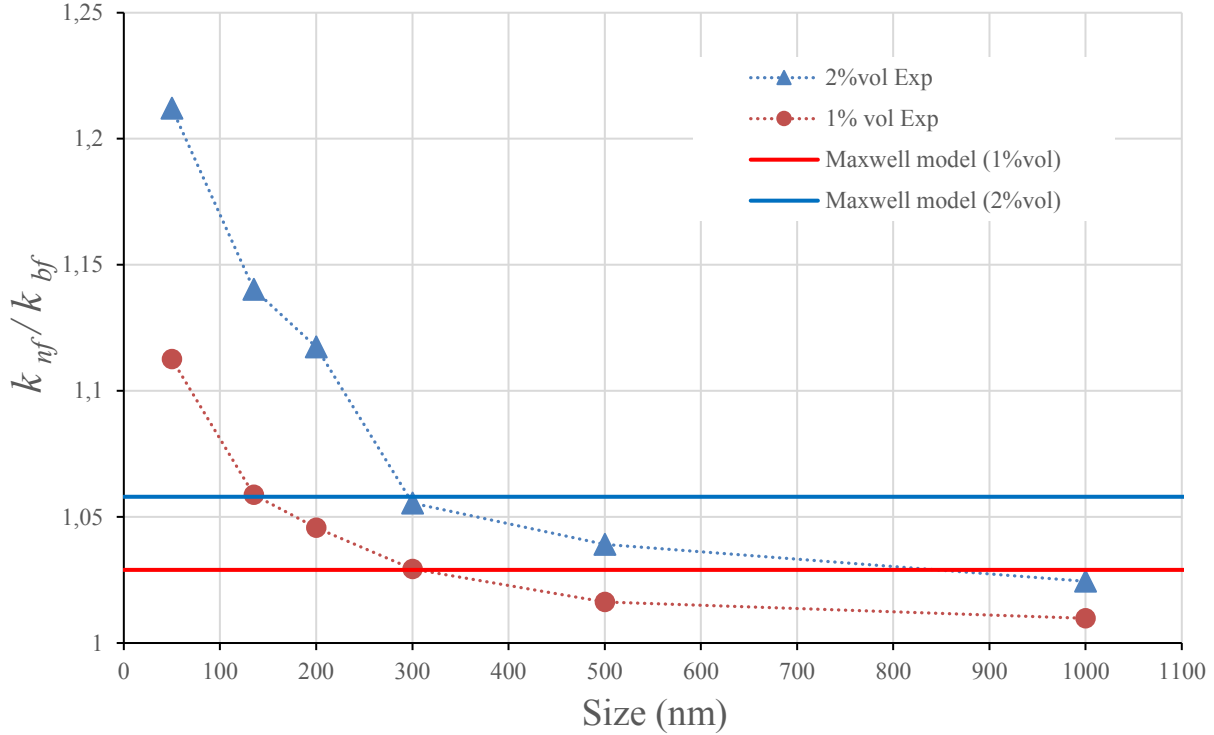


Figure II-13 Variation of the thermal conductivity ratio with the size of nanoparticles

As it can be seen in Fig. II-13, the thermal conductivity ratio decreases with the increase of the particle size for both concentrations of Al_2O_3 . Comparing the experimental results with the Maxwell's model [3], one can see that when the size of the nanoparticles becomes small (below 300 nm), there is a strong improvement of the thermal conductivity values. However, the Maxwell model gives almost a constant improvement for different sizes. Thus, one can conclude that this classical model is not valid for nanoparticles.

Fig. II-13 demonstrates that, by using the appropriate size and by optimizing the suspension stability, it is possible to observe an increase in the thermal conductivity of nanofluids, which do not follow the classical Maxwell's theory [3].

II-5.5 Effect of Nanoparticle Concentration on Thermal Conductivity

The last experiment of the present study investigates the effect of the nanoparticle concentration on the thermal conductivity. It is conducted using different volume fractions of Al_2O_3 as mentioned in Table II-8. Fig. II-14 shows the results of this experiment.

Tableau II-8 *Experimental Conditions (Concentration Effect)*

Diameter of nanoparticles (nm)	50
Volume fraction of Al ₂ O ₃	0.25 – 0.5 – 0.75 - 1 and 2 Vol. %
Weight fraction of SDBS	0
pH	5.7
Ultrasonication	12 h for 500 ml 20 min for each 50ml
Temperature	25 °C

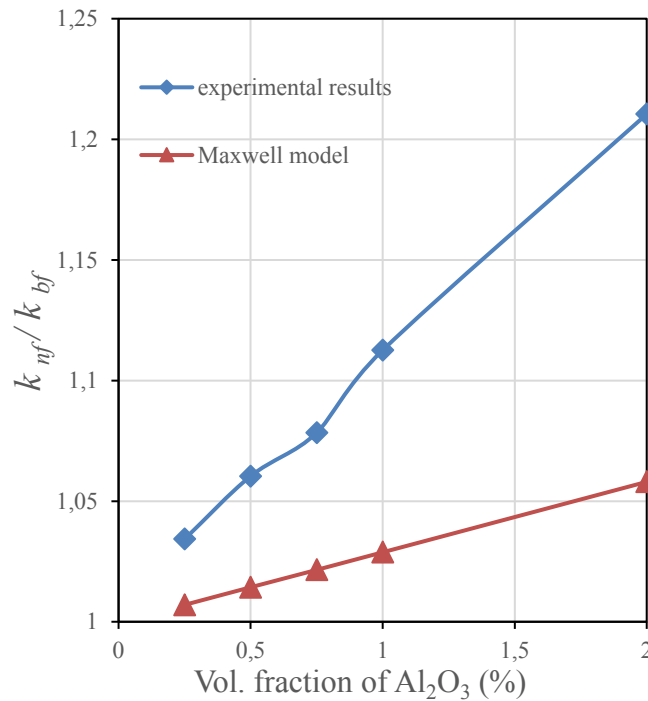


Figure II-14 *Evolution of the thermal conductivity ratio with the volume fraction of Al₂O₃*

As seen in Fig. II-14, when the concentration of nanoparticles increases, the ratio of the thermal conductivity also increases. An enhancement of 21% is observed for a 2% concentration. Compared to the Maxwell model [3], which uses microparticles, one can see that there is a strong improvement using nanoparticles. This allows us to validate once again the utility of nanofluids comparing to micro- or milli-sized ones.

II-6 Conclusion

In this paper, the thermal conductivity enhancement of Al₂O₃-water nanofluids was investigated under different pH values and different SDBS dispersant concentrations. The effect of

these two parameters was identified by direct measurements of the conductivity based on the THW method. The stability of nanofluids has a direct influence on the thermal conductivity. Better preparation conditions lead to the higher thermal conductivity of nanofluids. The optimization of the pH value and SDBS concentration can result in the highest thermal conductivity of the nanofluids. Hence, the isolated and combined adjustment with both the pH and surfactant concentration was found to increase the thermal conductivity of nanofluids. Improving nanofluids can be done by optimizing different parameters such as pH value and SDBS concentration, but also by changing the particle size and particle concentration in the base fluid. Therefore, after identifying the optimal preparation conditions, both effects of size and particle concentration on the thermal conductivity were examined.

The major challenge of this work was the stability of nanofluids, as the suspension tries always to agglomerate. As well as fixing an optimal protocol to conduct the different experiments. By establishing an experimental protocol allowing the control of the parameters and the separation of their effects, the impact of each factor was studied and the different outcomes are presented in the following:

- Adding SDBS surfactant causes the variation of pH as well as the thermal conductivity. Moreover, the conductivity cannot be well improved by adjusting the SDBS concentration when the pH value is not in the optimal range.
- Adding surfactant does not necessarily enhance the thermal conductivity and in some cases, a degradation of the thermal conductivity is observed using surfactant.
- pH is the key parameter for stabilizing nanofluids. The variation of the thermal conductivity with the pH is not linear and the optimal value ranges for the three particle sizes i.e. 50, 135 and 200 nm between 5.4 and 5.8. For these values and without addition of surfactant, an increase of the conductivity of more than 20% can be observed with 50 nm/2 Vol.% mixtures. This level of enhancement was not reached with the use of the SDBS at random pH values.
- The optimal SDBS concentration for 50 nm size was found to be 0.01 wt.% with a fixed pH at 5.7.
- The maximum enhancements of the thermal conductivity are 21.7%, 14.2% and 11.7% for 50 nm, 135 nm and 200 nm respectively for a fixed nanoparticle concentration of 2 vol.%.
- Thermal conductivity improves decreasing the size of particles.

- Thermal conductivity improves when the particle concentration in the base fluid increases and the maximum enhancement for 50 nm size is found to be 21.7% at 2 vol%.

Finally, one can conclude that by using appropriate measurement techniques and by optimizing the preparation conditions, it is possible to observe an increase in the thermal conductivity of nanofluids, much higher than the one predicted by the classical Maxwell's theory [3].

Acknowledgments

Mitacs is gratefully acknowledged for its financial support through the acceleration grant of N. Bouguerra and the Globalink program for A. Khabou. The authors would like to thank also the Sigma Energy Storage Company for its financial support and Cyril Soccodato for his involvement in preliminary tests.

II-7 References

- [1] Choi S. U. S. and Eastman J.A. (1995), Enhancing thermal conductivity of fluids with nanoparticles, In ASME International Mechanical Engineering Congress and Exposition, November 12-17, 1995, San Francisco, CA.
- [2] S. K. Das, S. U. S. Choi, W. Yu, and T. Pradeep, *Nanofluids: Science and Technology*, Wiley, 2008.
- [3] J. C. Maxwell, *A Treatise on Electricity and Magnetism*, 2 edition, vol.1, Clarendon Press, Oxford, 1881.
- [4] J.A. Eastman, S.U.S. Choi, L. J. Thompson, and S. Lee, "Enhanced Thermal Conductivity Through the Development of Nanofluids," in *Mater. Res. Soc. Symp. Proc.*, Boston, vol. 457, p.3-11, 1996.
- [5] M.-S. Liu, M. C.-C. Lin, I.-T. Huang, and C.-C. Wang, "Enhancement of Thermal Conductivity with CuO for Nanofluids," *Chem. Eng. Technol.*, vol. 29, no. 1, pp. 72–77, 2006.
- [6] Y. Hwang, H. S. Park, J. K. Lee, and W. H. Jung, "Thermal conductivity and lubrication characteristics of nanofluids," *Curr. Appl. Phys.*, vol. 6, pp. e67–e71, 2006.
- [7] W. Yu, H. Xie, L. Chen, and Y. Li, "Investigation of thermal conductivity and viscosity of ethylene glycol based ZnO nanofluid," *Thermochim. Acta*, vol. 491, no. 1, pp. 92–96, 2009.
- [8] H. A. Mints, G. Roy, C. T. Nguyen, and D. Doucet, "New temperature dependent thermal conductivity data for water-based nanofluids," *Int. J. Therm. Sci.*, vol. 48, no. 2, pp. 363–371, 2009.
- [9] J. Buongiorno, D. C. Venerus, and T. McKrell, "A benchmark study on the thermal conductivity of nanofluids," *J. Appl. Phys.*, vol. 106, no. 9, pp. 94312-1-94312–14, 2009.
- [10] J. Huang, X. Wang, Q. Long, X. Wen, Y. Zhou, and L. Li, "Influence of pH on the Stability Characteristics of Nanofluids," in *2009 Symposium on Photonics and Optoelectronics*, Wuhan, 2009, pp. 1–4.

- [11] H. Xie, J. Wang, T. Xi, Y. Liu, F. Ai, and Q. Wu, "Thermal conductivity enhancement of suspensions containing nanosized alumina particles," *J. Appl. Phys.*, vol. 91, no. 7, pp. 4568-4572, 2002.
- [12] M. A. Khairul, K. Shah, E. Doroodchi, R. Azizian, and B. Moghtaderi, "Effects of surfactant on stability and thermo-physical properties of metal oxide nanofluids," *Int. J. Heat Mass Transf.*, vol. 98, pp. 778–787, 2016.
- [13] B. Lotfizadeh Dehkordi, S. N. Kazi, M. Hamdi, A. Ghadimi, E. Sadeghinezhad, and H. S. C. Metselaar, "Investigation of viscosity and thermal conductivity of alumina nanofluids with addition of SDBS," *Heat Mass Transf.*, vol. 49, no. 8, pp. 1109–1115, 2013.
- [14] L. Godson, D. M. Lal, and S. Wongwises, "Measurement of Thermo Physical Properties of Metallic Nanofluids for High Temperature Applications," *Nanoscale Microscale Thermophys. Eng.*, vol. 14, no. 3, pp. 152–173, 2010.
- [15] H. Xie, H. Gu, M. Fujii, and X. Zhang, "Short hot wire technique for measuring thermal conductivity and thermal diffusivity of various materials," *Meas. Sci. Technol.*, vol. 17, no. 1, pp. 208–214, 2006.
- [16] V. Sridhara and L. N. Satapathy, "Al₂O₃-based nanofluids: a review," *Nanoscale Res. Lett.*, vol. 6, no. 1, p. 456, 2011.
- [17] S. Mukherjee and S. Paria, "Preparation and Stability of Nanofluids-A Review," *IOSR J. Mech. Civ. Eng.*, vol. 9, no. 2, pp. 63–69, 2013.
- [18] M. F. Zawrah, R. M. Khatib, L. G. Girgis, H. El Daidamony, and R. E. Abdel Aziz, "Stability and electrical conductivity of water-base Al₂O₃ nanofluids for different applications," *HBRC J.*, 2015.
- [19] T. Mori, I. Inamine, R. Wada, T. Hida, T. Kiguchi, H. Satone, and J. Tsubaki, "Effects of particle concentration and additive amount of dispersant on adsorption behavior of dispersant to alumina particles," *J. Ceram. Soc. Japan*, vol. 1178, pp. 917–921, 2009.
- [20] L. J. Felicia, J. C. Johnson, and J. Philip, "Effect of Surfactant on the Size, Zeta Potential and Rheology of Alumina Nanofluids," *J. Nanofluids*, vol. 3, no. 4, pp. 328–335, 2014.
- [21] W. Xian-Ju and X.-F. Li, "Influence of pH on Nanofluids' Viscosity and Thermal Conductivity," *Chin. Phys. Lett.*, vol. 26, no. 5, pp. 56601-1-4, 2009.

- [22] R. Sadeghi, S. G. Etemad, E. Keshavarzi, and M. Haghshenasfard, "Investigation of alumina nanofluid stability by UV-vis spectrum," *Microfluid. Nanofluidics*, vol. 18, no. 5–6, pp. 1023–1030, 2015.
- [23] E. V. Timofeeva, A. N. Gavrilov, J. M. McCloskey, Y. V. Tolmachev, S. Sprunt, L. M. Lopatina, and J. V. Selinger, "Thermal conductivity and particle agglomeration in alumina nanofluids: Experiment and theory," *Phys. Rev. E*, vol. 76, no. 6, Article ID 1203, 2007.
- [24] X. Wang, X. Li, and S. Yang, "Influence of pH and SDBS on the Stability and Thermal Conductivity of Nanofluids," *Energy & Fuels*, vol. 23, no. 5, pp. 2684–2689, May 2009.
- [25] G. Xia, H. Jiang, R. Liu, and Y. Zhai, "Effects of surfactant on the stability and thermal conductivity of Al_2O_3 /de-ionized water nanofluids," *Int. J. Therm. Sci.*, vol. 84, pp. 118–124, 2014.
- [26] L. Godson, D. M. Lal, and S. Wongwises, "Measurement of Thermo Physical Properties of Metallic Nanofluids for High Temperature Applications," *Nanoscale Microscale Thermophys. Eng.*, vol. 14, no. 3, pp. 152–173, 2010.
- [27] H. Xie, H. Gu, M. Fujii, and X. Zhang, "Short hot wire technique for measuring thermal conductivity and thermal diffusivity of various materials," *Meas. Sci. Technol.*, vol. 17, no. 1, pp. 208–214, 2006.
- [28] S. Mukherjee and S. Paria, "Preparation and Stability of Nanofluids-A Review," *IOSR J. Mech. Civ. Eng.*, vol. 9, no. 2, pp. 63–69, 2013.

Chapitre III Régimes de dispersion des nanofluides à base d'eau et d'alumine : mesures simultanées de la conductivité thermique et de la viscosité dynamique.

Titre de l'article:

Dispersion regimes in alumina/water-based nanofluids: Simultaneous measurements of thermal conductivity and dynamic viscosity

Auteurs et affiliations :

¹Nizar Bouguerra : Étudiant au doctorat, Université de Sherbrooke, Faculté de Génie, Département de Génie mécanique.

²Sébastien Poncet : Professeur agrégé, Université de Sherbrooke, Faculté de Génie, Département de Génie mécanique.

³Saïd Elkoun: Professeur, Université de Sherbrooke, Faculté de Génie, Département de Génie mécanique.

Date de soumission : Décembre 2017

Date d'acceptation : Février 2018

Statut actuel: Publié

Journal: International Communications in Heat and Mass Transfer.

Vol. 92, p.51-55

III-1 Résumé français

Cette étude présente une analyse expérimentale détaillée des régimes de dispersion dans les nanofluides. Dans cette optique, des mesures simultanées de la conductivité thermique et de la viscosité dynamique ont été effectuées sur des nanofluides à base d'eau et d'alumine à des concentrations volumiques φ allant de 0.2 à 2%. Selon les valeurs du pH, cinq régimes de dispersion ont été identifiés pour les valeurs intermédiaires de φ . Le régime bien dispersé caractérisé par un maximum local de la conductivité thermique et un minimum absolu de la viscosité dynamique n'est pas observé pour $\varphi = 2\%$, tandis que le régime d'agglomération en chaîne n'est pas présent quand $\varphi = 0.2\%$. Les résultats sont corroborés par la distribution du nombre de Mouromtseff, qui apparaît comme un paramètre fiable permettant d'identifier les nanofluides les plus efficaces. Pour un nanofluide optimisé, une efficacité comparable peut être obtenue même à faible concentration $\varphi = 0.2\%$.

III-2 Abstract

The present work proposes a detailed experimental analysis of the dispersion regimes within nanofluids. For this purpose, simultaneous measurements of thermal conductivity and dynamic viscosity are performed for alumina/water-based nanofluids at volumetric concentrations ϕ ranging from 0.2 to 2%. Depending on the pH values, five dispersion regimes have been identified for intermediate values of ϕ . The well-dispersed regime characterized by a local maximum of the thermal conductivity and an absolute minimum of the dynamic viscosity is not recovered for $\phi=2\%$, while the chain-like agglomeration regime is not observed for $\phi=0.2\%$. The results are corroborated by the distribution of the Mouromtseff number, which appears as a reliable parameter to identify the most efficient nanofluids. For an optimized nanofluid, comparable efficiency may be achieved even at low concentration $\phi=0.2\%$.

Keywords: Alumina/water-based nanofluids, Dispersion regimes, Thermal conductivity, Dynamic viscosity, Chain-like aggregation.

III-3 Introduction

Nanofluids (Nfs) are innovative heat transfer fluids with improved thermophysical properties obtained by suspending nanoparticles (Nps) into conventional fluids. A complete, unique and well-grounded definition regrettably does not exist to date. This may be due to the fact that the field is relatively new and some concepts, especially heat transfer enhancement mechanisms, are not yet fully understood. Nevertheless, numerous definitions can be found, most of them derive from the first definition proposed by Choi and Eastman [1] and enriched in a revisited version [2] in which the authors emerge dispersion as key element. Due to their small size (< 100 nm), nanoparticles benefit from a large surface/volume ratio (S/V) allowing them to provide much higher thermal conductivity (k) than that predicted by the classical theories [1, 3-7]. However, due to the challenges associated with the preparation of similar nanofluids, the literature results are often contradictory. As an example, Buongiorno et al. [8] proposed an experimental benchmark on the thermal conductivity of various nanofluids. The authors did not observe noticeable enhancement due to the inaccuracy of some measurement techniques [9, 10]. Actually, some methods, originally designed for solid thermal conductivity measurements, are indeed not appropriate for liquids, being very affected by natural convection. The KD2Pro Thermal Property Analyzer is the most significant example. This apparatus is erroneously frequently presented as a measuring system based on the transient hot-wire (THW) method while it is not as reliable.

Studies are constantly carried out to better understand the underlying mechanisms responsible for the improved thermal conductivity of nanofluids [11-15]. The lack of adequate experimental methods allowing to correlate the macroscopic effects to the nanoscale behavior of the particles makes this task hard. In fact, most of the works are based on theoretical models and when experiments exist, they focus much more on the stability indicators (zeta potential, absorbency, particle size ...) (see in [16-18]). Unfortunately, these techniques based mainly on the light scattering method are only suitable for very low particle concentrations far from the concentrations used in real applications. It remains a challenge and a subject of intense debate to identify clearly the heat transfer mechanisms in nanofluids [19]: higher specific surface area of nanoparticles, dispersion and electric charge, Brownian motion, interfacial nanolayer, collision between particles and linear nanoclusters like chains that can produce thermal bridges within the nanofluid. On the contrary, the scientific community agrees that nanoparticle aggregation plays a

significant role in thermal transport [18]. Clustering is a complex process that depends on the properties of the host fluid and the surface energy of the particles. The electric charges in the solution govern the level of aggregation and consequently the configuration of the particles within the base fluid which can lead to different dispersion regimes, namely: well dispersed (WD), weakly attracted (WA), chain-like agglomeration (CL Agg.), partially agglomerated (P Agg.) and fully agglomerated (F Agg.) [19]. Each of the possible mechanisms behind thermal conductivity enhancement may be either accentuated or attenuated by these different dispersion regimes. Controlling the agglomeration becomes then crucial for understanding the physics of nanofluids. Especially, always more studies report that an optimum level of agglomeration may achieve a maximum k enhancement by nanoclustering effect and that excessive particle clustering is unfavorable [18]. Many observations from scanning electron microscopy (SEM) show the presence of chain-like aggregation [20-22]. Nevertheless, this technique cannot evaluate clustering in real suspensions since it requires drying the base fluid.

Adding nanoparticles affect the other properties of the base fluid, particularly the dynamic viscosity (μ) [23]. Most of experimental studies deal with the thermal conductivity of colloids and few works examine their viscosity, and when they exist, these data are rarely coupled. The nanofluid viscosity is also very sensitive to agglomeration. Clustering has indeed an effect on the organization of the nanoparticles, by changing their average starting sizes, the particle size distribution, their shape and aspect ratio. As for k , each of these parameters has a direct influence on μ [24]. As an example, Bhanushali et al. [25] investigated the effect of particle shape on the properties of nanofluids using a range of distinct filler particle shapes. They concluded that higher aspect ratio favors the thermal conductivity and is detrimental for the viscosity. Simultaneous measurements of k and μ could then inform us about the state of dispersion and bring response elements on the heat transport mechanisms in nanofluids, which is the main objective of the present paper. Such experimental data, made simultaneously on the same sample with accurate equipments, can also be exploited to establish trustworthy global energy performance criteria allowing to select the proper nanofluids for use in energy systems.

III-4 Experimental methods

The two-step method has demonstrated to be suitable to prepare oxide Nfs [2]. Alumina/water-based Nfs have been selected here for their experimental flexibility unlike metallic

Nfs which must absolutely be prepared with the one-step method. The Al_2O_3 nanoparticles are purchased from US Research Nanomaterials and exhibit the following properties: purity of 99.9%, averaged diameter of 50 nm.

Water-based nanofluids allow a direct control on the degree of interaction between nanoparticles by regulating the pH. The preparation step requires indeed to use the appropriate surfactant, to control the pH of the solution and to disperse the Nps by ultrasound techniques. In a former study [26], a careful experimental investigation on the stability of Al_2O_3 -water based nanofluids has identified the pH as a key parameter for dispersing and stabilizing suspensions. The pH is controlled here using hydrochloric acid (HCl) and sodium hydroxide (NaOH) in analytical grade. Being temperature dependent, it is measured with LabQuest 2 from Vernier (Beaverton, USA) coupled to a temperature probe. One will mainly focus, in the following section, on the optimal pH range [4.5–6.5] identified by Bouguerra et al. [26]. The pH of the mother solution is set to 5.5 and pH is later adjusted to the desired value during the primary magnetic stirring.

The thermal conductivity of suspensions is measured with the THWL1 Liquid Thermal Conductivity System from Thermtest Instruments. This device offers an accurate and fast measure avoiding the error due to natural convection. The measuring cell is integrated into a system controlling the temperature with an accuracy of 0.1 °C (heat exchanger+ thermostat bath circulator). The principle, description and advantage of THW-method are detailed in [26]. Before each series of measurements, calibration and validation steps have been performed using distilled water and glycerin test fluids. The repeatability and the uncertainty of the measurements remain better than 0.5%.

The rheological properties of nanofluids are performed on a stress controlled rheometer (TA HR-2) using a DIN coaxial cylinder geometry. A Peltier cylinder regulates temperature with an accuracy of 0.1 °C. For low viscosity fluids, the rheometer may have a maximum beyond which it is no longer able to measure the angular velocity accurately. Then, one first delimits the validity range of the shear rate ($\dot{\gamma}$) relative to the present gap (5917.1 μm) by carrying out preliminary experiments on distilled water. The results compare very well with the literature values (uncertainty<3%, repeatability<0.5%). During the experiments on nanofluids, ones evaluate μ of all samples as a function of $\dot{\gamma}$. Whatever the operating conditions, the present nanofluids exhibit a Newtonian behavior over the range [0.01–100] s^{-1} .

As explained above, we present an experimental approach including a careful preparation step and the most appropriate measurement techniques for alumina/water based nanofluids. Particular attention is paid to the synchronization of the thermal and rheological tests. The first step in the experimental procedure is the weighing of the nanoparticles. Colloids with an ultra-precise concentration are prepared by homogenizing particles in water using a magnetic stirrer. The effective dispersion is achieved out by applying ultrasonic vibrations. Using this method, an initial solution of 800 ml of nanofluid is sonicated for 12 h. Mahbubul et al. [27] showed that the sonification time has no longer influence on the viscosity of alumina/water-based nanofluids for temperatures between 10 °C and 50 °C after 2 h. The required samples volumes for THW and rheological measurements are 45 ml and 25 ml, respectively. Therefore, the initial solution is divided into samples of 80 ml, the pH of each sample is adjusted to the desired value and a sonication of 15 mn is carried out before each test. The homogenization of the samples is performed with the Q700-Sonicator (Qsonica), while the initial solution is sonicated using the UIP1000hdT (1000 W, Hielscher Ultrasonics) which is more suited for large volumes. The next step is the calibration of the measuring instruments and the setting of the test temperature (25 °C). Once the test cell of each device is filled, simultaneous measurements of k and μ from the same sample can begin. The above procedure is repeated for different pH values and volume concentrations of nanoparticles (vol%). Temperature is fixed to 25°C for all measurements and controlled by incorporating a jacketed glass beaker connected to a thermostat bath circulator at all stages of preparation.

III-5 Results and discussion

Figures. III-1 to III-4 show the effective thermal conductivity (k_{nf}/k_{bf}) and dynamic viscosity (μ_{nf}/μ_{bf}) of the nanofluids as a function of pH for different volume percent concentration (from 0.2% to 2%). Here, k_{nf} and μ_{nf} are the thermal conductivity and dynamic viscosity, respectively, of the nanofluid whereas k_{bf} and μ_{bf} are that of the base fluid. Examination of the results represented by all of these measuring points makes it possible to correlate the consequences of the agglomeration on k and μ .

Indeed, changes in the thermal and rheological behaviors occur simultaneously in the same pH ranges. This can be explained by the structural modifications and the variation of the nanoparticle's arrangement in the base fluid. The pH of the solutions affects the surface charge of

the particles, which cause their repulsion or attraction, resulting in many states of colloidal dispersion. A high surface charge results in well-dispersed particles, while a fully developed agglomeration occurs when the surface charges vanish (point of zero charge). Between these two limit states, different levels of charge can lead to other dispersions regimes. The WD regime is characterized by the smallest particle size, which results in a decrease of μ and is accompanied by an increase in k . An inverse variation of these two quantities is observed during the F.Agg. regime, which leads to a larger particle size. Consequently, the combined analysis of k and μ curves can provide reliable information on the dispersion state.

Given the opposite variations of k and μ , it is not clear whether a nanofluid is efficient or not. It is then necessary to find a global parameter able to quantify its global quality for heat exchanges. The Mouromtseff number (Mo) [28] is a factor of merit based on four properties of the fluid: density (ρ), dynamic viscosity (μ), thermal conductivity (k) and heat capacity (C_p). Higher values of Mo indicate higher heat transfer capabilities.

$$Mo = \frac{\rho^{0.8} k^{0.67} C_p^{0.33}}{\mu^{0.47}} \quad (\text{III- 1})$$

Figures III-1 to III-4 display also the efficiency ratio of suspensions (Mo_{nf}/Mo_{water}) defined as the Mouromtseff number of the nanofluid divided by that of the base fluid (water). To calculate Mo_{nf} , the experimental data of k_{nf} and μ_{nf} are used, while ρ_{nf} and $C_{p,nf}$ are evaluated as a function of the volumetric fraction (φ) by applying equations (III-2) and (III-3) [29]:

$$\rho_{nf} = \varphi \cdot \rho_{np} + (1 - \varphi) \rho_{bf} \quad (\text{III-2})$$

$$\rho_{nf} \cdot C_{p,nf} = \varphi \cdot \rho_{np} \cdot C_{p,np} + (1 - \varphi) \rho_{bf} C_{p,bf} \quad (\text{III-3})$$

where the subscripts nf , np and bf refer to nanofluid, nanoparticle and base fluid, respectively. Note that using the improved model of Sharifpur et al. [30] instead of Eq. (III-2) would lead to similar results.

The results can be classified into three categories according to the dispersion regimes reflected by the number of k -peaks. Figures. III-1 and III-2 illustrate the characteristics of the nanofluids for $\varphi=1\%$ and 0.5% , respectively. These intermediate volume fractions exhibit all the dispersion regimes encountered here. They are characterized by the presence of two peaks of k

accompanied by a peak and a valley of μ . This constitutes the 2-peak configuration. For small ($\phi=0.2\%$) or large (2%) concentrations, one of the two peaks of k disappears revealing two other different configurations with an isolated peak of k (Figs. III-3 and III-4).

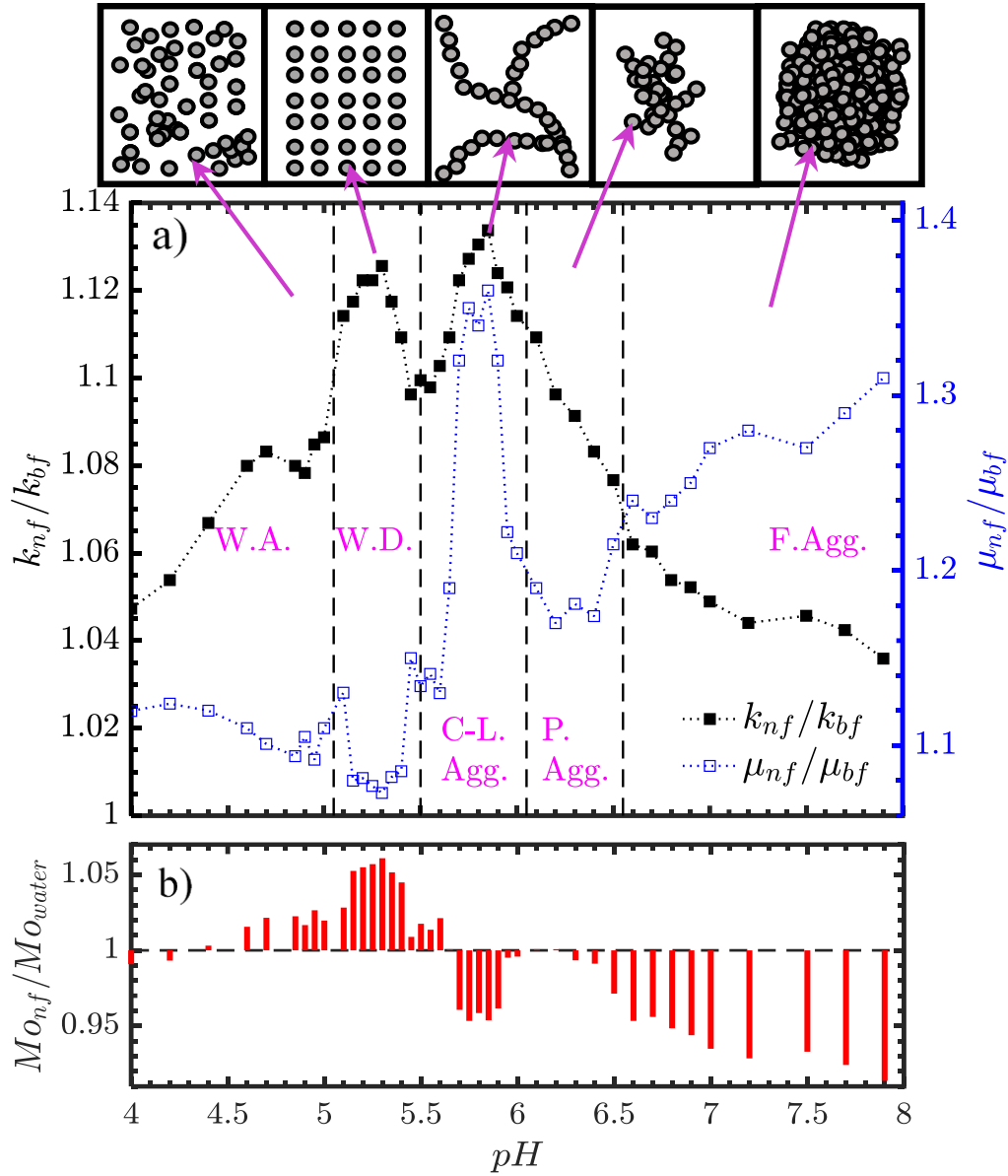


Figure III-1 (a) Ratios of the effective thermal conductivity and dynamic viscosity as a function of pH for $\phi=1\%$; (b) corresponding efficiency ratio.

Figure III-1 shows the existence of a first peak of k for a pH value between 5 and 5.5 while μ exhibits its lowest level. This region should correspond logically to the WD regime. These monodispersed nanoparticles promote the improvement of k since they accentuate some mechanisms proposed to explain the atypical enhancement. Indeed, this particle's arrangement benefits from a high specific surface. Surface/volume ratio can increase by several orders of magnitude, which emphasizes the importance of the nanoscale [2]. In this configuration, the liquid-solid interfaces are more important, which leads to an increase in the number of interfacial nanolayers. In fact, liquid in contact with a solid forms an ordered nanolayer of solid-like structure. As the organization of the liquid inside the interfacial nanolayer approaches that of the solids, nanolayer can lead to an increase in k . This contribution is increasingly pronounced when the particle size is decreasing [11]. Even if the role of the Brownian motion in the increase of the thermal conductivity is controversial, one can note that the WD regime accentuates this mechanism. Indeed, the diffusion coefficient for isolated Brownian particle is inversely proportional to its diameter [13, 16, 18]. Moreover, the WD regime allows better distribution of the particles in the host fluid, which reduces the interparticle distances and limits the zones of low k in the nanofluid [2]. Even if most theoretical models dedicated to the viscosity of nanofluids connect it only to the volume concentration of nanoparticles [24], the experimental studies which have treated the effect of the stability parameters on the rheological properties confirm that a well dispersed suspension results in a decrease of μ . Conversely, excessive agglomeration leads to an increase in μ [31]. Large aggregates have a size that makes them losing the advantageous characteristics of nanoparticles and leads to a deterioration of k . So, it is possible to identify the pH range between 6.5 and 8 in Fig. III-1 as a F.Agg. region. A second k -peak is recorded in the pH range between 5.5 and 6. Unlike the first one, a peak of μ accompanies it. The values of μ in this range rise sharply exceeding even those of the F.Agg. zone and announcing the existence of a particular aggregation. This is in perfect agreement with the optimized agglomeration theory suggested by Prasher et al. [32, 33]. According to this model, the optimized aggregation size, which is not the smallest, can lead to the unexpected enhancements of k thanks to special aggregates. They are found in the literature under the name of chain-like aggregation, fractal-like aggregates and linear aggregation [20-22, 32-34]. This aggregation structure in the form of chains can create highly conducting path network (bridges) that can conduct heat more efficiently [13, 16, 18, 19]. Unlike F.Agg., where all the advantages of the WD state are lost, this chain structuring continues

to benefit from a relatively high surface/volume ratio, which ensures a large surface area for exchange with the liquid and allows the nanolayer to occupy a larger portion of the volume. On the other side, this organization can nullify the effect of the Brownian motion since the size of structures moves away from that of the molecules of the base fluid.

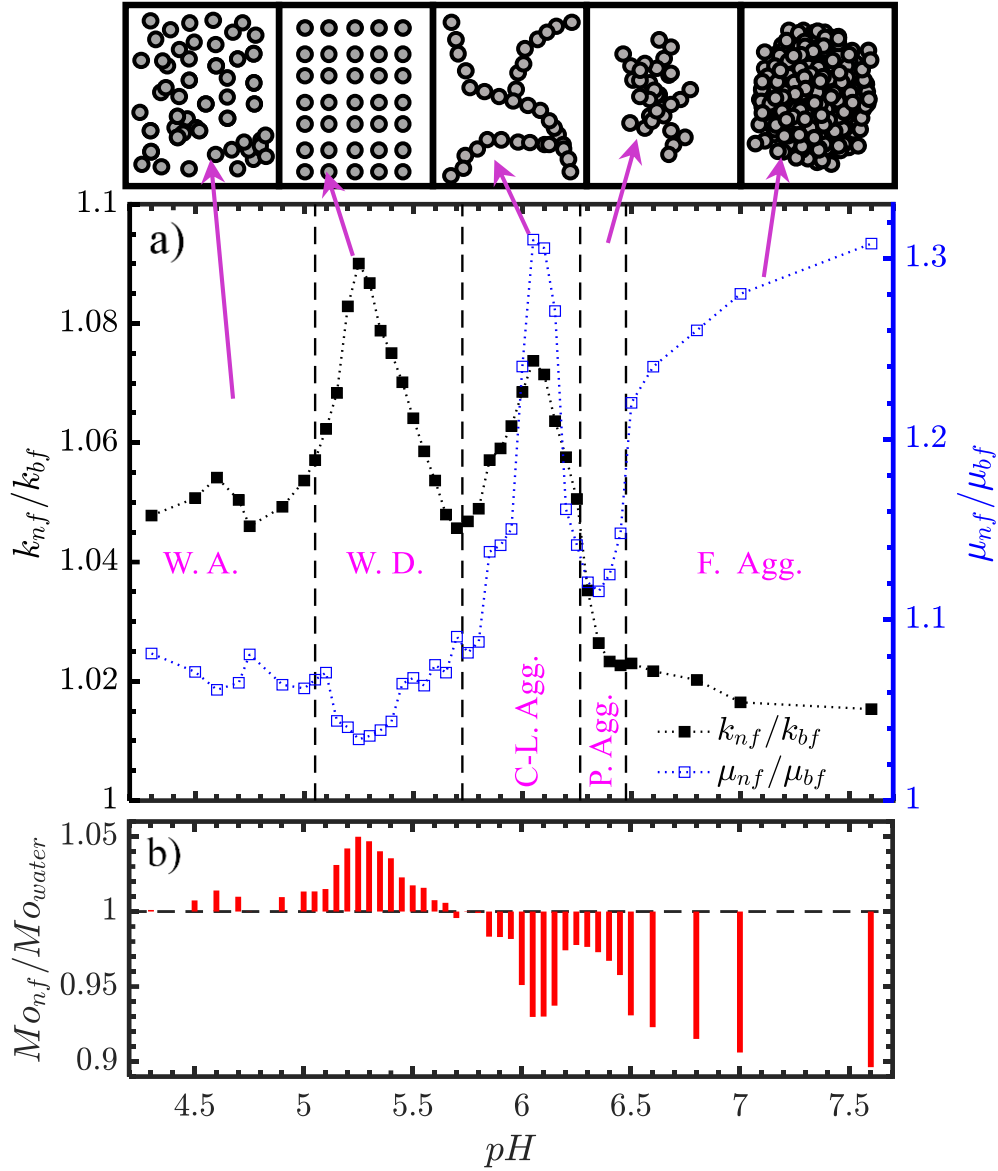


Figure III-2 Same legend as Figure III-1 for $\phi=0.5\%$.

Figure III-2 shows the same trends as Figure III-1. The amplitudes are however different. Indeed, the k -peak relative to W.D. state is more pronounced for $\phi=0.5\%$, while that of CL Agg. is

more marked for $\varphi=1\%$. The amplitude of these two peaks is balanced at a volumetric fraction $\varphi=0.7\%$, which is not present here for sake of clarity.

In Figure III-3, which groups the data relating to $\varphi=0.2\%$, chain-like agglomeration is not observed. The W.D. state is the only particle's arrangement able to provide an increase in k at this concentration level. The disappearance of the CL Agg. regime may be due to the lack of particles. Indeed, the chains can be formed locally in reduced number (slices of bridge) but not enough to create a complete path network able to ensure the transmission of the heat flux efficiently from end to end.

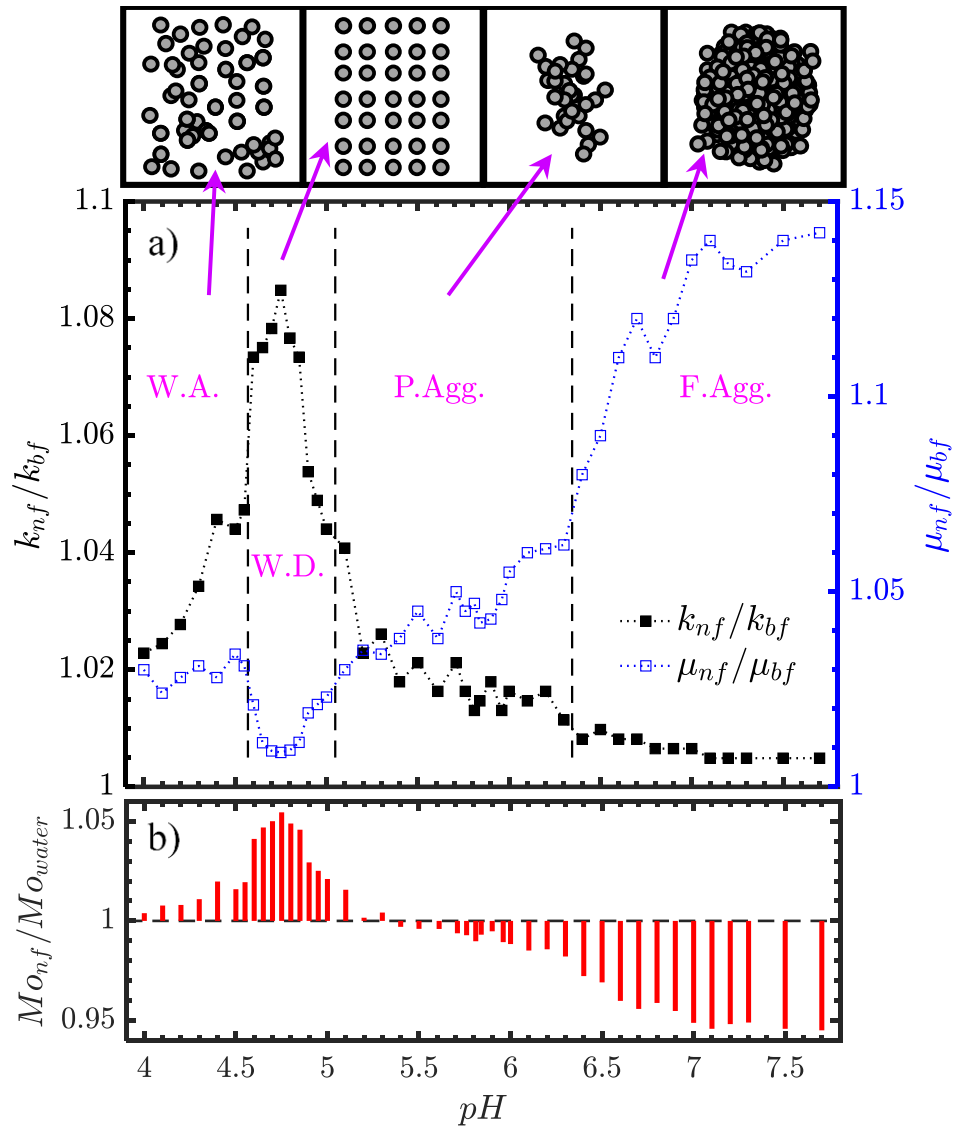


Figure III-3 Same legend as Figure III-1 for $\varphi=0.2\%$.

In Figure III-4, which groups the data relating to $\varphi=2\%$, the WD state is not observed. An increase of μ accompanies the enhancement of k and reveals the configuration of the isolated k -peak resulting from the CL Agg. regime. This high level of φ can increase the probability of interparticles collisions, thus complicating the appearance of the monodispersed state.

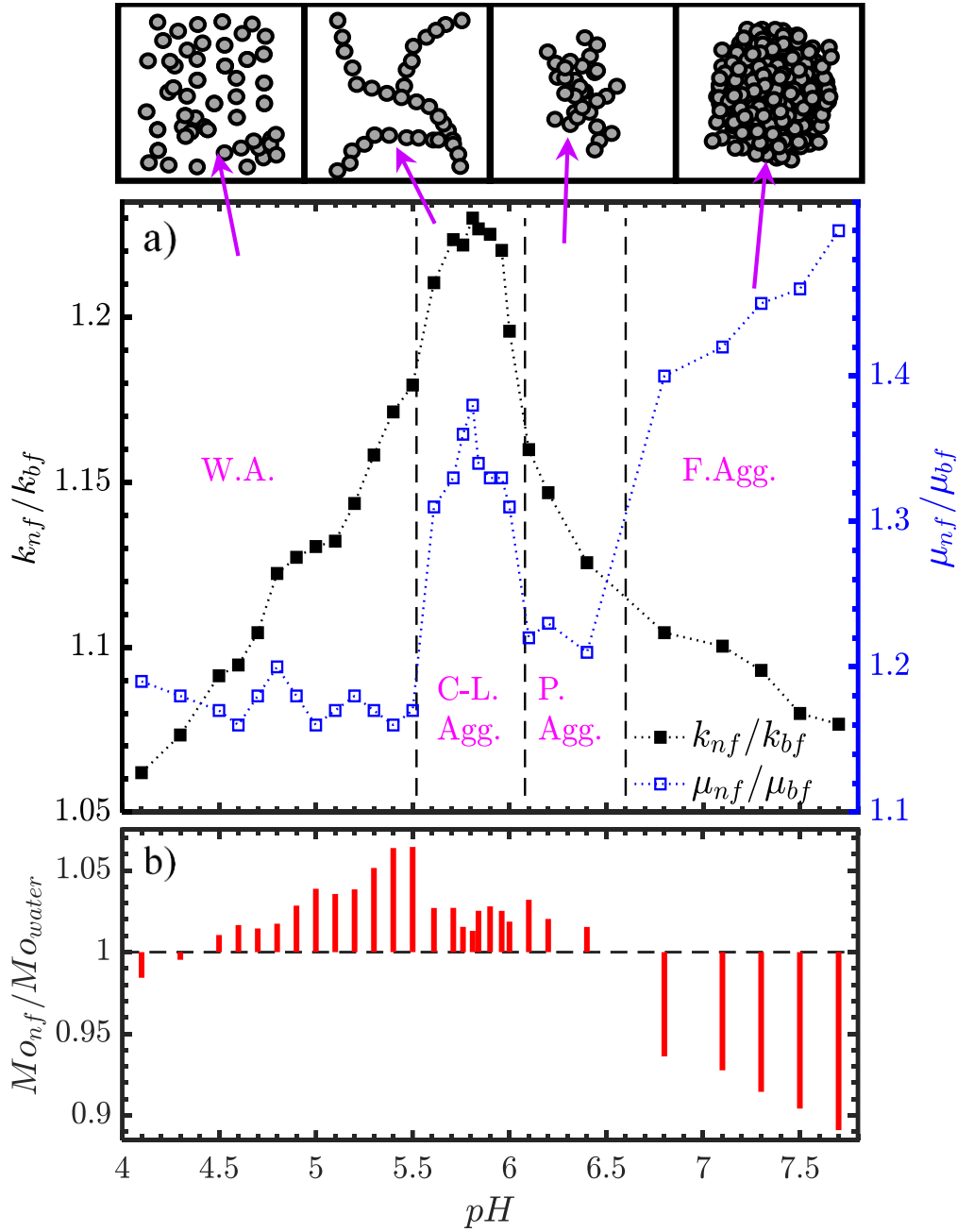


Figure III-4 Same legend as Figure III-1 for $\varphi=2\%$.

The distributions of the Mouromtseff number Mo of all studied concentrations show that, when the WD regime exists, it must be prioritized. Compared to the CL agg. regime, this dispersion state presents better overall energy performance. The increase of ϕ does not lead to any significant improvement in Mo . When the dispersion is optimized, comparable efficiency can be obtained even at very low ϕ levels (0.2%). However, in applications where thermal requirements prevail, and where pumping costs are less important, nanofluids having a high concentration may be beneficial since they provide an enhancement of k by more than 23% for only $\phi=2\%$. The enhancement of k is reached thanks to the CL agg. structure which yields to a non-penalizing μ increase since the nanofluid remains more efficient than the base fluid.

III-6 Conclusions

The dispersion regimes in alumina/water-based nanofluids have been studied experimentally by simultaneous measurements of thermal conductivity and dynamic viscosity using advanced and appropriate techniques for volume fractions of nanoparticles between $\phi=0.2\%$ and 2% at 25 °C. By varying the pH of the solutions between 4 and 8, five dispersion patterns have been identified except for the two extremum concentrations. At $\phi=0.2\%$, the chain-like agglomeration is not recovered, whereas at $\phi=2\%$, it was not possible to highlight the well-dispersed regime. The Mouromtseff number was then used to identify the most efficient nanofluid for practical applications [35]. If the nanoparticles are well dispersed, comparable efficiency may be achieved even at low ϕ values ($\phi=0.2\%$).

A considerable number of research papers focus on the thermal conductivity k of nanofluids. However, the dynamic viscosity μ is another important property that requires the same attention due to its critical effect on the overall performance of thermal energy plants. Consequently, the dynamic viscosity of Nfs should be systematically examined before use in heat transfer applications. Indeed, viscosity is a principal flow property of fluids. Pumping power or pressure drop in convective heat transfer are directly linked to the viscosity of fluids. In other words, the dual examination of the thermal conductivity and the viscosity is fundamental to determine the thermo-fluidic behavior of nanofluids.

Acknowledgments

This project is part of the research program of the NSERC Chair on Industrial Energy Efficiency, established at Université de Sherbrooke in 2014, with the support of Hydro-Québec, Natural Resources Canada and Rio Tinto Alcan. The Sigma Energy Storage company and the Canadian Foundation for Innovation (John R. Evans Leaders Fund number 34582) are also gratefully acknowledged.

Conflicts of interest

None.

III-7 References

- [1] S. U. S. Choi, J.A. Eastman, Enhancing thermal conductivity of fluids with nanoparticles, Proc. of the ASME Int. Mech. Eng. Congress & Exposition, San Francisco, California, 1995.
- [2] S. Das, S. U. S. Choi, W. Yu, T. Pradeep, Nanofluids: Science and Technology, John Wiley and sons Inc., Hoboken, USA, 2008.
- [3] J. A. Eastman, S. U. S. Choi, L. Thompson, S. Lee, Enhanced thermal conductivity through the development of nanofluids, Mater. Res. Soc. Symp. Proc., Boston, USA, 1996.
- [4] M. Liu, M. Lin, I. Huang, C. Wang, Enhancement of thermal conductivity with CuO for nanofluids, Chem. Eng. Technol. 29 (1) (2006) 72–77.
- [5] Y. Hwang, H. Park, J. Lee, W. Jung, Thermal conductivity and lubrication characteristics of nanofluids, Curr. Appl. Phys. 6 (2006) 67–71.
- [6] W. Yu, H. Xie, L. Chen, Y. Li, Investigation of thermal conductivity and viscosity of ethylene glycol based ZnO nanofluid, Thermochim. Acta 491 (1) (2009) 92–96.
- [7] H. Mintsas, G. Roy, C. Nguyen, D. Doucet, New temperature dependent thermal conductivity data for water-based nanofluids, Int. J. Therm. Sci. 48 (2) (2009) 363–371.
- [8] J. Buongiorno, D. Venerus, T. McKrell, A benchmark study on the thermal conductivity of nanofluids, J. Appl. Phys. 106 (9) (2009) 94312-1–94312-14.
- [9] H. Xie, J. Wang, T. Xi, Y. Liu, F. Ai, Q. Wu, Thermal conductivity enhancement of suspensions containing nanosized alumina particles, J. Appl. Phys. 91 (7) (2002) 4568–4572.

- [10] J. Huang, X. Wang, Q. Long, X. Wen, Y. Zhou, L. Li, Influence of pH on the stability characteristics of nanofluids, *Proc. Symposium on Photonics and Optoelectronics*, Wuhan, China, 2009, pp. 1–4.
- [11] P. Keblinski, S. Phillpot, S. U. S. Choi, J. A. Eastman, Mechanisms of heat flow in suspensions of nano-sized particles (nanofluids), *Int. J. Heat Mass Transf.* 45 (4) (2002) 855–863.
- [12] P. Keblinski, J. A. Eastman, D. Cahill, Nanofluids for thermal transport, *Mater. Today* 8 (6) (2005) 36–44.
- [13] M. Chandrasekar, S. Suresh, A review on the mechanisms of heat transport in nanofluids, *Heat Transf. Eng.* 30 (14) (2009) 1136–1150.
- [14] V. Terekhov, S. Kalinina, V. Lemanov, The mechanism of heat transfer in nanofluids: state of the art (review). Part 1. Synthesis and properties of nanofluids, *Thermophys. Aeromech.* 17 (1) (2010) 1–14.
- [15] H. Machrafi, G. Lebon, The role of several heat transfer mechanisms on the enhancement of thermal conductivity in nanofluids, *Contin. Mech. Thermodyn.* 28 (5) (2016) 1461–1475.
- [16] J. Wang, R. Zheng, J. Gao, G. Chen, Heat conduction mechanisms in nanofluids and suspensions, *Nano Today* 7 (2) (2012) 124–136.
- [17] M. Patil, J. Seo, S. Kang, M. Lee, Review on synthesis, thermo-physical property, and heat transfer mechanism of nanofluids, *Energies* 9 (10) (2016) 1–17.
- [18] R. Vidonscky Pinto, F. Augusto, S. Fiorelli, Review of the mechanisms responsible for heat transfer enhancement using nanofluids, *Appl. Therm. Eng.* 108 (2016) 720–739.
- [19] E. Michaelides, Transport properties of nanofluids. A critical review, *J. Non-Equilib. Thermodyn.* 38 (1) (2013) 1–79.
- [20] H. Patel, S. Das, T. Sundararajan, A. Sreekumaran Nair, B. George, T. Pradeep, Thermal conductivities of naked and monolayer protected metal nanoparticle based nanofluids: manifestation of anomalous enhancement and chemical effects, *Appl. Phys. Lett.* 83 (14) (2003) 2931–2933.
- [21] H. Zhu, C. Zhang, S. Liu, Y. Tang, Y. Yin, Effects of nanoparticle clustering and alignment on thermal conductivities of Fe_3O_4 aqueous nanofluids, *Appl. Phys. Lett.* 89 (2) (2006) 023123.
- [22] G. Paul, P. Das, I. Manna, Maneuvering the chain agglomerates of colloidal superparamagnetic nanoparticles by tunable magnetic fields, *Appl. Phys. Lett.* 105 (18) (2014) 183108.

- [23] K. Bashirnezhad, S. Bazri, M. Safaei, M. Goodarzi, M. Dahari, O. Mahian, A. Dalkilica, S. Wongwises, Viscosity of nanofluids: a review of recent experimental studies, *Int. Commun. Heat Mass Transf.* 73 (2016) 114–123.
- [24] J. Meyer, S. Adio, M. Sharifpur, P. Nwosu, The viscosity of nanofluids: a review of the theoretical, empirical, and numerical models, *Heat Transf. Eng.* 37 (5) (2016) 387–421.
- [25] S. Bhanushali, N. Jason, P. Ghosh, A. Ganesh, G. Simon, W. Cheng, Enhanced thermal conductivity of copper nanofluids: the effect of filler geometry, *ACS Appl. Mater. Interfaces* 9 (22) (2017) 18925–18935.
- [26] N. Bouguerra, A. Khabou, S. Poncet, S. Elkoun, Thermal conductivity of Al_2O_3 /water-based nanofluids: revisiting the influences of pH and surfactant, *Int. J. Mech. Aerosp. Ind. Mechatronic Manufact. Eng.* 10 (12) (2016) 1849–1858.
- [27] I. Mahbulul, R. Saidur, M. Amalina, M. Niza, Influence of ultrasonication duration on rheological properties of nanofluid: an experimental study with alumina-water nanofluid, *Int. Commun. Heat Mass Transf.* 76 (2016) 33–40.
- [28] I. Mouromtseff, Water and forced-air cooling of vacuum tubes nonelectronic problems in electronic tubes, *Proc. Inst. Radio Eng.* 30 (4) (1942) 190–205.
- [29] Y. Xuan, W. Roetzel, Conceptions for heat transfer correlation of nanofluids, *Int. J. Heat Mass Transf.* 43 (19) (2000) 3701–3707.
- [30] M. Sharifpur, S. Yousefi, J. Meyer, A new model for density of nanofluids including nanolayer, *Int. Commun. Heat Mass Transf.* 78 (2016) 168–174.
- [31] P. Keblinski, R. Prasher, J. Eapen, Thermal conductance of nanofluids: is the controversy over? *J. Nano Res.* 10 (7) (2008) 1089–1097.
- [32] R. Prasher, W. Evans, P. Meakin, J. Fish, P. Phelan, P. Keblinski, Effect of aggregation on thermal conduction in colloidal nanofluids, *Appl. Phys. Lett.* 89 (14) (2006) 88–90.
- [33] R. Prasher, P. Phelan, P. Bhattacharya, Effect of aggregation kinetics on the thermal conductivity of nanoscale colloidal solutions (nanofluid), *Nano Lett.* 6 (7) (2006) 1529–1534.
- [34] J. Sui, P. Zhao, B. Bin-Mohsin, L. Zheng, X. Zhang, Z. Cheng, Y. Chen, G. Chen, Fractal aggregation kinetics contributions to thermal conductivity of nano-suspensions in unsteady thermal convection, *Sci. Rep.* 6 (1) (2016) 39446.

[35] N. Che Sidik, I. Adamu, M. Jamil, G. Kefayati, R. Mamat, G. Najafi, Recent progress on hybrid nanofluids in heat transfer applications: a comprehensive review, *Int. Commun. Heat Mass Transf.* 78 (2016) 68–79.

Chapitre IV Effet de la température sur les nanofluides à base d'eau et d'Alumine : Relation entre le phénomène d'hystérésis et les régimes de dispersion.

Titre de l'article:

Alumina/water based nanofluids: Relationship between hysteresis phenomenon and dispersion regimes

Auteurs et affiliations :

¹ Nizar Bouguerra : Étudiant au doctorat, Université de Sherbrooke, Faculté de Génie, Département de Génie mécanique.

² Sébastien Poncet : Professeur agrégé, Université de Sherbrooke, Faculté de Génie, Département de Génie mécanique.

³ Saïd Elkoun: Professeur, Université de Sherbrooke, Faculté de Génie, Département de Génie mécanique.

IV-1 Résumé français

Cette étude examine à travers une étude expérimentale détaillée le phénomène d'hystérésis se développant lors des cycles de chauffage et de refroidissement des nanofluides à base d'eau et d'alumine. L'accent a été particulièrement mis sur la relation entre ce phénomène et les différents états de dispersion des nanoparticules. Ainsi, en effectuant des mesures simultanées de conductivité thermique et de viscosité dynamique, cinq régimes de dispersion ont été mis en évidence. L'influence de la température, dans la plage comprise entre 20 et 80 °C, sur ces deux propriétés ainsi que sur le pH de la solution a, par la suite, été étudiée pour six suspensions caractéristiques dans le régime bien dispersé et le régime d'agglomération en chaîne. Il a été démontré que tant que la température des nanofluides et, par conséquent, le pH ne dépassaient pas une valeur critique, aucun phénomène d'hystérésis ne se produit pendant les cycles de chauffage et de refroidissement. Finalement, il a été démontré que cette température critique dépend fortement du régime de dispersion et du pH initial du nanofluide.

IV-2 Abstract

The present paper deals with a comprehensive experimental study of the hysteresis phenomenon of alumina-water based nanofluids taking place during heating-cooling cycles. The emphasis was particularly put on investigating the relationship between this phenomenon and the dispersion state of alumina nanoparticles. Thus, by carrying out simultaneous thermal conductivity and dynamic viscosity measurements, five dispersion regimes were highlighted. The influence of the temperature on these two properties as well as the pH of the solution was then investigated for six characteristic conditions in the well-dispersed and chain-like agglomerated regimes and for temperatures between 20 and 80°C. It was shown that as long as the temperature of the nanofluids, and as a consequence the pH, was not exceeding a critical value, no hysteresis phenomenon leading to irreversible damages occurred during the heating and cooling processes. Eventually, it was shown that this critical temperature is strongly dependent on the dispersion regime and the initial pH of the nanofluid.

Keywords: Nanofluid; hysteresis; thermal conductivity; dynamic viscosity; alumina nanoparticles, temperature.

IV-3 Introduction

Nanofluids are generally defined as common or base fluids containing solid nanoparticles to enhance thermophysical properties of the fluids and, as a result, to make them suitable for various applications and, particularly for heat transfer fluids. This definition of nanofluids was initially proposed by Choi and Eastman [1] and, then, enriched by the same authors to take into account the preparation steps of nanofluids and the impact of the nanoparticles size [2]. This definition also pointed out the importance of the dispersion of the nanoparticles and stabilization of the solution during the preparation of nanofluid.

The Maxwell's theory [3] showed that an enhancement of the thermal conductivity (k) may be obtained by scattering micrometer-sized solid particles into a base fluid. Nevertheless, the major weakness of such large particles is their rapid settling. On the contrary, stabilized nanoparticles, with average size less than 100 nm, are not or less affected by the sedimentation phenomenon and exhibit surface/volume ratio 10^3 times larger than that of microparticles, leading to significantly higher thermal conductivity [2].

Numerous studies noticed an unusual improvement of the nanofluids' thermal conductivity that the classical theories of solid/liquid suspensions fail to explain [1, 4-8]. In addition and due to the difficulties in preparing similar nanofluids and controlling the experimental conditions, the reported results are often contradictory. Some researchers claimed that the non-detection of the unusual improvement in some works is due to the inaccuracies of the measurement techniques used [9-11]. Actually, some devices initially designed to measure the thermal conductivity of solid samples are widely used to characterize fluids. However, those apparatus are not suitable for liquids measurements because of natural convection. Among the available devices, the KD2Pro Thermal Property Analyzer is the most pertinent example. This apparatus is erroneously and recurrently presented as a measuring system based on the transient hot-wire (THW) method while it is not really the case [11]. In addition, the sensor of this device is very dependent on the environmental conditions such as temperature, vibration, and noise [11]. Obviously, this analyzer cannot be used if the temperature is one of the main parameters to be considered.

In addition to the enhancement of the thermal performances, other benefits expected from nanofluids for industrial applications include principally the decrease of the required pumping energy for fluid flow. Indeed, the presence of nanoparticles affects also the dynamic viscosity (μ)

and consequently the pressure drop [12]. The two key parameters that must be optimized to get an efficient nanofluid are then the thermal conductivity and dynamic viscosity [13-16]. Microscale particles cause abrasion, clogging of flow paths, pressure drop, and high pumping power requirements, which make their use not suitable. These problems could be overcome by better limiting the inherent increase of the dynamic viscosity by the addition of nanoparticles [17-19].

Nanofluids are complex fluids and their physical properties are dependent on several interdependent parameters such as the type of nanoparticles, their concentration, size distribution and shape, the base fluid, the dispersion methods and operating temperatures, to name just a few [2]. Many papers neglect some important factors including the stability of the suspensions and the agglomeration of the particles [7]. However, the stability of well-dispersed nanofluids is a crucial issue that must be addressed before any possible industrial applications. Indeed, excessive agglomeration of the nanoparticles leads, not only to settlement phenomenon and clogging channels but also, to the degradation of the thermal and rheological properties of the nanofluid [2]. Therefore, preparing a stable nanofluid over a long period of time is a mandatory prerequisite for industrial applications. The two-step preparation technique is generally the most widely used method. It is based on the dispersion of a dry powder in a base fluid. However, precautions must be taken and the preparation protocol must include different techniques that facilitate nanoparticles dispersion and allow, at each step of the procedure, to ensure the mixture quality [20]. The suspension of the nanoparticles is generally accompanied by mechanical (ultrasound) and/or chemical (surfactant and pH adjustment) processes, to homogenize the distribution of the solid particles in the base fluid and, to maintain the stability of the suspension by preventing or hindering the agglomeration [21]. In a previous paper, Bouguerra et al. [22] carried out a careful experimental investigation on the stability of alumina-water based nanofluids and pointed out that the pH of the solution is the key parameter for controlling dispersion and stabilization of the suspension and getting an optimum value for the thermal conductivity.

Colloid theory states that the sedimentation phenomenon in suspensions ceases when the particle size is smaller than a critical radius, below which there is a balance between gravity and Brownian forces. Accordingly, and with no surprise, the use of small particles has been regarded as an interesting solution for preparing stable nanoparticle suspensions without sedimentation. However, the smaller the particle size, the higher the surface energy, which contributes to the formation of particle agglomerates [20]. Indeed, nanoparticles in suspension are subjected to Van

Der Waals attractive and electrostatic repulsive forces. By decreasing the surface charges of the particles, interparticular distance may decrease below a critical distance and, consequently, favors agglomeration [23]. In other words, the electric charges in the solution govern the level of aggregation and, consequently, the arrangement of the particles within the base fluid which can lead to different dispersion regimes [24]. In the case of water-based nanofluids, interactions between nanoparticles can be controlled by the pH. Indeed, the pH of the solution affects the surface charges of the particles, which, in turn, changes repulsive or attractive forces. A high charge leads to well-dispersed particles, while large clusters form when the surface charges reduced (point of zero charge) [2]. Lee et al. [25] reported that the thermal conductivity of suspensions is significantly affected by the surface charges of the nanoparticles. They showed that the stability of the nanoparticles increases when the pH of the solutions is outside the zero charge zone (electrical neutrality). Therefore, the pH appears to be one of the main parameters to control and monitor the agglomeration and the distribution of nanoparticles within the base fluid. In a recent study Bouguerra et al. [26] investigated the relationships between the dispersion regimes, thermal conductivity and dynamic viscosity of alumina/water-based nanofluids at different concentrations ϕ ranging from 0.2 to 2 vol.%. Depending on the pH values, five dispersion regimes have been identified. By increasing the pH, the arrangement of nanoparticles goes from a weakly attracted (W.A.), well-dispersed (W.D.), chain-like agglomeration (C-L. Agg.), partially agglomerated (P. Agg.) to fully agglomerated (F. Agg.) regime. In the W.D. regime, characterized by the smallest particle size, a decrease of the dynamic viscosity and an increase of the thermal conductivity were observed. By contrast, opposite results were obtained in the fully agglomerated regime characterized by larger particle sizes. Between these two limit regimes, different levels of electrical charges, due to pH variations, lead to other dispersion regimes where the most interesting one is the chain-like agglomerated regime. Indeed, in this regime, both thermal conductivity and dynamic viscosity exhibit maximum values. The values of μ in this regime increase unexpectedly and may even exceed those of the F.Agg. region, revealing the presence of a particular aggregation. It is interesting to highlight that this type of agglomeration was successfully predicted by the optimized agglomeration theory suggested by Prasher et al. [27]. This peculiar dispersion regime is usually referred to as chain-like aggregation, fractal-like aggregates or linear aggregation [27-34]. In this aggregation structure, all particles are connected to each other, and form a highly heat conducting path or network (thermal bridges) [24, 35-37].

It is worth mentioning that the reported studies on nanofluid stability were carried out at room temperature whereas heat transfer fluids are subjected to different temperature levels. As an example, a heat exchanger usually involves two working fluids, which exchange thermal energy resulting in a variation of the inlet and outlet temperatures. Heat exchangers also impose a succession of heating and cooling cycles. Thus, nanofluids must then meet the requirement of repeatability and reproducibility during these cycles to ensure a proper functioning of the device. Increasing the temperature leads to an increase of thermal agitation, Brownian motion, particles collision and, as a result, can lead to agglomeration if these effects amplify too much. Moreover, it was also reported that an excessive increase of temperature can cause the degradation of the surfactant, used to stabilize the nanoparticles, which overall affects the suspension stability [38–40]. The variation of the temperature also leads to modification of solution pH that, in turn, may affect the suspension stability too. Ultimately, heating - cooling cycles may induce a change of the dispersion regime [2]. Therefore, investigating the stability of nanofluids as a function of temperature and heating-cooling cycles is crucial.

Only few experimental results have considered the dependence of nanofluids properties on temperature [8, 41-43]. The relevance of these works are questionable due to the reliability of the measuring equipment. Indeed, the measurements of the thermal conductivity are most of the time carried out using a KD2Pro probe, which is not appropriate when temperature is the main parameter of the study [11]. Similarly, several studies focused on the viscosity measurements using classical viscometers that are not very accurate and for which temperature regulation is less controlled.

One of the most intriguing phenomena when dealing with the effect of temperature on the nanofluids properties is the hysteresis phenomenon. This can compromise the eventual practical use of nanofluid since it is characterized by non-identical property values during the different heating and cooling ramps. Nguyen et al. [44, 45] and Said et al. [46] reported the presence of an hysteresis phenomenon by measuring dynamic viscosity of nanofluids as a function of temperature during different heating and cooling cycles. Nguyen et al. [44, 45] showed that this phenomenon occurs when the heating temperature exceeds a critical threshold. Through an experimental study, Nguyen et al. [44] examined the influences of the nanoparticles concentration and the temperature on the dynamic viscosity of alumina/water-based nanofluid. Measurements of viscosity were carried out using a circular Couette viscometer from room temperature until 75°C, with two different particle sizes, namely 36 and 47 nm, and particle concentration lying between 1 to 12 vol

%. The mixtures were obtained by diluting concentrated solutions in distilled water. The authors found that the dynamic viscosity of the nanofluids increases considerably with the increase of the particle concentration, but decreases markedly with an increase of temperature. They observed a decrease of the viscosity when the temperature was increased and, this effect was more pronounced in the temperature range between 22 and 40 °C. Beyond this temperature range, the viscosity tends to become almost constant regardless of the temperature. However, by further increasing the heating, the authors observed the presence of a critical temperature above which an irregular and irreversible change of the dynamic viscosity occurred. Indeed, for a given nanofluid, if the solution is heated beyond the critical temperature, a striking increase in viscosity occurs and, subsequently, if the sample is cooled down, an hysteresis phenomenon, characterized by different values of the viscosity during the heating and cooling ramps, appears. The authors emphasized the fact that this phenomenon is much more pronounced at high particle concentrations. It is important to mention that for a particles content of 9 vol%, Nguyen et al. [44] reported that beyond the critical temperature, the fluid became so viscous that the viscometer piston was stuck inside the measuring cylinder. The authors suggested a structural change within the nanofluids as a tentative explanation of the hysteresis phenomenon. Indeed, the naked eye observations of the samples, at the end of the heating ramp, showed a thickening of the fluid and agglomeration at the surface of the viscometer. Obviously, the stability of the suspensions was considerably altered by heating beyond the critical temperature. The authors ascribed this behavior to the degradation of the surfactant grafted on the nanoparticles surface, to ensure the stabilization and good dispersion. Overall, this peculiar hysteresis phenomenon remains, so far, not fully understood.

Unlike the suspensions of Nguyen et al. [44], which were prepared using commercial concentrated solutions, Said et al. [46] prepared their own mixtures by dispersing TiO_2 and Al_2O_3 nanoparticles powder in distilled water and examined the size distribution of the nanoparticles by the dynamic light scattering technique (DLS). The authors analyzed the stability of nanofluids by zeta potential measurements and particle morphology using a scanning electron microscope. They investigated the rheological and thermal behavior of nanofluids at concentrations ranging from 0.1 to 0.3 vol.%; much lower as compared to Nguyen et al.'s suspensions [44]. They were interested in determining the influence of temperature on the hydrothermal properties of the nanofluid subjected to several heating and cooling cycles over a temperature range from 25 to 80°C. To carry out their viscosity measurements, the authors connected the Brookfield viscometer to a thermostat

bath to control the temperature. As previously observed by Nguyen et al. [44], the experimental data of Said et al. [46] exhibited the hysteresis phenomenon on the viscosity as a function of temperature. The authors also showed the existence of a critical temperature beyond which the properties of the suspensions were drastically modified. They examined the evolution of the nanoparticle agglomeration as a function of time by comparing the results of DLS before and after using it in a solar collector. Their results revealed an increase in the average particle size and a relative decrease of the zeta potential. Such evolutions of these stability indicators are typical of the nanoparticles agglomeration [2]. In order to evaluate the thermal conductivity of nanofluids, the authors used the KD2Pro conductivity meter; which is, as mentioned previously, not suitable for measuring thermal conductivity of liquids. Since the volume concentrations of the nanoparticles were low as compared to reported data of Nguyen et al. [44], the observed hysteresis phenomenon was less pronounced.

Although it is of great interest, the hysteresis phenomenon has not been sufficiently explored and the few reported studies were focused on the characterization of the nanofluid properties without paying attention to the preparation conditions. Combining results of the previous investigations [22, 26] make it possible to determine optimal preparation conditions allowing to benefit from the best thermal and rheological properties of alumina/water-based nanofluids. One of our previous studies allowed, depending on the preparation conditions and concentration levels, to reveal the existence of different dispersion regimes. These dispersion regimes were not necessarily present at all concentration ranges [26]. Indeed the results showed that the well-dispersed regime (W.D.), characterized by a maximum of the thermal conductivity and a minimum of the dynamic viscosity, tends to disappear when the particle concentration increases. Conversely, the chain-like agglomeration regime (CL Agg.), which is predominant at high concentrations, was attenuated at low concentrations. These two dispersion regimes exhibited the best thermal performances and are present at intermediate concentration levels. The results showed that both regimes have similar amplitudes of thermal conductivity at their maximum peaks at $\phi = 0.7$ vol. %.

In contrast to Nguyen et al.'s work [44], the aim of this paper is to study the hysteresis phenomenon on the two main nanofluid properties, namely k and μ , as a function of temperature using carefully prepared nanofluids and appropriate measuring techniques. Thus, conductimeter, rheometer and pH-meter are combined to simultaneously assess thermal conductivity, dynamic

viscosity and stability of relevant dispersion regimes as a function of temperature. To the best of the authors' knowledge, the hysteresis phenomenon is discussed for the first time in light of the dispersion regimes.

IV-4 Experimental methods

IV-4.1 Thermal conductivity measurements

The thermal conductivity of suspensions was determined using the THW-L1 Liquid Thermal Conductivity System from Thermtest Thermophysical Instruments. The thermal conductivity, denoted k , is measured based on the THW method combined with a system monitoring the temperature (heat exchanger + thermostat bath circulator). This equipment allows a complete, direct, accurate and fast characterization of the nanofluid thermal conductivity within the ranges -40°C to 200°C and $0.01 \leq k \leq 2 \text{ W/ (m.K)}$. The main benefit of this method, when dealing with fluids, is its ability to exclude the effect of natural convection. The principle of the hot-wire method relies on an ideal and constant heating source, an infinitely long and thin continuous line aiming at dissipating the heat into an infinite test medium. A constant electrical current is delivered to the wire (platinum) to generate the temperature rise. The wire serves as both a heating source and a temperature sensor [47]. Heating the wire by Joule effect causes the variation of its resistance and allows to monitor its temperature variation as a function of time using a Wheatstone bridge and a data acquisition system. Finally, the thermal conductivity value is derived from the heating power and the slope of temperature change. The higher the thermal conductivity of the surrounding liquid is, the lower is the temperature rise of the wire [48]. The THW-L1 sensor has two main parts: (i) a thin platinum wire for heating the sample and recording electrical resistivity for the determination of the thermal conductivity; (ii) a PT100 Platinum resistance thermometer for independently measuring the temperature of the sample. The platinum wire is 0.1 mm in diameter and 35 mm in length. A platinum wire is selected owing to its well-known resistance–temperature relationship and its sensitivity over a wide temperature range. As suspensions containing metal particles are electrically conductive, a Teflon spray is then used to coat the platinum wire for electric insulation. The main experimental cell (sample cell) is in fact a part of the Wheatstone bridge circuit for which the resistance of the wire has to be measured. Two out of the four resistors of the Wheatstone bridge are the fixed resistors while the third one is variable which allows balancing the circuit. The THW sensor is positioned at the center of the

nanofluid sample cell and is placed in a heat exchanger connected to the thermostat bath circulator working with water to ensure the control of the temperature with an accuracy of $\pm 0.1^{\circ}\text{C}$.

Calibration and validation steps were performed using distilled water during the heating-cooling cycle. Fig.IV-1 shows the evolution of the thermal conductivity of the distilled water as a function of the temperature. The results are compared to the reference data presented by Incropera and Dewitt [49]. The repeatability and the uncertainty remain better than 0.5 %. Each measurement requires a stabilization of the sample temperature that can be achieved by a compromise between heating rate and holding time depending on the sample size. Stabilizing the temperature of the sample before each measurement is essential and can be achieved by a correct choice of the heating rate. The equipment used offers the ability to set the temperature ramps. Nevertheless, since the resistance temperature detector (RTD), in charge of controlling the set point temperature, is located in between the exchanger and the sample, an offset between the set and the actual temperature of the sample may occur if the heating or cooling rate is too high. This can result in a fictitious hysteresis due to the thermal lag. To avoid this offset, a measurement method allowing a temperature stabilization step prior to each measurement point was used. As shown in Fig.IV-1, the heating and cooling curves follow almost exactly the same path for two successive heating-cooling cycles.

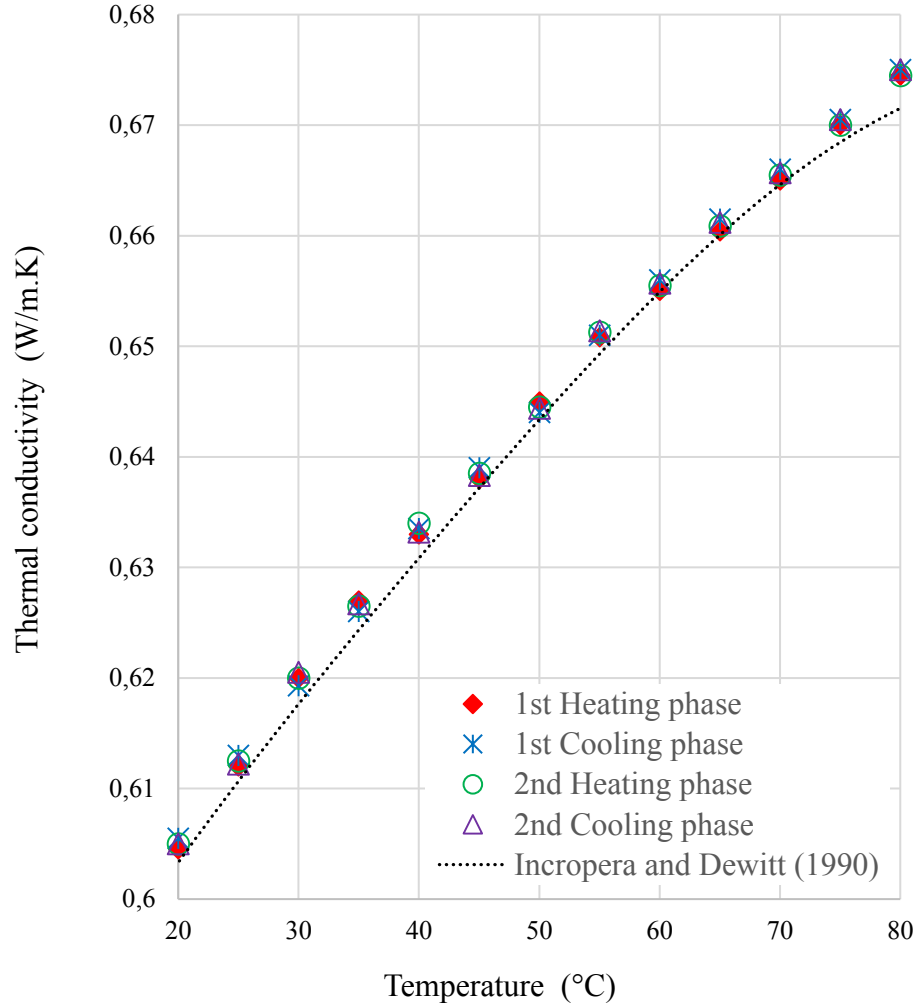


Figure IV-1 Variation of the thermal conductivity of distilled water as a function of temperature

IV-4.2 Dynamic viscosity measurements

The rheological properties of suspensions were obtained by means of an hybrid rheometer (TA Instruments HR-2) using a DIN coaxial cylinder geometry (diameter of 27.98 mm). A Peltier cylinder regulates temperature (T) with an accuracy of 0.1°C (inner diameter of 30.17 mm). Dehydration was prevented by using a wet steel cover insuring a water saturated atmosphere around the sample. For low viscosity fluids, angular velocity measurements may be wrong or inaccurate due to rheometer capabilities. Then, preliminary experiments on distilled water were carried out to determine the validity range of the shear rate ($\dot{\gamma}$) with respect to the gap (i.e. 5917.1 μm). Fig.IV-2 shows the dynamic viscosity as a function of temperature during 2 heating-cooling cycles. The obtained results during the first and second cycles were similar. Moreover, the measured viscosities

were also compared with calculated values using the equation (1) where μ (in cP) and T (in K) are the calculated dynamic viscosity and temperature respectively. As it can be seen in Fig.IV-2, the measured and calculated dynamic viscosities are quite similar (uncertainty < 3 %, repeatability < 0.5%) [50].

$$\mu_{bf} \times 10^4 = \exp \left[\frac{1.12646 - 0.039638 \times (T + 273.15)}{1 - 0.00729769 \times (T + 273.15)} \right] \quad (IV-1)$$

The uncertainty being very low, the viscosity variations and especially the hysteresis phenomenon on the dynamic viscosity displayed in the following sections cannot be due to the uncertainty of the rheometer.

The set temperature is controlled using an RTD probe located in the Peltier element. Similarly to the thermal conductivity measurements, a judicious choice of the heating rate is necessary to avoid any mismatch between set and real sample temperatures. As for the thermal conductivity measurements, a specific procedure allowing a temperature stabilization step prior to each measurement point was used. This allows to benefit from a much more stable temperature at each measurement point and to synchronize the viscosity and thermal conductivity measurements.

The dynamic viscosity μ of all nanofluid samples were assessed as a function of $\dot{\gamma}$. It is important to mention that, whatever the operating conditions, all investigated nanofluids exhibit a Newtonian behavior over the range [0.01 - 100 s⁻¹].

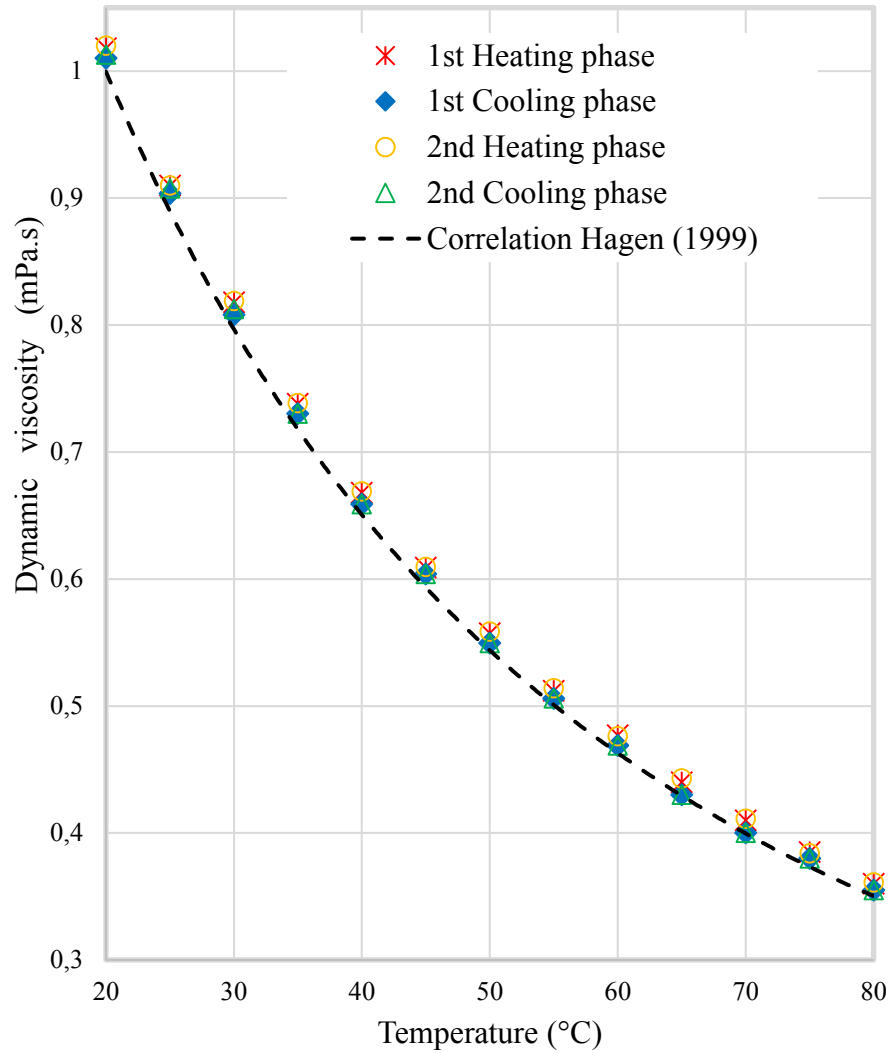


Figure IV-2 Variation of the dynamic viscosity of distilled water as a function of temperature.

IV-4.3 Preparation of alumina/water-based nanofluids and experimental procedure

To understand the hysteresis phenomenon of nanofluids, careful preparation and characterisation, in terms of dispersion regimes, is essential. In this study, preparation of alumina/water-based nanofluids was carried out using the two-step method, as it is well known to be efficient, economical and suitable for industrial scale up production [2]. This method consists in the dispersion of nanoparticles in powder form into the base fluid. Al_2O_3 nanoparticles powder was purchased from US Research Nanomaterials with a purity level of 99.9%, and an average

diameter of 50 nm. It is worth mentioning that the morphology and the average particle size were verified by scanning electron microscopy (SEM) and a Zetasizer (Nano ZS from Malvern Panalytical) for particle size distribution. Distilled water was chosen as it allows a direct control on nanoparticle interactions by adjusting the pH and, accordingly, the dispersion regimes [26].

As reported in a previous study, a surfactant is not required with this type of nanofluid for nanoparticle stabilization [22]. It was also shown that the pH is the key parameter to control the dispersion. In the present study, the pH was controlled by adding hydrochloric acid (HCl) and/or sodium hydroxide (NaOH) in analytical grade. pH of all suspensions was measured using LabQuest 2 (Vernier) coupled with a temperature probe and kept within the optimal range [4.5 - 6.5].

The purpose of the present paper is to study the effect of temperature on the properties of nanofluids, namely thermal conductivity and dynamic viscosity, in the two most interesting dispersion regimes (i.e. well dispersed and chain-like agglomerated) and, to figure out under which conditions the phenomenon of hysteresis occurs. Therefore, the experimental measurements were first devoted to determine the stability conditions of the different dispersion regimes as a function of pH and, subsequently, to investigate the effect of temperature and hysteresis phenomenon on selected samples. Consequently, the experimental procedure was split into 3 main steps as described below.

Preparation of the initial suspension (mother solution)

800 ml of an 0.7 vol. % suspension was prepared, at 25°C, by mixing Al_2O_3 powder and water. The suspension was homogenized using, initially, a magnetic stirrer and then, ultrasonic vibrations (UIP1000hdT Hielscher Ultrasonics) for 12 hours.

Preparation and characterization of samples for the identification of the dispersion regimes: synchronised thermal conductivity and viscosity measurements

This important task aimed at determining the boundaries of each dispersion regime as a function of the pH, for the selected concentration and, following the same experimental approach described in [26]. Thus synchronized measurements of thermal conductivity and dynamic viscosity were performed. As the THW and rheological measurements require 50 and 25 ml, respectively, the initial solution was split into 80 ml samples. The pH of each sample was then adjusted to the desired value as previously described and all the samples were sonicated for 15 min before each test using a Q700-Sonicator (Qsonica). This procedure was repeated for all desired pH. Temperature

was controlled and fixed at 25°C by incorporating a jacketed glass beaker connected to a bath circulator at all stages of preparation and characterization.

Preparation and characterisation of samples for investigating the effect of temperature and hysteresis phenomenon

Knowing the pH limits of the different dispersion regimes for 0.7 vol% concentration, samples with well-dispersed and chain-like agglomerated dispersion regimes were selected to investigate the effect of temperature and the hysteresis phenomenon. Bath Circulators connected to the THW and the rheometer were no longer used at this step to maintain the sample temperature at 25°C but to heat, cool down and hold the temperature constant during data acquisition between 20 and 80°C. Particular attention was paid to the synchronization of the thermal conductivity and rheological tests.

IV-5 Hysteresis phenomenon on the dynamic viscosity and thermal conductivity

Fig.IV-3 shows the relative thermal conductivity (k_{nf}/k_{bf}) and the relative dynamic viscosity (μ_{nf}/μ_{bf}) of the nanofluid as a function of pH. k_{nf} and μ_{nf} are the thermal conductivity and dynamic viscosity of the nanofluid, respectively, whereas k_{bf} and μ_{bf} are those of the base fluid (water). As expected, the five dispersion regimes described in details in a previous work [26] are also present with the investigated concentration $\phi=0.7$ vol%. This concentration is of particular interest as the well dispersed and the chain-like agglomerated regimes exhibit both the expected bell shape curve with a maximum of the relative thermal conductivity and similar amplitude.

To investigate the hysteresis phenomenon over a temperature range between 20 to 80°C, six suspensions, termed (a), (b), (c), (d), (e) and (f), located within the W.D. and C.-L. Agg regimes were selected (Fig.IV-3). Points (b) and (e) correspond to the maximum of the relative thermal conductivity while (a), (c), (d) and (f) are below and above these maximum in both regimes. pH of suspensions (a), (c), (d) and (e) are the beginning and the end or the boundaries of W.D. and C-L Agg. regimes respectively.

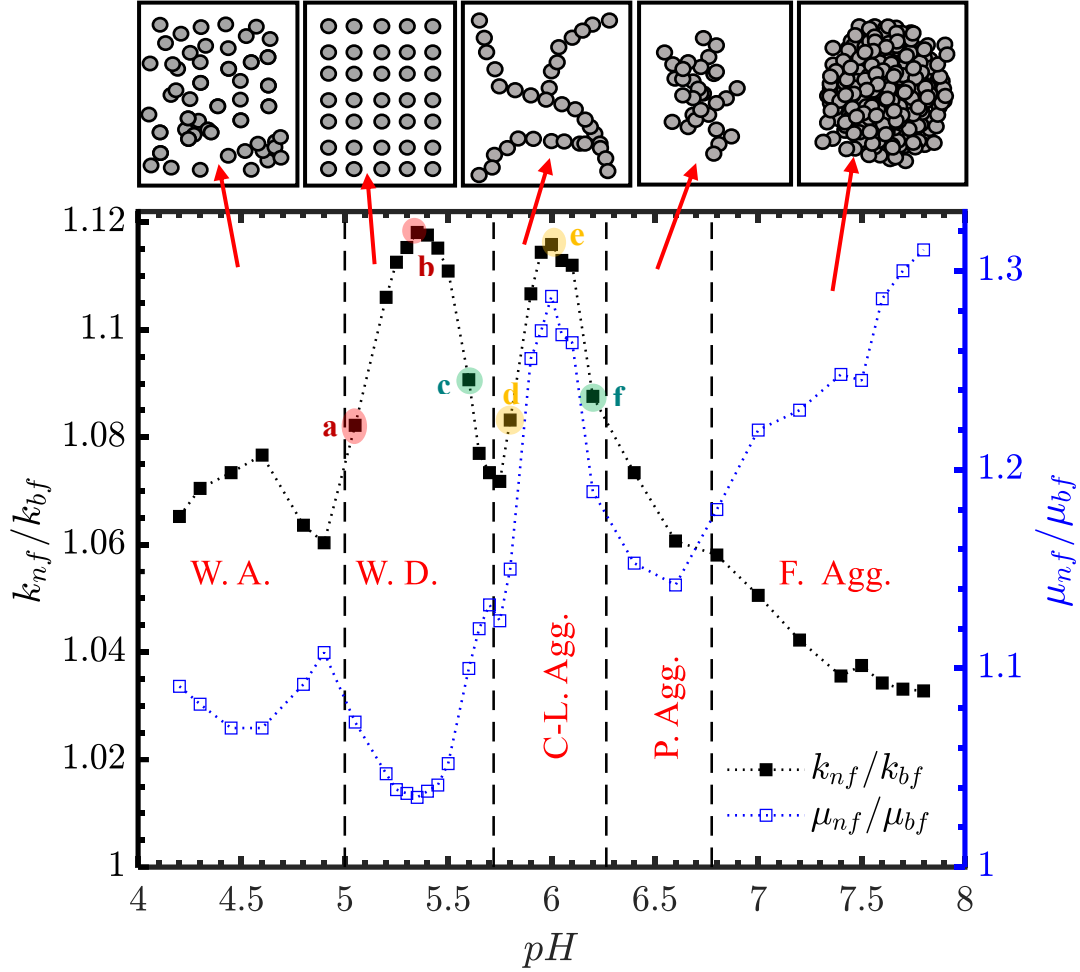


Figure IV-3 Dispersion regimes – Relative thermal conductivity and dynamic viscosity as a function of pH for $\phi = 0.7$ vol. % at $T = 25^\circ\text{C}$.

IV-5.1 Effect of temperature on suspensions with initial state located within the W.D. regime

Fig.IV-4 presents the influence of the temperature on the thermal conductivity, dynamic viscosity and pH for the suspension (b) (Center of W.D. regime area, initial pH = 5.35, at $T = 25^\circ\text{C}$, Fig.IV-3) and pure water, for the sake of comparison, during heating and cooling cycles. As expected and checked during calibration and validation protocols, pure liquid water exhibits no hysteresis phenomenon. (Figs. IV-1 and IV-2). The suspension was heated up to 80°C or below a critical temperature, T_{cr} , defined as the temperature at which a sudden change of the properties occurs. Each heating cycle was followed by cooling down to 25°C . Fig.IV-5 displays the corresponding relative thermal conductivity and dynamic viscosity as a function of temperature.

As it can be seen in Fig.IV-4c, any change in temperature induces a change in the pH of the solution, which can be correlated to the dispersion regimes of Fig. IV-3 and may, in turn, bring helpful information regarding agglomeration and the hysteresis phenomenon.

For the temperature range between 25 and 70°C, the pH of this suspension (b) is decreased during heating, followed, at about 70°C, by a sudden and irregular increase of the pH (Fig.IV-4c). Katiyar et al. [51] reported a similar pH decrease with an Alumina/water based nanofluid between 30 and 55°C. They ascribed it to a change of the hydronium ion concentration, $H_3O^+_{eff}$, in the colloidal system using analogy of standard definition of pH as:

$$pH = -\log [H_3O^+_{eff}]. \quad (IV-2)$$

$H_3O^+_{eff}$ is the effective hydronium ions. They suggested that the change of $[H_3O^+_{eff}]$ concentration is due to pull created on the water coming from the formation of the Electrical Double Layer (EDL) around the nanoparticles. In the case of the base fluid, an increase in temperature leads to an effective decrease in the net attractive force among the polar base fluid molecules because of a weakening of the hydrogen bond strength due to the increase of thermal fluctuations. Essentially, the effective polar nature is enhanced, causing a partial augmentation in the $[H_3O^+]$ ion concentration within the polar water molecules. This causes a slight dip in pH as temperature increases. Even though the authors were not dealing with high temperatures (i.e. above 55°C), the proposed explanation may be used to account for the observed increase in pH from 70°C. According to the DLVO theory developed by Derjaguin, Landau, Verwey, and Overbeek, the particle stability depends on its total potential energy [52]. The zeta potential, particle separation and the thickness of the EDL influence the state of the nanosuspension [2]. At higher temperatures due to enhanced thermal energy, the Brownian motion increases, which can increase the collision and cohesion of the particles. This may cause a possible agglomeration of particles. The initial dip in the pH value, due to the presence of well-dispersed nanoparticles, may be compromised. In the case of excessive agglomeration, water molecules under the influence of EDL decreases. As a result, the $[H_3O^+]$ concentration of the nanofluid decreases and therefore leads to an increase of the solution pH. Once the sample is heated above the critical temperature, the slope of the pH curve is reversed, the increase in temperature then causes an increase of the pH and an hysteresis phenomenon is observed during the subsequent cooling step. If sample temperature is not exceeding the critical temperature during the heating ramp, no hysteresis phenomenon occurs. This

phenomenon is observed for both thermal conductivity and viscosity measurements at the same critical temperature (Figures.IV-4a and IV-4b). The agglomeration formed beyond the critical temperature may be due to the excessive effect of Brownian motion at higher temperature, but may also be traced back to the dispersion regime transition caused by the remoteness of the pH value from the stability range. Indeed, Figure IV-3 shows that the lower limit of the well-dispersed regime area is at $\text{pH} = 5.05$. When the temperature rises and reaches the critical temperature, the pH of this sample (b) decreases from its initial value of 5.35 to 4.85. This may yield to a change from the W.D. to the weakly attracted (W.A.) regime.

Figure IV-5 depicts the relative thermal conductivity and relative dynamic viscosity as a function of temperature for suspension (b) (optimal suspension within the well-dispersed regime). The results show that the increase in thermal conductivity occurs unequally within the temperature range ($25^{\circ}\text{C} < T < 70^{\circ}\text{C}$). Indeed, one of the mechanisms of heat transfer explaining the unusual increase in the thermal conductivity of nanofluids is the Brownian motion. This movement can be regarded as the stochastic motion of the nanoparticles suspended in a fluid resulting from their collision with the fast-moving molecules in the base fluid. This mechanism depends on both particle size and temperature. In a well-dispersed regime (suspension b), the particles are at their smallest size, the movement of the base fluid molecules then has more impact on the particles and the Brownian motion is more important. The increase in temperature causes more thermal agitation bringing more nano-effect in the conducting behavior of the nanofluid. This explanation can be the reason for the improvement of the relative thermal conductivity of the suspension between 25 and 45°C . At more elevated temperatures, the effect of the Brownian motion becomes more pronounced, causing more collisions between particles and eventually agglomeration beyond the critical temperature. Once the critical temperature (T_{cr}) is reached, irreversible change appears and affects the properties of the suspensions since they are no longer able to reach the same levels of efficiency during the cooling phase. This results in a lower thermal conductivity and a higher dynamic viscosity, evolutions that go against the expected properties of an efficient nanofluid. What is even more important to note is the hysteresis curve which is developing and which is characterized by a shift of the measured values of the suspension properties between the heating and the cooling ramps. This phenomenon does not appear if the nanofluid temperature is not exceeding the critical temperature. As it can be seen in Figs. IV-4a and IV-4b, conductivity,

viscosity and pH curves during the cooling phase, when keeping the nanofluid below the critical temperature ($T < T_{cr}$), overlap quite well with those obtained during the heating phase.

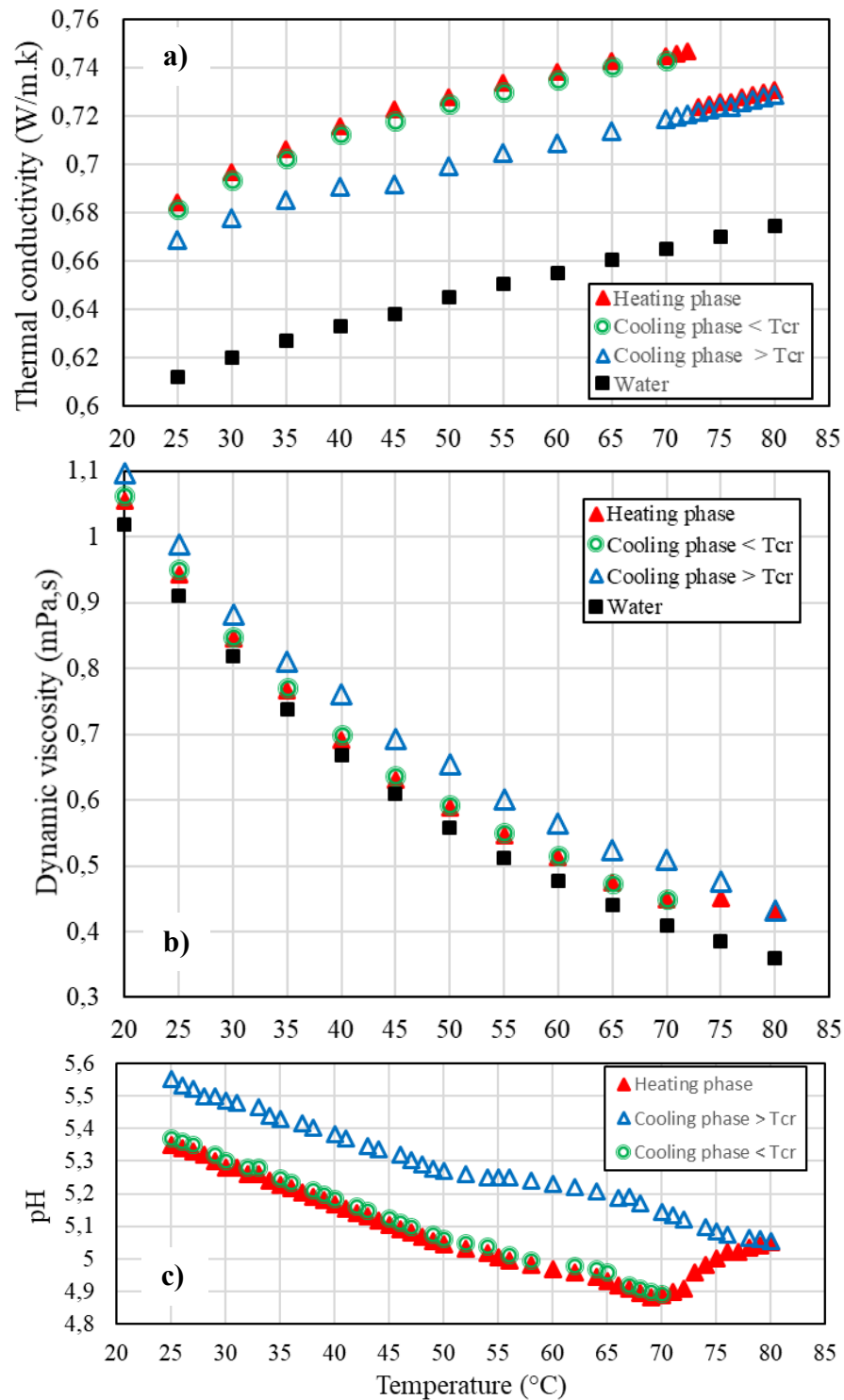


Figure IV-4 : Influence of the temperature on the (a) thermal conductivity, (b) dynamic viscosity and (c) pH for the suspension (b) (center of the W.D. zone: initial pH = 5.35 at T=25°C in Figure IV-3).

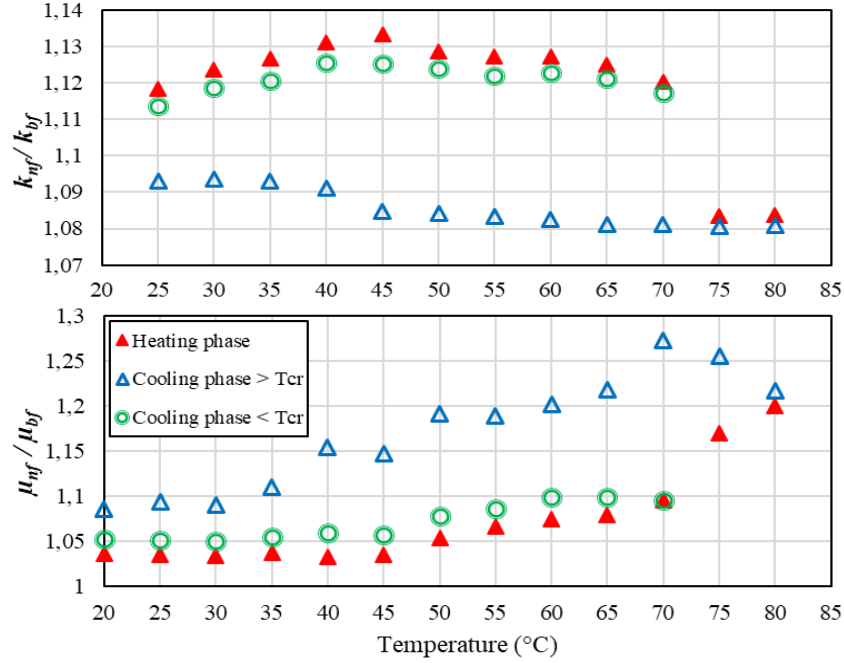


Figure IV-5 Relative thermal conductivity and dynamic viscosity as a function of temperature for the suspension (b) (center of the well-dispersed area: initial pH = 5.35 at $T=25^{\circ}\text{C}$ in Figure IV-3).

Figure IV-6 presents the influence of the temperature on the thermal conductivity, dynamic viscosity and pH for the sample from the low end of the well-dispersed area (suspension (a) with initial pH = 5.05 at $T=25^{\circ}\text{C}$ in Figure IV-3). Figure IV-7 depicts the corresponding relative thermal conductivity and dynamic viscosity as a function of temperature. As it can be seen in Figure IV-6c, the increase in temperature causes a decrease in pH, which can induce a change of the dispersion regime from the W.D. to the weakly attracted (W.A.) one. Similarly to suspension (b), this sample also exhibits the hysteresis phenomenon but with a lower critical temperature ($T_{cr} \sim 65^{\circ}\text{C}$).

As the temperature increases, the thermal conductivity of this sample increases significantly in a first step before experiencing a change from 45°C . As one can see in Fig. IV-7, the relative thermal conductivity increases between 25 and 45°C before experiencing a first drop between 45 and 50°C and, a second one larger beyond 65°C . The first drop in the relative thermal conductivity could be regarded as the signature of the transition to the weakly attracted (W.A.) regime. In this temperature range (50 to 65°C), k_{nf}/k_{bf} remains constant and no longer benefit that much from the effect of the Brownian motion. Indeed, in the W.A. regime, the particle size increases and requires more energy to be set into motion. When the temperature exceeds 65°C , an increase in the dynamic viscosity and a larger decrease in the relative thermal conductivity were observed. During

the heating ramp, this sample goes through three phases delimited by two key temperatures. The first temperature could be associated to the transition between the dispersion regimes and, the second one corresponds to the critical temperature beyond which irreversible damages alter the properties of the nanofluid. Indeed, and contrary to sample (b), for which no hysteresis appears as long as $T < T_{cr}$, this sample exhibits a low amplitude hysteresis phenomenon when temperature is between 25 and 45 °C. During the heating-cooling cycle, a slight shift of k , μ and pH appears whereas the temperature remains below T_{cr} . This could be explained by the fact that if the sample has left the well-dispersed zone during the heating ramp, then it is difficult for the suspension to get back to its initial state without external energy (e.g. sonification).

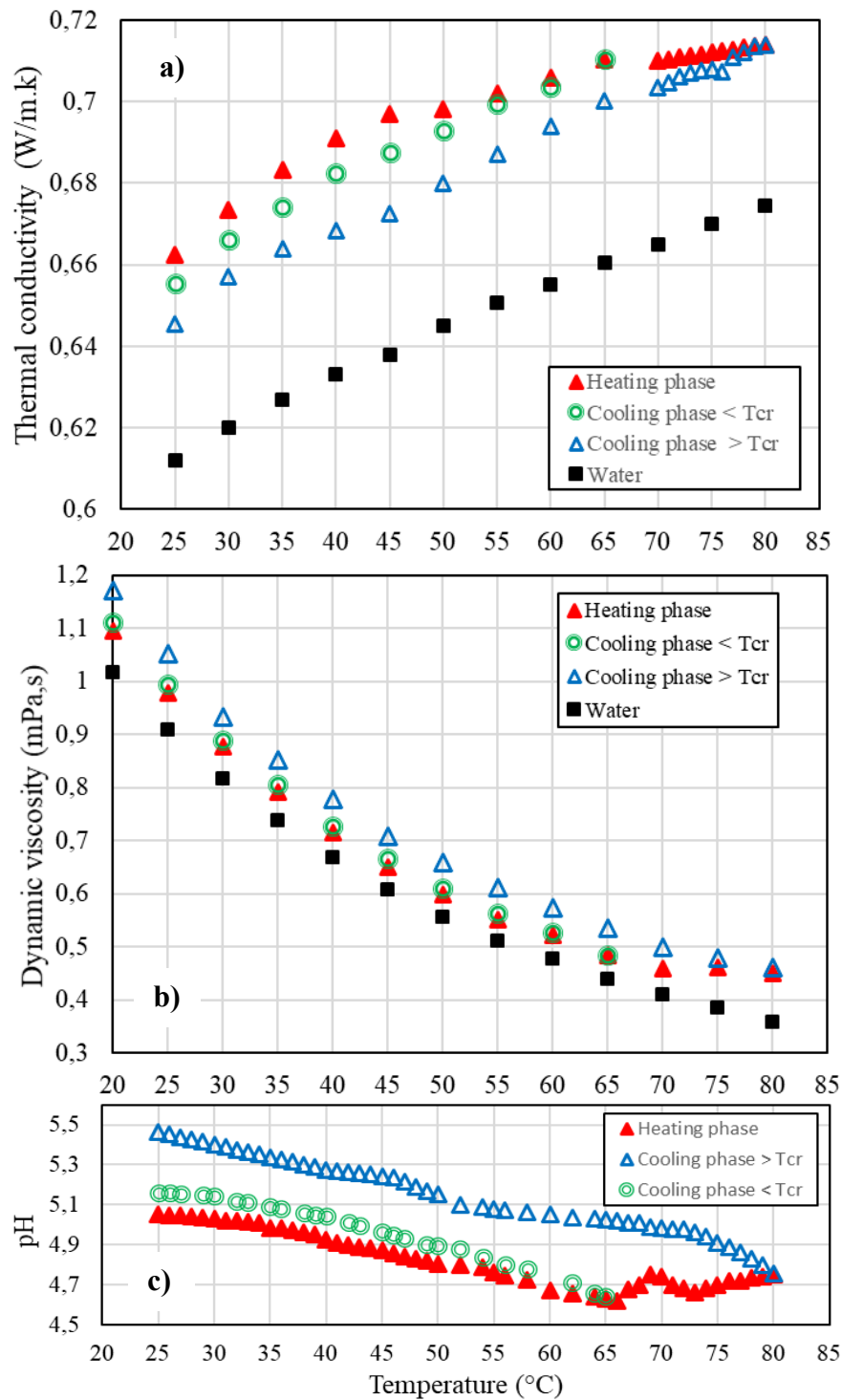


Figure IV-6 . Influence of the temperature on the (a) thermal conductivity, (b) dynamic viscosity and (c) pH for the suspension (a) (low end of the W.D. area: initial pH = 5.05 at T=25°C in Figure IV-3).

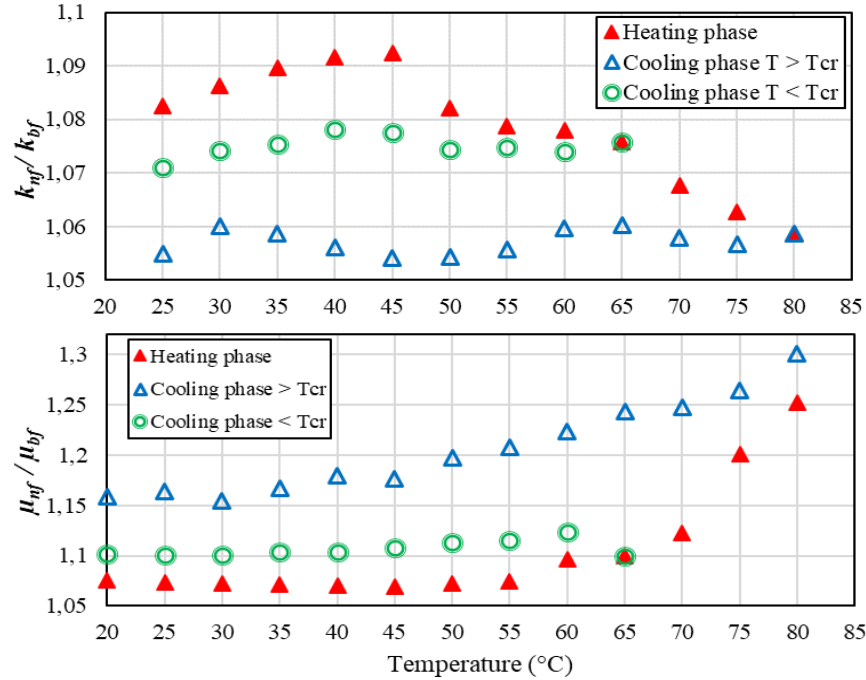


Figure IV-7 Relative thermal conductivity and dynamic viscosity as a function of temperature for the suspension (a) (low end of the W.D. area: initial pH = 5.05 at $T=25^{\circ}\text{C}$ in Figure IV-3).

Fig. IV-8 presents the influence of the temperature on the thermal conductivity, dynamic viscosity and pH for sample (c) (i.e. upper end of the W.D. regime pH = 5.6 at $T=25^{\circ}\text{C}$ in Fig. IV-3). Fig.IV-9 displays the corresponding relative thermal conductivity and dynamic viscosity as a function of temperature. As it can be seen in Fig.IV-8c, the increase in temperature causes a decrease in pH. Unlike samples (a) and (b) where the slopes of the curves were reversed when the samples were heated beyond their critical temperatures, the pH of sample (c) decreases continuously. At the initial state, before the heating process, this sample is at the upper limit of the well-dispersed zone. It means, according to Fig.IV-3, that it can take advantage of a wider window of pH for maintaining its dispersion regime during the heating phase. As a result, it is not surprising to observe no hysteresis phenomenon for this sample within the whole investigated temperature range (Fig.IV-8). It is also interesting to note that sample (c) exhibits an improved thermal conductivity at high temperatures. As one can see in Fig.IV-9, the relative thermal conductivity increases continuously. Similarly to sample (a) and (b), this sample (c) benefits also from the effect of Brownian motion but within a wider temperature range while maintaining its dispersion regime (i.e. well dispersed).

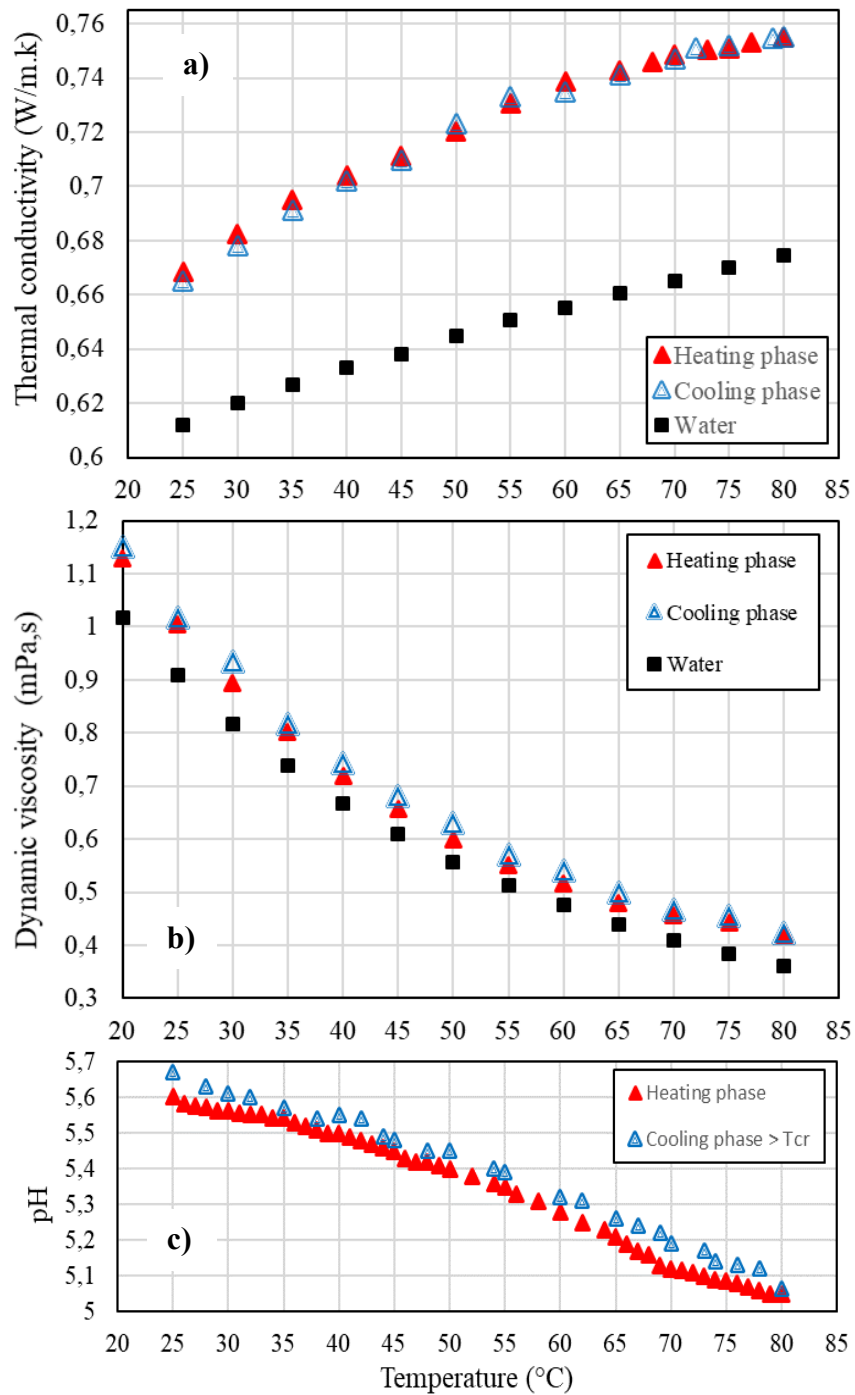


Figure IV-8 Influence of the temperature on the (a) thermal conductivity, (b) dynamic viscosity and (c) pH for the suspension (c) (upper end of the W.D. area: initial pH = 5.6 at T=25°C in Figure IV-3).

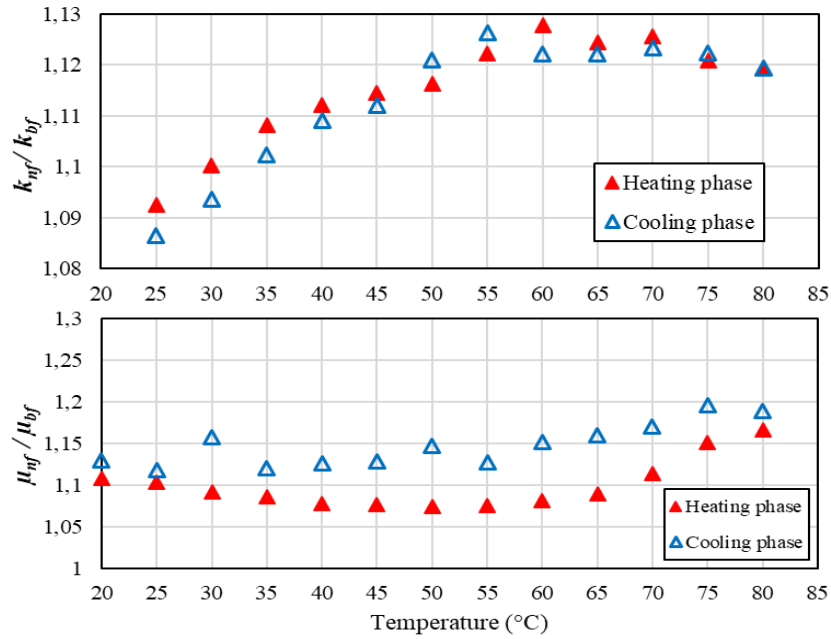


Figure IV-9 Relative thermal conductivity and dynamic viscosity as a function of temperature for the suspension (c) (upper end of the W.D. area: initial pH = 5.6 at T=25°C in Figure IV-3).

IV-5.2 Effect of temperature on suspensions with initial state located within the C-L.Agg. regime

Figure IV-10 presents the influence of the temperature on the thermal conductivity, dynamic viscosity and pH for the suspension (e) (center of the chain-like agglomerated zone: initial pH = 6 at T=25°C, Fig.IV-3). Fig.IV-11 displays the corresponding relative thermal conductivity and relative dynamic viscosity as a function of temperature. The initial state before the heating process corresponds to the peak value of the thermal conductivity in the C-L. Agg regime. This state of dispersion is characterized by an unexpected increase in viscosity (Fig.IV-3). Unlike the fully agglomerated regime, where all the benefits of the well-dispersed state disappear, this specific particle arrangement continues to benefit from a relatively high surface/volume ratio, which brings more exchange surface with the liquid and permits the nanolayer to occupy a larger part of the volume. On the other hand, this kind of particle arrangement can minimize the influence of Brownian motion since the size of the structures is moving away from that of the base fluid molecules. Indeed, unlike samples from the well-dispersed area, where their relative thermal conductivity takes advantage of the thermal agitation and increases as a function of temperature, this sample (e) has fairly equivalent conductivity ratios over the 25 to 55 °C temperature range. At

these temperature levels, the thermal conductivity increases continuously before going through a disturbance zone during which a sudden decrease in k_{nf} is noticed between 60 and 70 °C. As of 70 °C, k_{nf} increases with a similar slope (dk_{nf}/dT) obtained below 60°C. Over the temperature range between 70 and 80 °C, the increase in thermal conductivity is accompanied by a considerable decrease in dynamic viscosity, which provides information on a structural change of the suspension. Fig.IV-10c indicates that the pH of the sample decreases as a function of temperature and reaches, when the temperature is between 70 and 80 °C, values less than 5.5. According to Fig.IV-3, these values suggest that the arrangement of the particles is within the well-dispersed regime region. The disturbance zone between 60 and 70 °C may be related to the transition zone from the C-L. Agg to the W.D. regime. During this phase, the particle chains, responsible for the enhanced thermal conductivity, break and the suspensions no longer benefit from the highly conductive effect provided by this path network (thermal bridges). The breaking of this particle chain arrangement may also explain the relative decrease in dynamic viscosity over this temperature range. During the heating ramp, this sample goes, consequently, through three phases. Suspension (e) benefits from the advantages of the highly conductive C-L. Agg regime for low temperatures and those of the well-dispersed regime for high temperatures. Between these two states of dispersion, a disturbance zone delimits the transition phase between the two regimes. This transition zone is characterized by low relative thermal conductivity and intermediate viscosity ratios. Indeed, the value of the relative viscosity during this phase is between the high viscosity caused by the chain-like suspensions and the low viscosity, which is the characteristic of the well-dispersed state. This temperature seems to be the critical temperature since an hysteresis phenomenon was observed. However, since no irreversible damage was reported, T_{cr} is closer, in the case of sample (e), to a transition temperature than to the classical T_{cr} as observed in the case of the W.D. samples (*a and b*). During the cooling ramp, even if the values are not identical and the properties of the nanofluid go through a transition zone characterized by lower performances, this sample reaches, somehow, its initial performances. The hysteresis phenomenon is present but its amplitude is limited and has little effect on the properties. Even better, in the case of the dynamic viscosity, this phenomenon is beneficial since the values of μ during the cooling ramp are lower than that of the heating ramp. The hysteresis phenomenon does not appear if the critical temperature is not exceeded. As one can see in Figure IV-10, the conductivity, viscosity and pH curves during the cooling phase ($T < T_{cr}$) are similar to those of the heating.

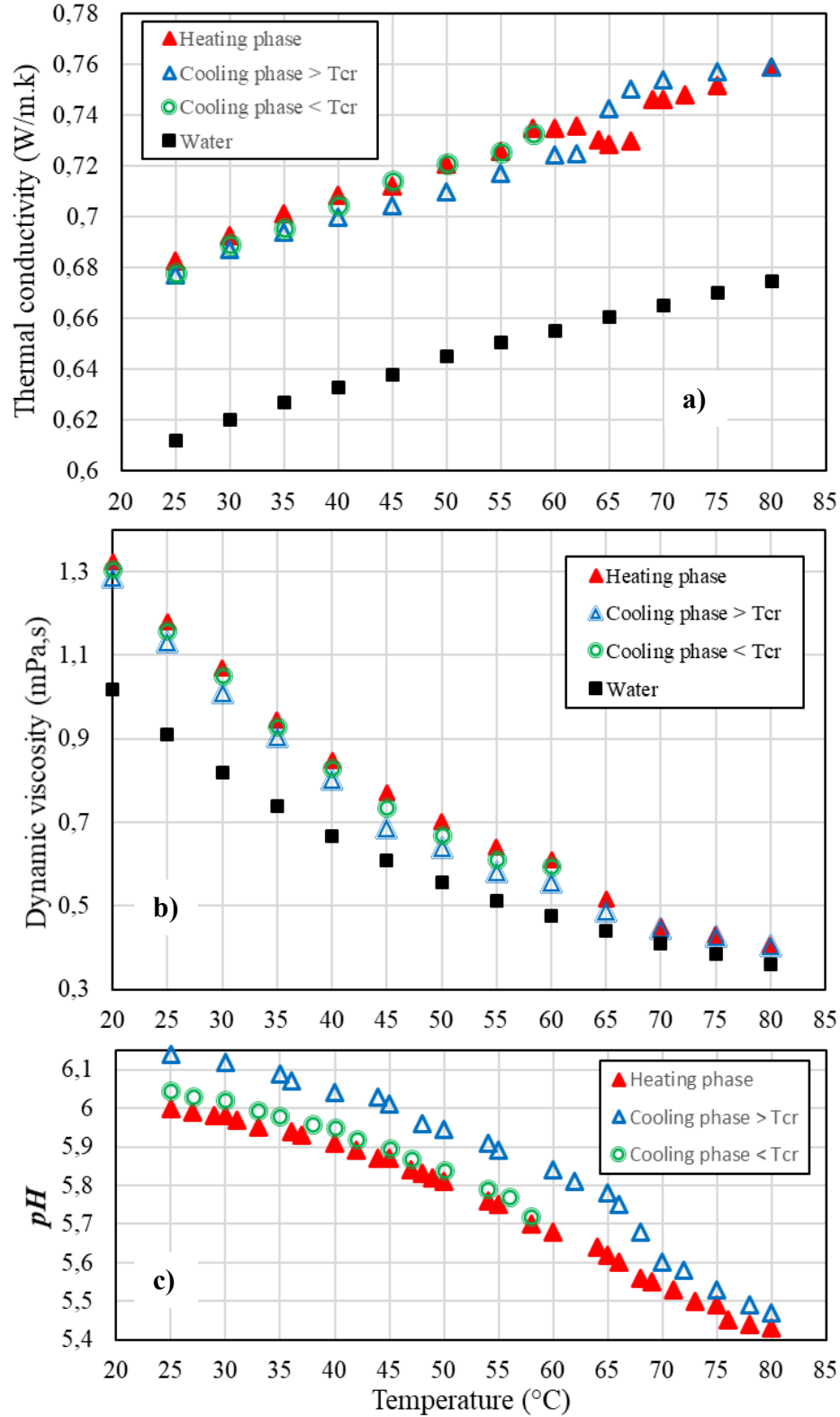


Figure IV-10 Influence of the temperature on the (a) thermal conductivity, (b) dynamic viscosity and (c) pH for the suspension (e) (center of C-L agg. zone: initial pH = 6 at T=25°C in Figure IV-3).

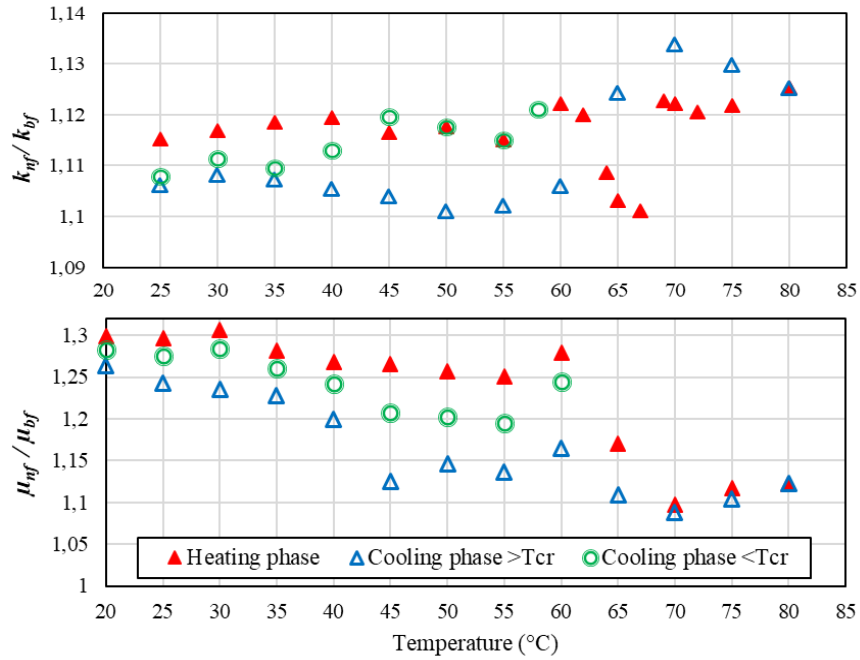


Figure IV-11 Relative thermal conductivity and dynamic viscosity as a function of temperature for the suspension (e) (center of C-L agg. Zone: initial pH = 6 at $T=25^{\circ}\text{C}$ in Figure IV-3).

Figure IV-12 presents the influence of the temperature on the thermal conductivity, dynamic viscosity and pH for the suspension (f) (upper end of the C-L. agg. area: initial pH = 6.2 at $T=25^{\circ}\text{C}$ in Figure IV-3). Figure IV-13 displays the corresponding relative thermal conductivity and relative dynamic viscosity as a function of temperature. In its initial state, before the heating process, this sample (f) is characterized by relatively high values of thermal conductivity and dynamic viscosity, but which remain lower than those obtained with the sample coming from the center of this zone (suspension (e)). As it can be seen in Fig.IV-12c, pH decreases as the temperature increases, which brings the pH of the suspensions (f) within the optimal range of the C-L. agg regime. As shown in Figs. IV-12a and IV-12b, the increase in temperature during the heating cycle results in an increase of the thermal conductivity and a decrease of the dynamic viscosity. This trend persists continuously over the entire investigated temperature range. Fig. IV-13 shows that the increase in thermal conductivity occurs unequally according to the temperature level. Unlike samples from the well dispersed regime where this increase was followed by a slight decrease of viscosity ratios or unchanged values, the viscosity ratios of sample (f) increases during the heating cycle ($20^{\circ}\text{C} < T < 65^{\circ}\text{C}$). This can therefore indicate that the enhancement of the thermal conductivity cannot be accounted for the accentuation of the Brownian motion but can be

linked to the reinforcement of the thermal path network generated by the magnification of the particle chains. In an attempt to summarize the concatenation of causes and effects, the temperature increase leads to the reduction of the solution pH and its displacement towards the optimum values of the chain-like agglomerated regime. This results in an increase of the relative thermal conductivity and the relative viscosity that reflects the growth of particle chains. At high temperatures ($T > 70\text{ °C}$), the trend reverses and the ratios start to decrease. The pH reaches values that should correspond to the lower limit of the C-L. agg. region. This does not affect the intrinsic values of the thermal conductivity, which continues to increase as a function of temperature but with a lower slope. The viscosity also continues to decrease and its relative increase is no longer important similarly to the first part of the heating ramp. During the entire heating step, this sample does not show any sign of excessive agglomeration or goes against the expected behavior of an efficient nanofluid. However, the cooling ramp reveals the appearance of a rather particular hysteresis phenomenon. In fact, the cooling of this sample (f) decreases the thermal conductivity at the beginning but at the end, k reaches higher values than those displayed during the heating ramp. Also, the viscosity at the end of the cooling ramp is higher than the one at the beginning of the heating ramp (initial state at 25°C). The hysteresis phenomenon, a priori without consequences for this case (sample f), does not appear if the critical temperature is not exceeded (here $T_{cr} \sim 65\text{°C}$).

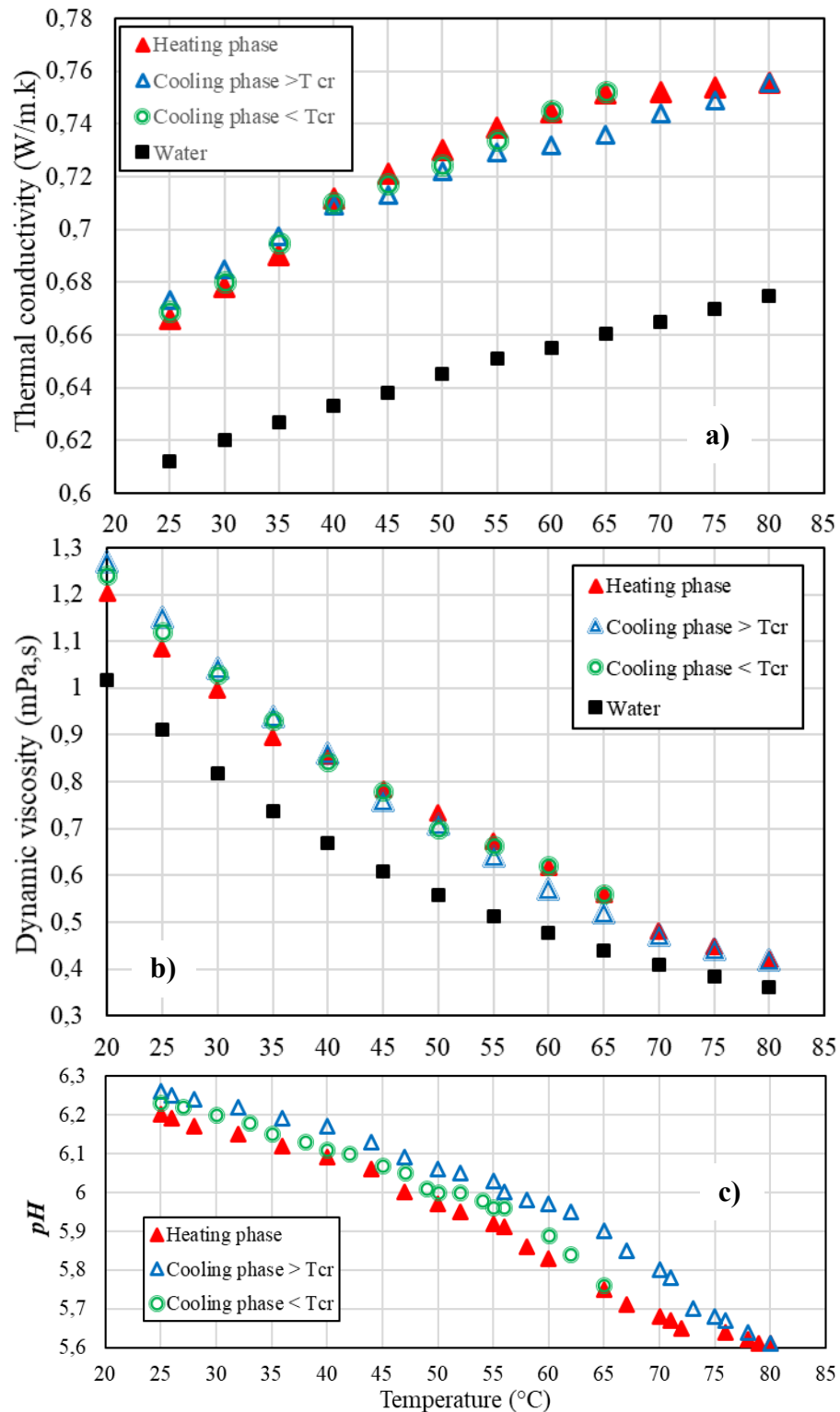


Figure IV-12 Influence of the temperature on the (a) thermal conductivity, (b) dynamic viscosity and (c) pH for the suspension (f) (upper end of C-L. agg zone: initial pH = 6.2 at T=25°C in Figure IV-3).

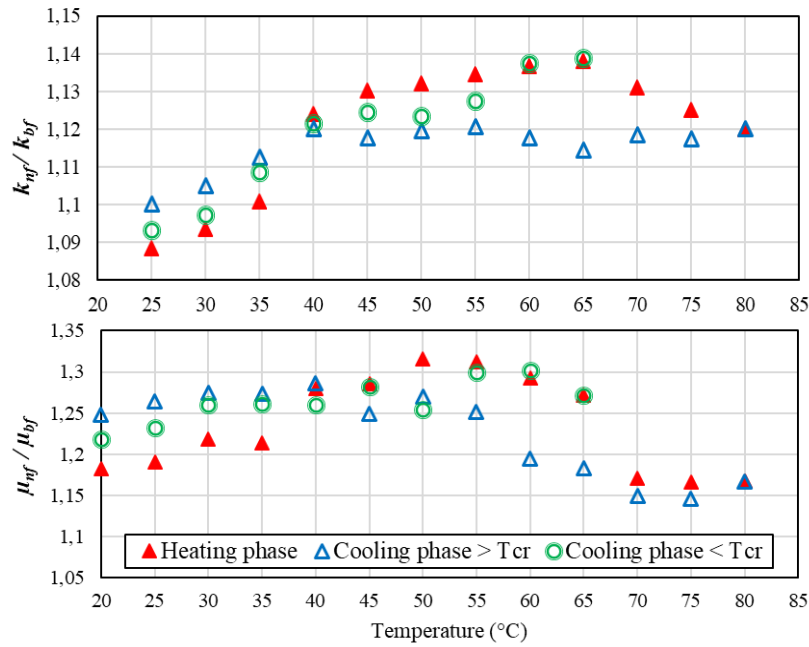


Figure IV-13 Relative thermal conductivity and dynamic viscosity as a function of temperature for the suspension (f) (upper end of C-L. agg. zone: initial pH = 6.2 at $T=25^{\circ}\text{C}$ in Figure IV-3).

Figure IV-14 presents the influence of the temperature on the thermal conductivity, dynamic viscosity and pH for the suspension (d) (lower end of the C-L. agg. zone: initial pH = 5.8 at $T=25^{\circ}\text{C}$ in Figure IV-3). Figure IV-15 displays the corresponding relative thermal conductivity and dynamic viscosity as a function of temperature. The results seem to indicate that the apparent behavior of this sample (d) is somehow similar to those of sample (e). The only difference between the two suspensions is the transition zone which shifted to lower temperatures ($\sim 40^{\circ}\text{C}$). This can be explained by the fact that at its initial state, this sample is in between the two dispersion regimes. The slight temperature increase seems to yield to a quick transition from the chain-like agglomerated regime to the well-dispersed regime.

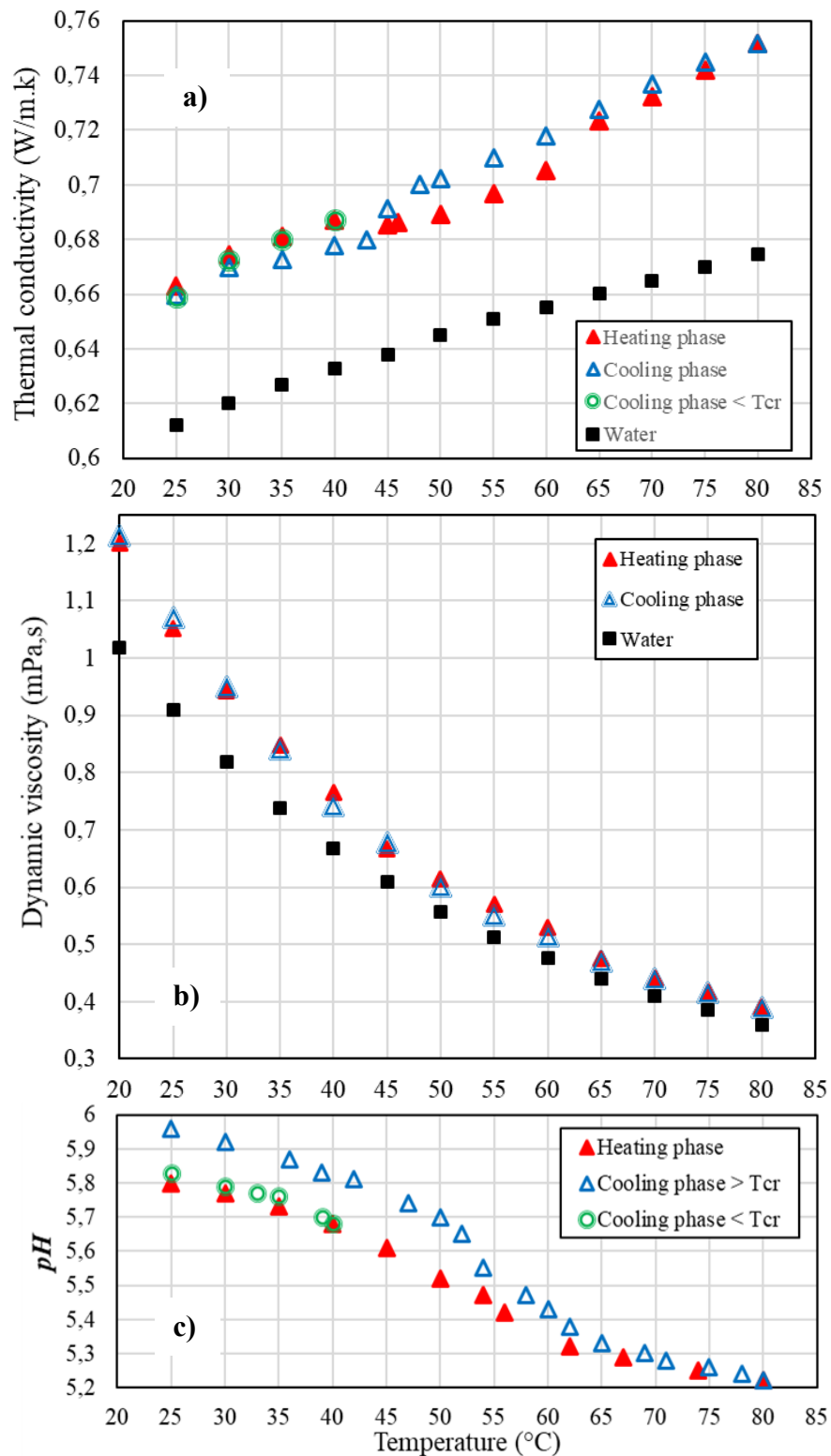


Figure IV-14 Influence of the temperature on the (a) thermal conductivity, (b) dynamic viscosity and (c) pH for the suspension (d) (lower end of C-L. agg. zone: initial pH = 5.8 at T=25°C in Figure IV-3).

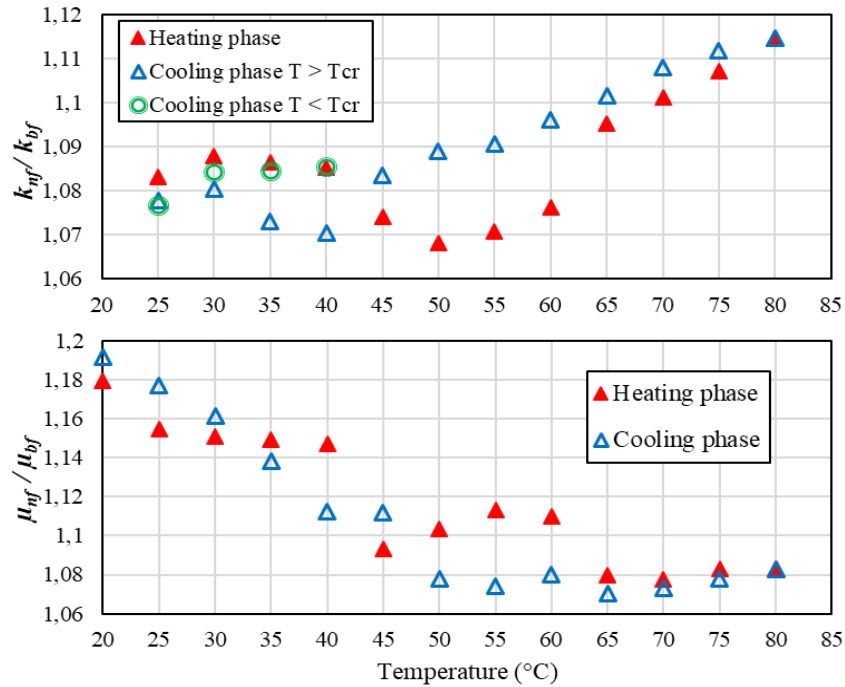


Figure IV-15 Relative thermal conductivity and dynamic viscosity as a function of temperature for the suspension (d) (lower end of C-L. agg. zone: initial pH = 5.8 at $T=25^{\circ}\text{C}$ in Figure IV-3).

IV-6 Conclusion

In this study, we have tried to understand the mechanisms leading to the presence of an hysteresis phenomenon on the thermophysical properties of nanofluids subjected to heating and cooling cycles. As the nanofluid was targeted to be used as a heat exchanger fluid, the $\text{Al}_2\text{O}_3/\text{water}$ nanofluid was chosen and, thermal conductivity and dynamic viscosity were determined simultaneously. Thus, a $\text{Al}_2\text{O}_3/\text{water}$ nanofluid suspension was thoroughly prepared and characterized. Then, simultaneous measurements of the thermal conductivity and dynamic viscosity of the suspension were carried out, at room temperature, in order to investigate the effect of the pH on the dispersion state and the stability of Al_2O_3 nanoparticles. As expected, 5 dispersion states, referred to as dispersion regimes, were observed. Among the 5 dispersion regimes, only the W.D regime, characterized by an optimal dispersion and small size of the nanoparticles, and C-L.Agg. regime, with chain-like arrangement of nanoparticles, exhibit a maximum of the thermal conductivity. These 2 regimes are consecutive and stable within 5 to 5.6 and 5.6 to 6.3 pH range respectively.

In order to understand the effect of temperature on suspension stability and hysteresis phenomenon, 6 different suspensions initially located within the WD and C-L.Agg regimes were selected. 2 suspensions with the pH for which a maximum of the thermal conductivity was found in both regimes while, the other 4 were chosen close to the pH boundaries of each regime. The results evidenced the existence of two critical temperatures that lead to the hysteresis phenomenon. This latter was ascribed to different mechanisms depending on the temperature and the pH of the initial suspension. When the suspension temperature is sufficiently high and above a critical temperature, an irreversible damage was inferred along with an hysteresis phenomenon during the subsequent cooling step. This result was explained by an increase of the thermal agitation and the Brownian motion that led to more particles collision and agglomeration and, eventually, to a definitive loss of the dispersion state. A second critical temperature leading to a less pronounced hysteresis phenomenon, present at lower temperature as compared to the first one, was observed. This critical temperature was accounted for by a dispersion regime transition. Indeed, as temperature was increased, the pH of the suspension decreased and a change in the dispersion regime was inferred. Eventually, both mechanisms (i.e. loss of dispersion state and change of dispersion regime) may take place simultaneously depending on the temperature as well as dispersion regime and the pH of the initial suspension.

Acknowledgement

The authors would like to acknowledge the Centre de Caractérisation des Matériaux (CCM) of the Université de Sherbrooke for their help in nanoparticles characterization, Sigma Energy Storage Inc. for allowing us to use their THW apparatus for thermal conductivity measurements and, department of chemistry of the Université de Sherbrooke for allowing us to work in their laboratories and use their zetasizer for particles size characterization.

IV-7 Références

- [1] S.U.S. Choi, J.A. Eastman, Enhancing thermal conductivity of fluids with nanoparticles, in: Proc. ASME Int. Mech. Eng. Congr. Expo., San Francisco, CA, 1995.
- [2] S.K. Das, S.U.S. Choi, W. Yu, T. Pradeep, Nanofluids : Science and Technology, John Wiley & Sons, Hoboken, USA, 2008.
- [3] J.C. Maxwell, A Treatise on Electricity and Magnetism, 2nd Edition, Clarendon Press, Oxford, 1881.
- [4] J.A. Eastman, S.U.S. Choi, L.J. Thompson, S. Lee, Enhanced Thermal Conductivity Through the Development of Nanofluids, MRS Proceedings 457, (1996) 3-11.
- [5] M.S. Liu, M.C.C. Lin, I.T. Huang, C.C. Wang, Enhancement of Thermal Conductivity with CuO for Nanofluids, Chem. Eng. Technol. 29 (2006) 72–77.
- [6] Y. Hwang, H.S. Park, J.K. Lee, W.H. Jung, Thermal conductivity and lubrication characteristics of nanofluids, Curr. Appl. Phys. 6 (2006) 67–71.
- [7] W. Yu, H. Xie, L. Chen, Y. Li, Investigation of thermal conductivity and viscosity of ethylene glycol based ZnO nanofluid, Thermochim. Acta. 491 (2009) 92–96.
- [8] H.A. Mints, G. Roy, C.T. Nguyen, D. Doucet, New temperature dependent thermal conductivity data for water-based nanofluids, Int. J. Therm. Sci. 48 (2009) 363–371.
- [9] J. Huang, X. Wang, Q. Long, X. Wen, Y. Zhou, L. Li, Influence of pH on the Stability Characteristics of Nanofluids, in: 2009 Symp. Photonics Optoelectron., IEEE eXpress Conference Publishing, Wuhan, 2009: pp. 1–4.
- [10] H. Xie, J. Wang, T. Xi, Y. Liu, F. Ai, Q. Wu, Thermal conductivity enhancement of suspensions containing nanosized alumina particles, J. Appl. Phys. 91 (2002) 4568–4572.
- [11] J.H. Lee, S.H. Lee, S.P. Jang, Do temperature and nanoparticle size affect the thermal conductivity of alumina nanofluids?, Appl. Phys. Lett. 104 (16) (2014), 161908.
- [12] K. Bashirnezhad, S. Bazri, M.R. Safaei, M. Goodarzi, M. Dahari, O. Mahian, A.S. Dalkılıç, S. Wongwises, Viscosity of nanofluids: A review of recent experimental studies, Int. Commun. Heat Mass Transf. 73 (2016) 114–123.

- [13] J.H. Lee, K.S. Hwang, S.P. Jang, B.H. Lee, J.H. Kim, S.U.S. Choi, C.J. Choi, Effective viscosities and thermal conductivities of aqueous nanofluids containing low volume concentrations of Al_2O_3 nanoparticles, *Int. J. Heat Mass Transf.* 51 (2008) 2651–2656.
- [14] J.A. Eastman, S.R. Phillpot, S.U.S. Choi, P. Keblinski, Thermal Transport in Nanofluids, *Annu. Rev. Mater. Res.* 34 (2004) 219–246.
- [15] S. El Bécaye Maïga, S.J. Palm, C.T. Nguyen, G. Roy, N. Galanis, Heat transfer enhancement by using nanofluids in forced convection flows, *Int. J. Heat Fluid Flow.* 26 (2005) 530–546.
- [16] M.M. Heyhat, F. Kowsary, A.M. Rashidi, M.H. Momenpour, A. Amrollahi, Experimental investigation of laminar convective heat transfer and pressure drop of water-based Al_2O_3 nanofluids in fully developed flow regime, *Exp. Therm. Fluid Sci.* 44 (2013) 483–489.
- [17] S.M.S. Murshed, K.C. Leong, C. Yang, Thermophysical and electrokinetic properties of nanofluids - A critical review, *Appl. Therm. Eng.* 28 (2008) 2109–2125.
- [18] X.Q. Wang, A.S. Mujumdar, A review on nanofluids - Part II: Experiments and applications, *Brazilian J. Chem. Eng.* 25 (2008) 631–648.
- [19] R.S. Vajjha, D.K. Das, P.K. Namburu, Numerical study of fluid dynamic and heat transfer performance of Al_2O_3 and CuO nanofluids in the flat tubes of a radiator, *Int. J. Heat Fluid Flow.* 31 (2010) 613–621.
- [20] S.U. Ilyas, R. Pendyala, N. Marneni, Preparation, Sedimentation, and Agglomeration of Nanofluids, *Chem. Eng. Technol.* 37 (2014) 2011–2021.
- [21] L. Chen, H. Xie, Y. Li, W. Yu, Nanofluids containing carbon nanotubes treated by mechanochemical reaction, *Thermochim. Acta.* 477 (2008) 21–24.
- [22] N. Bouguerra, A. Khabou, S. Poncet, S. Elkoun, Thermal Conductivity of Al_2O_3 /Water-Based Nanofluids: Revisiting the Influences of pH and Surfactant, *Int. J. Mech. Aerospace, Ind. Mechatron. Manuf. Eng.* 10 (2016) 1849–1858.
- [23] K. Holmberg, B. Jönsson, B. Kromberg, B. Lindman, Surfactants And Polymers In Aqueous Solutions, 2nd ed., John Wiley and Sons Ltd, Hoboken, USA, 2002.
- [24] E.E. Michaelides, Transport properties of nanofluids. A critical review, *J. Non-Equilibrium Thermodyn.* 38 (2013) 1–79.
- [25] D. Lee, J.-W. Kim, B.G. Kim, A new parameter to control heat transport in nanofluids: surface charge state of the particle in suspension, *J. Phys. Chem. B.* 110 (2006) 4323–4328.
- [26] N. Bouguerra, S. Poncet, S. Elkoun, Dispersion regimes in alumina/water-based nanofluids: Simultaneous measurements of thermal conductivity and dynamic viscosity, *Int. Commun. Heat Mass Transf.* 92 (2018) 51–55.
- [27] R. Prasher, P.E. Phelan, P. Bhattacharya, Effect of aggregation kinetics on the thermal conductivity of nanoscale colloidal solutions (nanofluid), *Nano Lett.* 6 (2006) 1529–1534.
- [28] H. Zhu, C. Zhang, S. Liu, Y. Tang, Y. Yin, Effects of nanoparticle clustering and alignment on thermal conductivities of Fe_3O_4 aqueous nanofluids, *Appl. Phys. Lett.* 89 (2006) 023123.
- [29] H.E. Patel, S.K. Das, T. Sundararajan, A. Sreekumaran Nair, B. George, T. Pradeep, Thermal conductivities of naked and monolayer protected metal nanoparticle based nanofluids:

Manifestation of anomalous enhancement and chemical effects, *Appl. Phys. Lett.* 83 (2003) 2931–2933.

[30] G. Paul, P.K. Das, I. Manna, Maneuvering the chain agglomerates of colloidal superparamagnetic nanoparticles by tunable magnetic fields, *Appl. Phys. Lett.* 105 (2014) 183108.

[31] R. Prasher, W. Evans, P. Meakin, J. Fish, P. Phelan, P. Keblinski, Effect of aggregation on thermal conduction in colloidal nanofluids, *Appl. Phys. Lett.* 89 (2006) 88–90.

[32] J. Sui, P. Zhao, B. Bin-Mohsin, L. Zheng, X. Zhang, Z. Cheng, Y. Chen, G. Chen, Fractal aggregation kinetics contributions to thermal conductivity of nano-suspensions in unsteady thermal convection, *Sci. Rep.* 6 (2016) 39446.

[33] P.D. Shima, J. Philip, B. Raj, Magnetically controllable nanofluid with tunable thermal conductivity and viscosity, *Appl. Phys. Lett.* 95 (2009) 1–4.

[34] J. Philip, P.D. Shima, B. Raj, Enhancement of thermal conductivity in magnetite based nanofluid due to chainlike structures, *Appl. Phys. Lett.* 91 (2007) 89–92.

[35] M. Chandrasekar, S. Suresh, A Review on the Mechanisms of Heat Transport in Nanofluids, *Heat Transf. Eng.* 30 (2009) 1136–1150.

[36] R. Vidonscky Pinto, F. Augusto, S. Fiorelli, Review of the mechanisms responsible for heat transfer enhancement using nanofluids, *Appl. Therm. Eng.* 108 (2016) 720–739.

[37] J.J. Wang, R.T. Zheng, J.W. Gao, G. Chen, Heat conduction mechanisms in nanofluids and suspensions, *Nano Today*. 7 (2012) 124–136.

[38] J.S. Duncan, Introduction to Colloid and Surface Chemistry, 4th Edition, Elsevier Science Ltd., Liverpool, 1992.

[39] R.M. Pashley and M.E. Karaman, Applied Colloid and Surface Chemistry, John Wiley & Sons Ltd, Australia, 2004.

[40] R. Zhang, P. Somasundaran, Advances in adsorption of surfactants and their mixtures at solid/solution interfaces, *Adv. Colloid Interface Sci.* 123–126 (2006) 213–229.

[41] S.K. Das, N. Putra, P. Thiesen, W. Roetzel, Temperature Dependence of Thermal Conductivity Enhancement for Nanofluids, *J. Heat Transfer* 125 (2003) 567–574.

[42] X. Zhang, H. Gu, M. Fujii, Effective thermal conductivity and thermal diffusivity of nanofluids containing spherical and cylindrical nanoparticles, *Exp. Therm. Fluid Sci.* 31 (2007) 593–599.

[43] J. Shah, M. Ranjan, V. Davariya, S.K. Gupta, Y. Sonvane, Temperature-dependent thermal conductivity and viscosity of synthesized α -alumina nanofluids, *Appl. Nanosci.* 7 (2017) 803–813.

[44] C.T. Nguyen, F. Desgranges, G. Roy, N. Galanis, T. Maré, S. Boucher, H. Angue Mintsa, Temperature and particle-size dependent viscosity data for water-based nanofluids – Hysteresis phenomenon, *Int. J. Heat Fluid Flow*. 28 (2007) 1492–1506.

[45] C.T. Nguyen, F. Desgranges, N. Galanis, G. Roy, T. Maré, S. Boucher, H. Angue Mintsa, Viscosity data for Al_2O_3 –water nanofluid—hysteresis: is heat transfer enhancement using nanofluids reliable?, *Int. J. Therm. Sci.* 47 (2008) 103–111.

- [46] Z. Said, R. Saidur, A. Hepbasli, N.A. Rahim, New thermophysical properties of water based TiO₂ nanofluid-The hysteresis phenomenon revisited, *Int. Commun. Heat Mass Transf.* 58 (2014) 85–95.
- [47] L. Godson, D.M. Lal, S. Wongwises, Measurement of Thermo Physical Properties of Metallic Nanofluids for High Temperature Applications, *Nanoscale Microscale Thermophys. Eng.* 14 (2010) 152–173.
- [48] H. Xie, H. Gu, M. Fujii, X. Zhang, Short hot wire technique for measuring thermal conductivity and thermal diffusivity of various materials, *Meas. Sci. Technol.* 17 (2006) 208–214.
- [49] F.P. Incropera, D.P. Dewitt, *Fundamentals of heat and mass transfer*, 2th ed, Wiley, USA, 1990.
- [50] K.D. Hagen, *Heat Transfer with Applications*, Prentice-Hall, New Jersey, 1999.
- [51] A. Katiyar, A.R. Harikrishnan, P. Dhar, Influence of temperature and particle concentration on the pH of complex nanocolloids, *Colloid Polym. Sci.* 295 (2017) 1575–1583. doi:10.1007/s00396-017-4132-7.
- [52] E.J.W. Verwey, J.T.G. Overbeek, *Theory of the Stability of Lyophobic Colloids. The interaction of Particles Having an Electric Double Layer.*, in: Elsevier, New York - Amsterdam, 1948: p. 631-636.

Chapitre V Conclusion générale

Les travaux de recherche réalisés au cours de cette thèse de doctorat ont permis d'examiner en profondeur les aspects liés à l'élaboration, la stabilisation et la caractérisation thermique et rhéologique des nanofluides à base d'eau et d'alumine afin d'essayer de mieux comprendre les mécanismes physicochimiques qui gouvernent ces suspensions et d'être en mesure d'évaluer les effets des différents paramètres pouvant influencer leurs propriétés. Dans cette optique et dans un cadre plus large que la simple caractérisation des propriétés, une attention particulière a été accordée à la mise en place d'un protocole expérimental adéquat.

Dans un premier temps et puisque les résultats expérimentaux issus de la littérature dévoilent des divergences voire même des contradictions, il était primordial alors de cerner les origines de ce manque de consensus. L'analyse bibliographique a permis d'identifier les conditions de préparation des nanofluides et surtout les méthodes de mesure employées comme étant les principaux facteurs pouvant expliquer ces écarts. Notre démarche s'est alors orientée vers la mise en place d'un programme expérimental le plus complet possible menant à la caractérisation fine des mélanges tout en intégrant systématiquement les différentes étapes de préparation et de stabilisation. De plus, un processus de sélection des dispositifs de mesure les plus adéquats a été engagé et dans ce sens la THW s'est imposée comme l'unique méthode appropriée à la mesure de la conductivité thermique des nanofluides.

Les résultats les plus importants de cette thèse ont fait l'objet de trois articles scientifiques, dont les principales conclusions sont reprises ci-dessous :

Dans le deuxième chapitre de ce manuscrit, l'effet de la variation du pH et de la concentration en tensioactif sur la conductivité thermique des nanofluides à base d'eau et d'alumine a été examiné expérimentalement. Les résultats ont montré que la stabilité des nanofluides a une influence directe sur la conductivité thermique. Un meilleur control des conditions de préparation et l'optimisation des valeurs du pH et de la concentration en tensioactif mènent à une amélioration de la conductivité thermique. Les effets de la taille et de la concertation des particules ont aussi été examinés dans les conditions optimales de préparation. Le principal défi de cette étude était la stabilisation des suspensions et l'élaboration d'un protocole expérimental

rigoureux permettant de contrôler les différents paramètres de l'étude et d'isoler leurs effets. Ainsi l'impact de chaque facteur a été évalué et les conclusions majeures sont listées dans ce qui suit :

- L'ajout du tensioactif SDBS provoque la variation du pH de la solution et n'améliore pas forcément la conductivité thermique, pire encore, dans certains cas elle mène même à sa dégradation. La conductivité thermique ne peut être améliorée en ajustant la concentration en SDBS que lorsque la valeur du pH est dans la plage optimale. Plus que tous les autres paramètres, le pH se démarque comme étant le paramètre clé pour la stabilisation de ces nanofluides.
- Plus la taille des nanoparticules est petite, meilleure est la conductivité thermique.
- La conductivité thermique augmente quand la concentration en particules augmente.

Au-delà de l'évaluation et la quantification des effets des différents paramètres précédemment énoncés sur la conductivité thermique des nanofluides, les résultats du chapitre 2 ont permis de démontrer expérimentalement qu'en utilisant les techniques de mesure appropriées et en optimisant les conditions de préparation, il est possible d'observer une augmentation de la conductivité thermique des nanofluides, beaucoup plus élevée que celles prédites par les modèles théoriques classiques [1].

Dans le troisième chapitre de ce manuscrit, une analyse expérimentale détaillée des régimes de dispersion que peuvent présenter les nanofluides à base d'eau et d'alumine a été exposée. Pour ce faire, des mesures simultanées de la conductivité thermique et de la viscosité dynamique ont été réalisées à des niveaux de concentration volumique ϕ allant de 0.2 à 2%. Il a été possible de contrôler l'agglomération des mélanges en faisant varier le pH. Les mesures simultanées de k et de μ ont permis de nous renseigner sur le possible état de dispersion des particules et ainsi d'apporter des éléments de réponse sur les mécanismes de transport de chaleur dans les nanofluides, ce qui était l'objectif principal de cette étude. En effet, examiner les résultats représentés par les différents points de mesure a rendu possible la corrélation des conséquences de l'agglomération sur les évolutions de k et de μ puisque les changements des comportements thermiques et rhéologiques se produisaient de façon simultanée dans les mêmes gammes de pH. En faisant varier le pH des solutions, cinq régimes de dispersion ont été identifiés pour les valeurs intermédiaires de ϕ . Deux arrangements de particules différents pouvaient fournir les

maxima d'augmentation de la conductivité thermique. Le régime bien dispersé caractérisé par un maximum local de la conductivité thermique et un minimum absolu de la viscosité dynamique n'est pas observé quand la concentration en particule était élevée ($\varphi = 2\%$) tandis que le régime d'agglomération en chaîne n'était pas présent aux faibles concentrations ($\varphi = 0.2\%$). Contrairement au régime bien dispersé, un pic de μ accompagnait l'augmentation de k dans le *C-L.agg*. Les valeurs de μ relatives à ce régime de dispersion avaient augmenté de façon à dépasser même celles du régime fortement aggloméré ce qui a permis de révéler l'existence d'une agglomération particulière pouvant assurer un transfert de chaleur efficace : *Chaîne-Like Agglomération*. Ce résultat vient confirmer expérimentalement le concept théorique d'*agglomération optimisée* prédit avec succès par Prasher et al. [2,3]. Les résultats de cette étude ont également été corroborés par la distribution du nombre de Mouromtseff Mo, critère de mérite permettant d'identifier les nanofluides les plus efficaces. La distribution de Mo a permis de constater que, pour un nanofluide optimisé, une efficacité comparable peut être obtenue même à faible concentration $\varphi = 0.2\%$.

Cette étude a de plus permis de mettre en évidence la nécessité de considérer avec plus d'intérêt la viscosité des nanofluides. En effet, un nombre considérable des travaux de recherche se concentrent sur l'évaluation de la conductivité thermique des nanofluides alors que la viscosité dynamique est aussi une propriété qui ne manque pas d'importance en raison de son impact sur les performances globales des nanofluides lors de leur utilisation dans des systèmes énergétiques. Par conséquent, la viscosité dynamique des nanofluides devrait être systématiquement estimée et le double examen de k et de μ est fondamentale pour l'évaluation du comportement thermo-fluidique des nanofluides.

Dans le quatrième chapitre de ce manuscrit, une étude expérimentale détaillée a été menée afin de comprendre les origines du phénomène d'hystérésis se développant lors des cycles de chauffage et de refroidissement des nanofluides à base d'eau et d'alumine. L'accent a été particulièrement mis sur la relation qui lie ce phénomène aux différents états de dispersion des nanoparticules. Ainsi, en effectuant des mesures simultanées de conductivité thermique et de viscosité dynamique à la température ambiante, les cinq régimes de dispersion rencontrés et examinés dans le chapitre 3, ont aussi été mis en évidence pour une nouvelle concentration volumique $\varphi = 0.7\%$. Cette concentration a suscité un intérêt particulier pour cette étude puisque

les régimes d'agglomération en chaîne (*C-L.agg.*) et bien dispersé (*W.D.*) présentait des courbes dont les pics de conductivité thermique relative avait la même amplitude. L'influence de la température, dans la plage comprise entre 20 et 80 °C, sur k et μ ainsi que sur le pH de la solution a, par la suite, été étudiée pour six conditions caractéristiques dans ces deux régimes. Il a été démontré que dépendamment de l'état de préparation et des conditions de stabilisation des nanofluides, il existerait une température critique au-delà de laquelle un phénomène d'hystérésis pouvait apparaître pendant les cycles de chauffage et de refroidissement. Cette température critique dépend fortement du régime de dispersion et du pH initial du nanofluide. En effet, il a été observé que tout changement de température induit un changement du pH de la solution, qui peut être corrélé aux régimes de dispersion et peut, à son tour, apporter des informations utiles concernant l'agglomération des nanoparticules et le phénomène d'hystérésis. Les expériences menées dans le cadre de cette étude ont permis d'identifier les conditions dans lesquelles le phénomène d'hystérésis pouvait apparaître et ainsi apporter des éléments de réponse sur les configurations à privilégier lors de la préparation des nanofluides afin d'atténuer, et si c'est possible éviter, ce phénomène indésirable, ce qui constituait l'objectif central du chapitre 4.

Dans le cas des nanofluides dont l'état de dispersion de départ les plaçait dans la fenêtre de pH relative au régime bien dispersé (*W.D.*), aucun phénomène d'hystérésis n'apparaissait tant que la variation de la température n'induisait pas une transition vers le régime de particules faiblement liées (*Weakly-attracted*). L'augmentation de la température ayant pour effet de déplacer le pH vers les faibles valeurs, il a été constaté que préparer un nanofluide avec un pH initial le situant à la limite supérieure de la zone bien dispersée assure une meilleure stabilité de la suspension vis-à-vis de la température. A l'inverse, les échantillons dont le pH initial les rapprochait de la zone de transition entre le régime bien dispersé (*W.D.*) et le régime de particules faiblement liées (*Weakly-attracted*) étaient beaucoup plus instables et leurs cycles de chauffage-refroidissement faisaient apparaître une hystérésis dont l'incidence sur les propriétés des solutions avait un effet irréversible. En effet, au cours du chauffage de ces nanofluides et quand la température critique était dépassée, la conductivité thermique chutait de façon considérable alors que la viscosité augmentait et la phase de refroidissement était incapable de ramener le fluide à ses performances de départ. Plus le pH initial de la solution s'éloignait de

cette zone de transition, plus la température critique était repoussée vers de hautes valeurs et par conséquent le phénomène d'hystérésis était retardé.

Les résultats relatifs aux échantillons issus du régime bien dispersé ont aussi permis de mettre en évidence le possible effet du mouvement brownien. En effet, il a été observé que, lors de la chauffe des échantillons, l'augmentation relative de la conductivité thermique se produisait de façon inégale dépendamment du niveau de température. Le mouvement brownien étant la résultante des collisions des nanoparticules avec les molécules du fluide de base et, de ce fait, très dépendant de la taille des particules et de la température, est susceptible d'être d'autant plus accentué en régime bien dispersé puisque les particules sont à leur plus petite taille. L'augmentation de la température provoque davantage d'agitation thermique, ce qui apporte plus d'effet nano (nano-convection provoquée par le sillage de la particule en mouvement dans le fluide de base) et pourrait être à l'origine de l'amélioration de la conductivité thermique relative des suspensions dans la première partie de la phase de chauffe. Aux températures élevées, l'effet du mouvement brownien est d'autant plus prononcé, pouvant mener à plus de collisions entre particules [4] et éventuellement, avec un effet combiné à la variation du pH des solutions induite par la température, expliquer l'agglomération qui se produit au-delà de la température critique.

Le phénomène d'hystérésis qui a été observé lors du chauffage-refroidissement des échantillons instables du régime bien dispersé (*W.D.*) est alarmant dans le sens où il risque de compromettre l'utilisation sereine de pareils nanofluides dans des applications industrielles puisque les propriétés de ces suspensions pourraient subir des dégradations au cours des différents cycles d'exploitation. Cependant, et comme l'hystérésis n'apparaît pas tant que la température critique n'est pas dépassée, l'utilisation de ces suspensions dans des installations industrielles dont les températures de travail ne dépasseraient pas T_{cr} ne devrait pas poser de problème de fonctionnement. Bien évidemment, et si les plages de variation de la température de l'application visée étaient réduites et coïncidaient avec la fenêtre de stabilité de la suspension issue du centre de la zone bien dispersée (*W.D.*), ces conditions de préparation devront être considérées en priorité puisqu'elles assurent le maximum d'augmentation de la conductivité thermique et le minimum absolu de viscosité assurant ainsi les meilleures performances énergétiques globales. Par ailleurs, il a été observé que les nanofluides dont le pH initial les plaçait à la limite supérieure de la zone bien dispersée pouvaient tirer profit d'une fenêtre de pH

beaucoup plus large permettant de mieux maintenir leur régime de dispersion pendant la phase de chauffage et ainsi présenter une meilleure stabilité thermique. Leurs propriétés thermophysiques ne subissent aucune hystérésis sur une large plage de température et leurs conditions de préparation devront être privilégiées si les applications industrielles visées nécessitent des niveaux de température de fonctionnement élevés. Bien qu'ils aient une conductivité thermique initiale (à 25 °C) inférieure à celle des suspensions issues du centre de la zone bien dispersée, ces dispersions subissent une meilleure augmentation de la conductivité thermique relative à haute température.

Dans le cas des nanofluides dont l'état de dispersion de départ les plaçait dans la fenêtre de pH relative au régime d'agglomération en chaîne, les expériences ont montré que le phénomène d'hystérésis, quand il a été observé, avait une amplitude limitée et son effet sur les propriétés des suspensions était minime. En effet, au-delà de la température critique à laquelle ce phénomène apparaissait, les propriétés du fluide ne subissaient aucun dommage irréversible. Cette T_{cr} semblait alors plus correspondre à une température de transition entre les deux régimes *C-L.agg.* et *W.D* qu'à la T_{cr} classique observée dans le cas des échantillons issus du régime *W.D*. Effectivement, dans le cadre de cet état de dispersion, les échantillons pour lesquels l'hystérésis apparaissait, bénéficiaient des avantages des chaînes de particules hautement conductrices à basses températures et ceux du régime bien dispersé à hautes températures. Plus le pH initial des solutions se situait proche de la limite inférieure de la fenêtre relative au *C-L.agg régime*, plus la transition vers le *W.D régime* s'effectuait à des températures faibles.

L'éventuelle intégration des nanofluides dont l'état de dispersion des particules présenteraient un arrangement en chaîne dans les installations industrielles ne devrait pas poser de problème. Cependant, et dans le cas précis où le pH initial de l'échantillon le situait sur la limite supérieure de la fenêtre relative au *C-L.agg régime*, la phase de refroidissement pouvait amener la viscosité, à la fin du cycle, à des niveaux légèrement supérieurs à ses valeurs initiales. Étant donné que le dimensionnement des installations est généralement basé sur la valeur de viscosité la plus élevée que le fluide connaît au cours de son cycle de travail, il faudra alors penser à prendre en compte l'augmentation possible de la viscosité lors de la conception des installations. Le *C-L.agg régime* étant caractérisé par une viscosité plus élevée que celle du *W.D régime* devra être considéré dans le cas des applications pour lesquelles les besoins thermiques priment. Le phénomène

d'hystérésis, a priori sans conséquence pour cet arrangement de particules, n'apparaissait pas tant que la température critique n'était pas dépassée. Les résultats montrent aussi que contrairement au *W.D.* régime, le mouvement brownien ne semble pas faire partie des mécanismes de transfert de chaleur qui sont à l'origine de l'amélioration de la conductivité thermique dans le *C-L.agg régime*. Ceci s'explique par le fait que le développement des chaînes de particules les éloigne de l'échelle moléculaire ce qui les rend difficiles à faire bouger par les molécules du fluide de base.

Les résultats recueillis dans le cadre de cette thèse de doctorat sont concluants et prometteurs, cependant beaucoup de questions demeurent en suspens tant au niveau fondamental qu'au niveau des éventuelles approches pouvant amener les nanofluides à un degré de maturité suffisant pour être utilisé de manière efficace dans des installations thermiques réelles. Ainsi, il serait intéressant :

- D'évaluer leurs performances dans un échangeur de chaleur en milieux convectif. Le design et la conception d'un montage expérimental d'échangeur de chaleur à l'échelle pilote a aussi été effectué dans le cadre de cette thèse. Le banc d'essais a été imaginé de façon à être finement instrumenté pour permettre de quantifier les performances globales du système et mesurer les transferts locaux. Ce banc d'essais permettra de comparer les comportements rhéologique et thermique des nanofluides dans un échangeur de chaleur dont les conditions opératoires sont similaires à celle des échangeurs retrouvés dans les applications industrielles. Il servira à tester les nanofluides pour diverses conditions (températures aux entrées, débits massiques, niveaux de flux, puissance d'homogénéisation par ultrason ...), il permettra de mesurer les coefficients de transfert thermique, de déterminer les pertes de charge, de calculer un facteur de mérite liant la puissance de pompage à l'amélioration des échanges et de sélectionner les mélanges les plus performants. Ce banc d'essais expérimental aura l'originalité d'inclure une boucle secondaire de préparation des mélanges annexée à l'échangeur et un système à ultrason en ligne qui pourra être utilisé pour disperser les nanofluides en cycle continu. La boucle comportera aussi une sonde de mesure de conductivité thermique et un viscosimètre en ligne qui permettront d'évaluer dans les conditions réelles de fonctionnement les propriétés thermohydrauliques des mélanges. Il est aussi prévu de modifier le banc lors d'une phase ultérieure pour inclure un accès optique, ce qui permettra de pouvoir faire des mesures locales de vitesse (PIV) et d'avoir un accès à la structure de l'écoulement.

- D'étudier le vieillissement des nanofluides sur plusieurs cycles de fonctionnement.
- D'étudier l'effet du phénomène d'hystérésis sur les autres propriétés des nanofluides, à savoir la densité et la capacité calorifique. L'étude de l'éventuel effet des états de dispersion sur la masse volumique pourrait valider expérimentalement la contribution de la couche *nanolayer* au transfert thermique des nanofluides si la notion d'excès de volume est confirmé.
- D'essayer de généraliser les résultats de cette thèse à d'autres types de nanoparticules et d'autres fluides de base.
- D'essayer de créer un nanofluide multiéchelle en mixant deux tailles de particules, de préférence séparées par un ordre de grandeur ($\sim 10\text{nm}$ et $\sim 100\text{nm}$).

Références:

- [1] J. C. Maxwell, (1881). A Treatise on electricity and magnetism, Second Edition. Clarendon, Oxford.
- [2] R. Prasher, W. Evans, P. Meakin, J. Fish, P. Phelan, P. Keblinski, Effect of aggregation on thermal conduction in colloidal nanofluids, Appl. Phys. Lett. 89 (14) (2006) 88–90.
- [3] R. Prasher, P. Phelan, P. Bhattacharya, Effect of aggregation kinetics on the thermal conductivity of nanoscale colloidal solutions (nanofluid), Nano Lett. 6 (7) (2006) 1529–1534.
- [4] S.K. Das, S.U.S. Choi, W. Yu, T. Pradeep, Nanofluids : Science and Technology, John Wiley & Sons, Hoboken, USA, 2008.